UTILIZATION OF WASTE RUBBER TIRES IN ARTIFICIALLY CEMENTED ALLUVIAL CLAY

A THESIS SUBMITTED TO
THE BOARD OF GRADUATE PROGRAMS
OF
MIDDLE EAST TECHNICAL UNIVERSITY, NORTHERN CYPRUS CAMPUS

BY

LUTF NAGI AHMED AL-SUBARI

IN PARTIAL FULFILLMENT OF THE REQUIREMENTS
FOR
THE DEGREE OF MASTER OF SCIENCE
IN SUSTAINABLE ENVIRONMENT AND ENERGY SYSTEMS PROGRAM

JULY 2022

Approval of the Board of Graduate Programs

Prof. Dr. Cumali Sabah
Chairperson

I certify that this thesis satisfies all the requirements as a thesis for the degree of Master of Science

Assoc. Prof. Dr. Ceren Ince
Program Coordinator

This is to certify that we have read this thesis and that in our opinion it is fully adequate, in scope and quality, as a thesis for the degree of Master of Science.

Assoc. Prof. Dr. Pedro Miguel Vaz Ferreira
Co-Supervisor

Asst. Prof. Dr. Abdullah Ekinci
Supervisor

Examining Committee Members

Prof. Dr. Murat Fahrioğlu	Electrical and Electronics Engineering Dept., METU NCC	
Assoc. Prof. Dr. Ayşe Pekrioğlu Balkis	Civil Engineering Dept., CIU	
Asst. Prof. Dr. Abdullah Ekinci	Civil Engineering Dept., METU NCC	

I hereby declare that all information in this document has been obtained and presented in accordance with academic rules and ethical conduct. I also declare that, as required by these rules and conduct, I have fully cited and referenced all material and results that are not original to this work.

Name, Last name: Lutf Nagi Ahmed, Al-Subari

Signature:

ABSTRACT

UTILIZATION OF WASTE RUBBER TIRES IN ARTIFICIALLY CEMENTED ALLUVIAL CLAY

Al-Subari, Lutf Nagi Ahmed
Master of Science, Sustainable Environment and Energy Systems Program
Supervisor: Asst. Prof. Dr. Abdullah Ekinci
Co-Supervisor: Assoc. Prof. Dr. Pedro Miguel Vaz Ferreira

July 2022, 135 pages

Problematic soils possess unfavorable engineering properties that need to be treated before usage, whilst cement is one of the most common materials used for such purpose. However, cement production is one of the highest contributors to global CO_2 emissions that cause global warming. On the other hand, a massive amount of waste rubber tires is being generated annually, which commonly are being disposed of in landfills causing many environmental and health problems. In this context, this study investigates the performance of waste rubber tire inclusion in alluvial clay stabilized with ordinary Portland cement. For this purpose, samples of various mixes were prepared, containing soil, cement content (7%, 10%, and 13%) of the dry mass of the soil, and two types of rubber tires (i.e., powder [TRP] and fiber [TRF]) proportioned as (0%, 2.5%, 5%, 10%, and 20%) of the cement quantity. The blends were compacted at (1600 and 1800 kg/m^3) dry densities and 7, 28 and 60 days of curing. After curing, strength (unconfined compressive strength, and stiffness), durability (wet/dry cycles), and microstructural (SEM, XRD, XRF) evaluations were performed. Furthermore, life cycle assessment (LCA) of employing the tires in cemented soils was performed to highlight the environmental impacts of such technique. Overall, the results showed that the inclusion of 2.5% to 5% TRF or TRP

replacing cement is the ideal range of rubber tire content in the composites studied concerning strength, stiffness, and weathering resistant performances. Furthermore, LCA results confirmed the significant contribution of this method to the environment.

Keywords: Clay, Stabilization, Tires, Cement, Sustainability

ÖZ

ATIK LASTİKLERİN ÇİMENTO KATKILI ALÜVYAL KİLDE KULLANIMI

Al-Subari, Lutf Nagi Ahmed
Yüksek Lisans, Sürdürülebilir Çevre ve Enerji Sistemleri
Tez Yöneticisi: Dr. Öğr. Üyesi Abdullah Ekinci
Ortak Tez Yöneticisi: Doç. Dr. Pedro Miguel Vaz Ferreira

Temmuz 2022, 135 sayfa

Günümüzde problemli zeminlerin mühendislik uygulamalarında kullanılmı öncesi çimento ile ıslahı yaygın olarak kullanılmaktadır. Ancak çimento üretimi, küresel CO_2 emisyonlarına en fazla katkıda bulunan yapı malzemelerinden biridir. Öte yandan, her yıl yüksek miktarda atık lastik üretilmekte ve bunlar genellikle atık depolama alanlarına veya vahşi depolama alanlarına atılarak çevre ve sağlık sorunlarına sebebiyet vermektedir. Bu çalışmada atik lastiklerin çimento katkili alüvyal kilde kullanimi incelenmiştir. Ön testlerden elde edilen veriler ışığında, referans oluşturmak makasdı ile kil (%7, %10, ve %13) oranında çimento ile karıştırılmıştır. Daha sonra çimento içeriğinin yerine (%0, %2.5, %5, %10, ve %20) oranında iki farklı lastik türü (lastik kauçuk tozu (LKT) ve lastik kauçuk lifi (LKL)) kullanılmıştır. Tüm karışımlar için numuneler hazırlanmış ve üç farklı yaşta (7, 28 ve 60 gün) kürlenmiştir. Kür işleminden sonra, dayanım (serbest basınç dayanımı ve kayma modülü), dayanıklılık (ıslak/kuru döngüler) ve mikroyapısal (SEM, XRD, XRF) değerlendirmeler yapılmıştır. Ayrıca, böyle bir tekniğin çevresel etkilerini vurgulamak için lastiklerin çimento ile iyileştirilmiş zeminlerde kullanılmasına ilişkin yaşam döngüsü analizi gerçekleştirilmiştir. Genel olarak sonuçlar, %2,5 ila

%5 lastik katkılı çimentonun, serbest basınç dayanımı, kayma modülü ve hava koşullarına dayanıklılık açısından ideal kauçuk lastik içeriği aralığı olduğunu göstermiştir. Ayrıca, yaşam döngüsü sonuçları, bu yöntemin çevreye önemli ölçüde olumlu katkısını doğrulamıştır.

Anahtar Kelimeler: Kil, Stabilizasyon, Atık, Çimento, Sürdürülebilirlik

To My Family

ACKNOWLEDGMENTS

I would like to express my sincere gratitude to my supervisor Asst. Prof. Dr. Abdullah Ekinci and my co-supervisor Assoc. Prof. Dr. Pedro Miguel Vaz Ferreira for their guidance, advice, criticism, encouragement, and insight throughout the research. My gratitude also extends to the SEES program and civil engineering faculties for giving me the opportunity to do this research.

I would like to thank the thesis defense jury members Prof. Dr. Murat Fahrioğlu and Assoc. Prof. Dr. Ayşe Pekrioğlu Balkis for their comments and suggestions.

I would also like to thank Assoc. Prof. Dr. Ertug Aydin for his contribution and help in the microstructure analysis.

I would like to thank civil engineering graduates of METU NCC: Maen Ghanem, Said Baathman, Iqbal Hassan, and Amin Hassan, for their great help during the laboratory work.

I am also grateful for all the help and support I have received from my friends and colleagues throughout the period of this research.

Finally, I could not have undertaken this journey without the support and encouragement of my family, especially my parents (my father: Nagi, and my mother: Saqia), whose sincere prayers accompanied me through all good and challenging times. Special thanks to my old brother Hezam for his endless support and encouragement. To the love of my life, my finance, and my future wife: Omaima Al-Subari, I am genuinely grateful for all the love, support, and motivation you showed me throughout this journey.

TABLE OF CONTENTS

LIST OF TABLES

TABLES

LIST OF FIGURES

FIGURES

CHAPTER 1

INTRODUCTION

1.1 Background and Problem Statement

It is a well-known fact that early settlements were constructed next to fertile lands, soft alluvium soils rich with minerals needed for farming, whilst homes were built on stronger grounds. However, increasing population lead to an increase in housing and infrastructure needs. With such demand, people were forced to build on problematic soils which are covering large land areas worldwide. Such soils are not preferable for development due to the problems encountered in their use. Low strength [1], extensive settlement [2], high compressibility [1], and propensity to expand and shrink because of seasonal changes [3,4] characterize the stability and durability of structures and foundations resting on these soils [5].

This type of soil can be improved through soil stabilization, which is a collective term for any method employed to improve soil properties, thus reinforcing the soil for proper service [6]. One of the well-known and common techniques worldwide is the practice of blending cement in the soil; such method has been widely used to enable the use of weak soils as foundation reinforcement, road subgrade, and other projects [7–12]. This method can enhance geotechnical properties such as the soil's strength and durability [13,14]. Nevertheless, the cement manufacturing process is environmentally unfriendly due to the usage of considerable quantities of energy and

resources, along with the release of vast amounts of carbon dioxide (CO_2) [15–17], where, according to a study on global carbon dioxide (CO_2) emissions from cement manufacturing between 1928 to 2018 (Figure 1.1), accumulative carbon dioxide (CO_2) emissions were 38.3 plus/minus 2.4 gigatons [18]. In line with this, many researchers are exploring alternative approaches to reducing emissions to address such global sustainability issue [19–22].

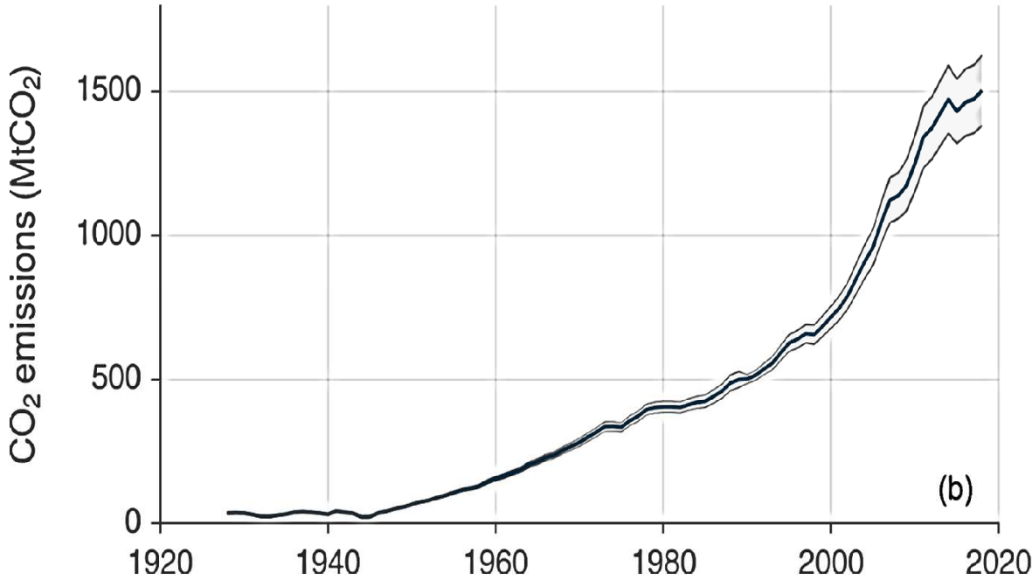

Figure 1.1. Global CO_2 emission resulting from cement production between 1928-2018 [18].

On the other hand, although solid waste management is being used to control such waste dumping in some developed nations, developing countries, particularly poor, swarmed urban communities, do not have sustainable management plans for solid waste dumping. Besides, such wastes are disposed of in landfills, creating environmental contamination, endangering human wellbeing and ecosystems around it. Waste rubber tires are probably the most environmentally hostile solid wastes.

Around 1.5 billion tires are being produced worldwide consistently, and nearly two-thirds of them reach End-of-Life Tires (ELTs) [23]. The ELTs are tires at the end of their useful lifecycle; thus, they are no longer be utilized for their main purpose and are considered waste. Although few nations, like the USA, Japan, and the European Union, have embraced sustainable methodologies to diminish their ELTs, most of the ELTs in agricultural nations are disposed wildly, causing numerous environmental issues [24].

Therefore, this study will provide an environmentally friendly alternative for the disposal of waste rubber tires while employing it to decrease the cement content used for soil stabilization.

1.2 Objective of the Study

This study aims to utilize waste tire rubber in two forms (powder and fiber) to improve the physical and mechanical characteristics of cemented clays, thus reducing the environmental burden due to cement manufacturing and waste tire dumping. The main objectives are listed as follows:

- To investigate the effectiveness of employing two types of shredded tire rubber (Tire Rubber Powder (TRP), and Fiber (TRF)) on the strength and stiffness of soft soil stabilized with cement.
- To examine the durability performance of tire-cemented-clay blends considering the effect of severe climate conditions (through wet/dry cycles) on mass loss.
- To examine the microstructure (SEM, XRD, XRF) evaluations of the blends after specific period of curing times.
- To correlate the mechanical properties with the porosity/binder index as a factor controlling such properties of the blends.

- To investigate the environmental impacts of such soil stabilization technique using the mentioned inclusions through life cycle assessments.

1.3 Thesis Outline

While this chapter introduce general background, problem statement and explanation of the thesis objectives, the following chapters will be divided as follows:

- **Chapter 2**: Literature review which includes findings from previous research works to build up general background of clay stabilization using various additives and fibers.
- **Chapter 3**: Experimental program and methodology; this chapter describes the materials, preparation of samples and testing procedures. It also includes description of the methods used for data analysis followed in this study.
- **Chapter 4:** Results and discussion includes the interpretation of the results obtained from analysis of the laboratory data. Strength, stiffness, durability, microstructure, and life cycle assessment results of the blends are discussed in this chapter.
- **Chapter 5:** Conclusions; this chapter presents the summary points of the study findings as well as limitations and recommendations for future work.

CHAPTER 2

LITERATURE REVIEW

This chapter will begin by describing the clay of Cyprus from where the soil in this study was collected. After that, a general description of the ground improvement techniques is presented, followed by a discussion of previous work in ground improvement methods similar to the one adopted in this study. Moreover, studies that investigated waste tires with or without cement in ground improvement are discussed. This chapter ends with a literature review of environmental assessment of ground improvement techniques.

2.1 Clay of Cyprus

According to Cyprus Geological Survey Department (GSD), Cyprus is geologically divided into six zones[25]. As shown in Figure 2.1. these zones are Kyrenia, Circum Troodos sedimentary succession, Troodos ophiolite, Mamonia, and Arakaps terrane.

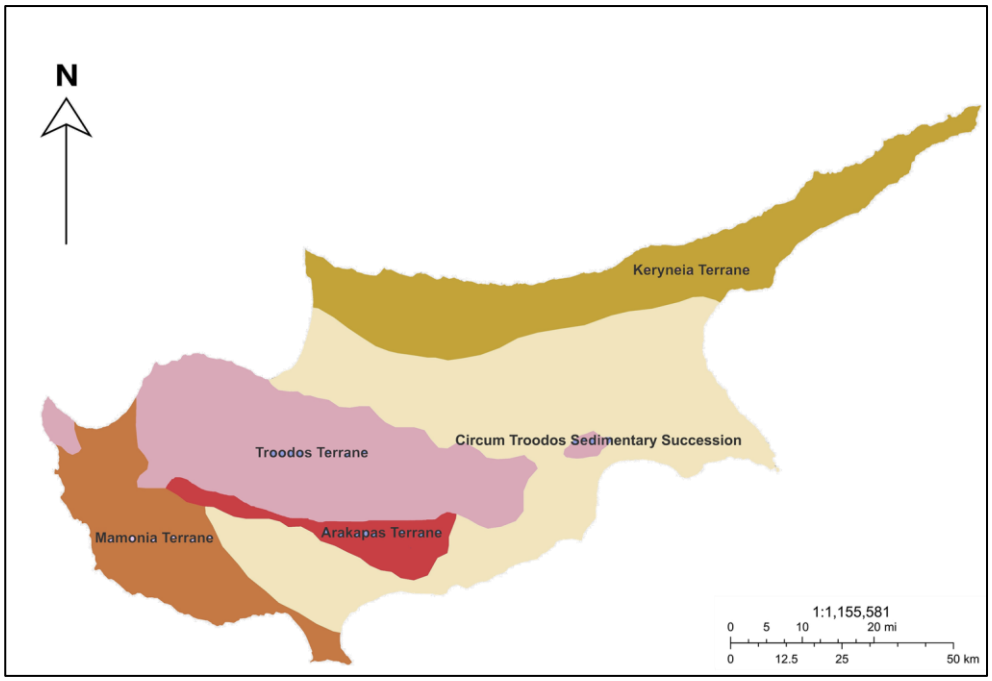

Figure 2.1. Geological zones of Cyprus (Retrieved from GSD [25])

The clays of Cyprus have been created as a result of Troodos ophiolite alterations and pelagic sedimentary cycles that followed the post Createceous period (In general, Cyprus clays possess high calcium carbonate content (Kyrenia zone) and chalks. Alluviums are mainly situated across Pedios river (southeast, southwest, and northeast) which have low bearing capacity and intermediate to high swelling potential. Cyprus clays are categorized as follows [25]:

- Alluvium clays
- Bentonitic clay group
- Mamonia clay group
- Kythrea clay group
- Nicosia Formation clay group

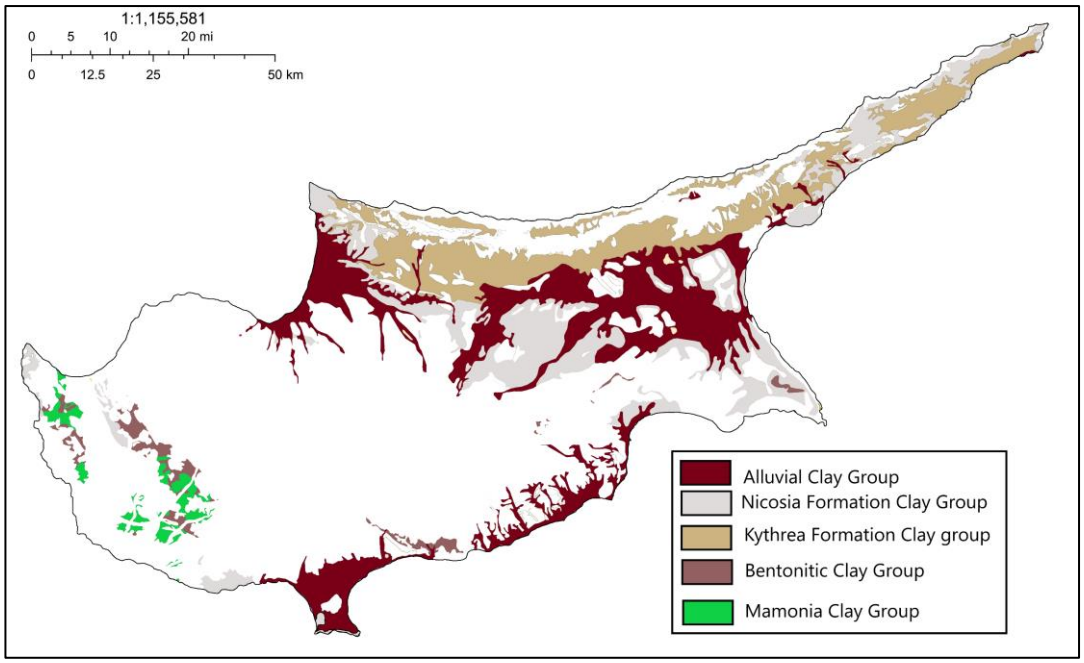

Figure 2.2. Clay of Cyprus (Retrieved from GSD [25])

2.2 Ground Improvement Techniques

Using tensile elements in soil to improve mechanical properties is not a new technique; 3000 years ago, for example, the Babylonians used palm branches to manufacture clay bricks [26]. Later, the Chinese used tree branches to reinforce clay and gravel for building the Great Wall of China, followed by the Romans, who used earth-reinforcing techniques along the Tiber River and the wharf of the port of Londinium. In the 1930s, Casagrande idealized the problem in the form of a weak soil reinforced by horizontally layered high-strength membranes. In the 1960s, Vidal placed flat reinforcement strips on frictional soil, generating a friction force that held the soil in place [27].

Since then, a vast range of ground improvement techniques has been developed to a point where they are regularly applied in most geotechnical applications. The application of these methods depends on various factors, such as soil type, the purpose of improvement, availability, and feasibility of applying such technology in

a specific location. Overall, the ground improvement methods have been categorized by TC211 -ISSMGE [28] as follows:

- Category A: Improving non-cohesive soils or fill materials without mixtures, which mainly includes the use of different compaction methods.
- Category B: Improving cohesive soil without mixtures. This category includes replacement/displacement, electro-kinetic and dynamic consolidation, preloading, thermal stabilization, and hydro-blasting compaction.
- Category C: Ground improvement using additives/inclusions. This method includes the use of stone columns, dynamic replacement, compacted sand piles, microbial additives, and the use of geosynthetics and geotextiles.
- Category D: Ground improvement grouting type admixtures. This category includes the use of different grouting (i.e., particulate, chemical, compaction, and compensation grouting) and mixing methods by treating weak soil with different additives and/or binders (such as cement and lime) to improve its physical and mechanical properties.
- Category E: Earth reinforcement. This category covers the methods used for stabilizing slope instability and it includes the use of vegetation, anchors, soil nailing, and geosynthetic or mechanical stabilized earth retaining walls.

The ground improvement technique adopted in this study is a combination of both fiber inclusion (category C) and grouting-like additive (category D). Therfore, the following literature review will focus on the investigations of such ground improvement technques.

2.2.1 Soil Stabilization Using Pozzolanic/Cementitious Additives

Various chemical additives are being used to improve soils' properties. The amount and type of additive used in soil stabilization depend on project specifications, soil type and soil characteristics to be treated.

The use of cement in ground improvement techniques in general and as an additive in soil stabilization is the most common material. When mixing cement with soil and water, the hydration (chemical reaction) of cement takes place and continues until the hardening of cement occurs. This process forms a crystal form of hardened cement that interlocks the soil particles, which significantly improves the soil's engineering properties [29]. The improvement is significant in the first several days although a slight enhancement is attained afterward. The resulted mixture of such process is called cement-soil. Various studies have been investigating the effectiveness of cement in the engineering properties of different soil types. The advantages of cement usage highly dependent on the soil type. For clayey soil, cement decrease its plasticity, swelling potential and increase strength, and stiffness [7–12,30]. Additionally, cement transform the clay into brittle material, which effects the deformation characteristics [31].

Blending small amounts of cement with soft clay increased the soils' mechanical strength, for example, bearing capacity improvement of lightweight constructions and base/sub-base layers of roads' pavement. Table 2.1 records the unconfined compressive strength (UCS) prerequisites following seven days of curing for the road base, sub-base, and rammed earth, as indicated by studies from various nations. It ought to be noticed that UCS requirements for roads emphatically rely on road class and material types.

Table 2.1. Requirements for the UCS of road base, subbase, and rammed earth.

Country	Specification Source	Unconfined Compressive Strength (MPa)			Reference
		Rammed earth	Subbase	Base	
USA	Standard Specifications for Construction of Roads and Bridges on Federal Highway Projects		1.4		[37]
USA	Soil Cement Laboratory Handbook		2.07	5.52	[38]
South African	Pavement Engineering Manual		2.0 - 4.0	4.0 - 8.0	[34]
UK	Stabilized materials for civil engineering purposes, General requirements.		2.5 - 4.5	4.5 - 7.5	[40]
UK	British practice in the design and specification of cement-stabilized bases and sub-bases for roads		1.7	3.5	[41]
Australia	Transport and Main Roads Specifications.		min - 3		[42]
China	Technical specifications for construction of highway roadbases.		> 2	> 4	[38]
New Zealand	Cement Stabilization.		min - 3		[39]
Turkey	Turkish Highway Technical Specification.			3.43 - 5.39	[40]
Australia	The Australian earth building handbook.	0.4 - 0.6			[41]
Australia	Bulletin 5. “Earth wall construction.	0.25			[42]
New Zealand	The New Zealand Standard for engineering design of earth buildings	0.5			[43]
USA	New Mexico Earthen Building Materials Code.	1.38			[44]

One of the drawbacks of using cement intensively in soil stabilization is the massive environmental impacts that its production causes. The other drawback with cement–soil stabilization is durability, that could be described as the capacity of a material to resist chemical attacks and preserve its integrity and stability over long periods of exposure to harmful weathering [45], where, according to Lu *et al.* [12], the benefits of cement stabilization decrease during weathering cycles. In this sense, the

development of alternative approaches that reduce cement usage and improve durability might be an option to mitigate those drawbacks.

Quicklime, hydrated lime, and lime slurry are calcium hydroxide products originated from limestone breakdown. Such materials have been widely investigated as binders in soil stabilization. The interaction between lime binder and soils is almost similar to cement-soil interaction. Furthermore, the effects of lime on the engineering properties of soil are mainly similar to cement [46]. However, the degree of enhancement is dependent on the soil type. For instance, high alkaline clay can be treated effectively with lime, whereas Portland cement would create detraction of its engineering properties. Overall, the general idea of using cement and lime for soil treatment is due to the pozzolanic reaction that develop strong bonds between soil particles. There are also various materials that possess such features and are called pozzolanic materials.

Pozzolanic materials are described as siliceous/siliceous-aluminous compounds containing no or very little cementitious matter. However, such materials (in a fine form) can react with calcium hydroxide with the existence of water to create a compound that has cementitious properties [47]. Pozzolans are divided, by origin, into two main categories: natural and artificial pozzolans. Natural pozzolans comes from volcanic or sedimentary origins[48], whereas artificial pozzolans are generally by-products of manufacturing and refinery activities. Various studies have investigated the influence of such materials as soil stabilizers.

Fly ash [49,50], bottom ash [51], and rice husk ash [52] are a few examples of the artificial pozzolans that have been blended with cemented clay, and laboratory examinations have been conducted to evaluate the performance of industrial wastes' blends. Such materials enhance the cemented clay's strength and stiffness behaviors when blended at a specific rate. The use of pozzolans refines the capillaries thus reducing the porosity which significantly strengthen the soil.

2.2.2 Soil Stabilization by Natural and Synthetic Fibers

As mentioned earlier, the use of fibers has been adopted in ancient history to improve the engineering properties of soils for different purposes. A wide range of fibers has been utilized for soil reinforcement. Those fibers can be categorized as follows:

- Natural fibers: this category includes plant fibers (such as coir, bamboo, rice husk, etc..), animal part fibers (such as silk, wool, etc..), and minerals (such as asbestos). Although natural fibers have various engineering applications, plant fibers are the most commonly used natural fibers in geotechnical engineering applications.
- Synthetic fibers: carbon, glass, steel, polypropylene, plastic, and much more fibers have been investigated as soil reinforcement elements. Moreover, geosynthetic materials have gained broad interest in geotechnical engineering applications due to the flexibility and efficiency of their usage for soil reinforcement.

Geosynthetics are generally distributed in an oriented way where other fibers (like, glass) are randomly scattered in the soil. Figure 2.3 illustrates the interaction between randomly distributed fibers and soil media [53].

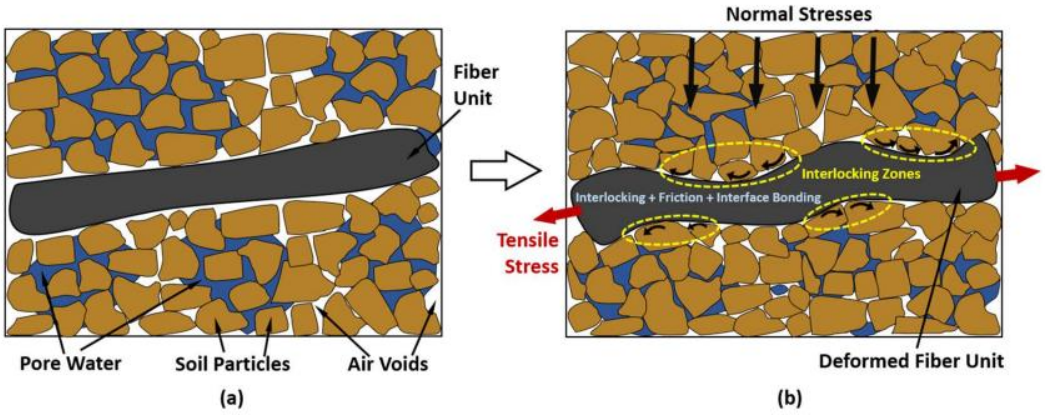

Figure 2.3. Fiber-Soil interaction (a) after mixing (b) During load application, retrieved from Gowthaman *et al* [53].

Research on fiber-reinforced soils consistently shows that the addition of fibers causes an increase in peak and post-peak shear strength. As one of the earlier research, Li and Zornberg [54] showed that the addition of fibers significantly increased the peak shear strength and limited the post peak loss of strength for both cohesive and granular soils. Li and Zornberg [55] and Freilich et al. [56] assessed the undrained shear response of fiber-reinforced clay and concluded that fibers distribute stresses more uniformly within the soil matrix. Similar conclusions were reached by the authors [56–59] when investigating the deformation modes of different fine-grained soils. The authors reported that unreinforced samples developed distinct slip planes, while reinforced specimens showed barreling type failure. Mirzababaei et al. [60] performed more comprehensive study on carpet waste reinforced clay and reported that unconfined compressive strength highly dependent on initial dry unit weight and moisture content of the soil. Authors further confirmed with earlier studies on other types of fiber that addition of carpet fiber enhanced compressive strength, reduce post peak strength loss, and change the failure behavior from brittle to ductile and failure pattern from localization to a more uniform barrel-shaped failure. Few other studies have been performed on other aspects of the technique. In one of those studies, Falorca and Pinto [61] evaluated the shear strength behavior of sandy and clayey soils reinforced with discrete polypropylene fibers having different texture and reported that no appreciable advantage is achieved on shear strength when using textured fibers. In another study, Mirzababaei et al. [62] evaluated the shear strength improvement of soft to stiff clays with discrete short fibers and reported that short fibers did not perform well in soft clays that have low density. Ekinci et al. [63] investigated the influence of Polypropylene fiber on the mechanical behavior of compacted Lambeth-group clays through triaxial testing. The authors reported a degradation of the mechanical properties after 100 kPa of confining stress. However, such inclusion transforms the plane failure of the tested samples from shear to barrel. Moreover, Ekinici et al. [64] studied the effect of several artificial fibers (i.e., basalt, carbon, polypropylene and glass) on the mechanical and durability properties of alluvial clays. The authors reported that

carbon fibers have the highest degree of strength improvement of the soil, compared to the other three other fibers. However, polypropylene fiber reinforced clay possessed the highest peak strain energy.

To reduce environmental impact caused by traditional stabilizers such as lime and cement, industrial wastes additives, such as tire waste as fiber have been used to replace cement. One of the earliest study of refire clay composite was performed by Al-Tabbaa and Aravinthan [65] on naturally over-consolidated fissured clays mixed with shredded tire. Authors studied mechanical behavior of the composite and reported compressive strength of the mixture was as low as 40% of the strength of the clay alone. Authors further report that the initial stiffness of the tire stabilized clay was half the clay alone specimens. Özkul and Baykal [58] performing drained and undrained triaxial tests to stabilize kaolinite reach clay with tire fibers. Authors reported that up to a critical confining stress, the peak strength of the composite is greater than the clay alone, whilst above the critical confinement, lower peak improvement was observed.

2.2.3 The Use of Porosity/Binder Index Stabilized Soil Evaluation

The porosity/binder index is ratio that combined the effect of both the binder content and the porosity (density) of soil-binder blends. Such factor was established by Pendola et al. [66] in 1969 to evaluate the tensile properties of cemented soils. Consoli *et al.* [67] examined the relationship between the volumetric voids and cement content on the compressive strength of cemented sand; they revealed that the porosity/cement index could be used to assess the compressive strength of cemented sand. Additionally, they proposed applying an exponential porosity/binder modified equation, which relies on the mixed ingredients. This way, the porosity/binder index has been viably applied to assess the compressive strength, stiffness, and tensile strength of treated coarse and fine grain soils. Porosity/binder index has been utilized to evaluate the unconfined compressive strength, tensile strength, and stiffness of cemented soils ([68], [69], [70], [71], and [72]). Moreover, it has been proposed to

utilize the porosity/binder index for soils treated with a double and triple binder. Ekinci *et al.* [73] found the porosity/double and triple binder index can be used to assess the strength of marine clay deposit treated with double and triple binders mix (i.e., Portland cement, hydrated lime, and copper slag). Moreover, this index can be utilized in a relevant construction project, and at that point, strength and stiffness can be compared by employing relationships developed in laboratory tests [74,75].

In a later study, Festugato et al. [76] investigated unconfined compressive strength and split tensile strength of polypropylene fiber reinforced cemented clayey sand and reported that both unconfined compressive and split tensile strength increase with respect to the increase in cement and fiber content. Authors further proposed a dosage relationship linking unconfined compressive strength and split tensile strength of the clayey soil with porosity/cement ratio developed by authors earlier and fiber length. In a more sophisticated attempt, Mirzababaei et al. [77] performed consolidated undrained triaxial tests to study the shear strength of carpet waste fibers and proposed a nonlinear regression model to predict the relationship between effective shear stress ratio, deviator stress and axial strain fiber reinforced soils samples with various fiber contents. Improving earlier studies on porosity/binder index, Festugato et al. [78] proposed a theoretical model for predicting the compressive strength - splitting tensile strengths ratio of artificially cemented fiber reinforced soils. Authors further reported that the developed model yields results of tensile to compression strength ratio closer to experimental observations and the ratio is slightly dependent on the fiber content.

Furthermore, subsequent studies examined the possibility of using this index (porosity/binder ratio) as durability and stiffness parameters of cemented soil to evaluate stiffness and durability indicators by considering the loss of mass after a number of wetting/drying cycles [9,79,80], and these studies demonstrated that proposed index is appropriate to predict loss of mass. In a more recent study, Hanafi *et al.* [81] investigated the porosity/binder ratio for cemented soil blends in terms of loss of mass. Additionally, Consoli *et al.* [82] conducted a study on low plasticity silty sand/chalky sand blended with a binder composed of coal fly ash and hydrated

lime and proposed a new approach that relates durability through wetting/drying cycles with stiffness results through the ultrasonic pulse velocity (UPV) test.

2.3 Previous Studies on Waste Rubber Tire Utilization in Soil Stabilization

Few researchers have investigated the utilization of waste rubber tires in ground improvement applications. Blending tires at certain rates of various forms (i.e., shreds, powders, fibers, grinds, and chips) with clay found to reduce the unconfined compressive strength (UCS) and stiffness of clay tire blends ([83],[84], [85], [86], [87]). The decreased UCS and stiffness realized by those researchers can be explained by the absence of bonding among clay and tire particles. Nonetheless, to a certain extent, a few researchers justified using rubber tires to somewhat improve soil's strength and stiffness properties. A substantial drop has been observed when the level of the rubber tire exceeds a certain restricting rate ([88], [89], [90]). Based on the author's knowledge, the use of waste rubber tires in cemented soil treatment has not been widely investigated. Shahin and Hong [91] revealed that 1%, 4%, and 7% shredded tires (440μm of tire powder and 4 mm of grain size tires) treated with 15% cement could reduce the strength and elastic modulus of rubber treated cemented clay as the level of tires in the blend increase. In any case, they likewise noticed an increase in the ductility behavior of the blend by adding the shredded tires. Ho *et al.* [92] led an exploratory investigation of the effect of adding 5 %, 10%, and 15% of rubber chips containing 2mm to 5mm grain tires on the compressibility of kaolinite clay treated with 2% and 4% cement and concluded an increase in the stiffness of treated clay. Yadav and Tiwari [90] performed a laboratory examination to analyze the effect of blending rubber powder of a 0.8mm to 2mm diameter on cemented clay's strength and stiffness properties. The Yadav and Tiwari [90] study examined the use of 3% and 6% of cement (by dry soil weight) in treating the weak soil where 2.5%, 5%, 7.5%, and 10% of crumb rubber (by dry soil weight) was blended in with cemented clay at the maximum dry densities and optimum moisture content of the blends. The incorporation of crumb rubber decreased the UCS of the

treated soil, and the rate of this decrease increased when more than 5% of crumb rubber was incorporated. Nonetheless, the addition of crumb rubber increased the longitudinal failure strain by decreasing the stiffness of treated clay [90]. Shahin and Hong [91] reported similar findings. Moreover, immersing the samples into the water by one day fundamentally reduced the UCS values because of the low resistivity of the lower proportions of cement in the blend [90].

Moreover, Chan [93] used granulated rubber waste in cement-stabilized clayey sand with 0-4% cement and rubber shreds or chips. The authors investigated the strength and stiffness response of the mixes via unconfined compressive strength and bender element tests and reported that both, specimen's strength, and stiffness were controlled by cement content and the increase in the rubber content resulted in an increase in ductility of the stabilized material. They also reported that a correlation between the strength (q_u) and stiffness (initial shear modulus, G_o and elastic modulus, E) parameters exist for the mixes. Yadav and Tiwari [94] utilized tire rubber fibers in cement treated soft clay. Authors used 2-3 mm size long tire threads as 2.5%, 5%, 7.5% and 10% and 3% and 6% cement content by the dry weight of the specimens. It was reported by the authors that addition of rubber fibers reduces the unconfined compressive and split tensile strength of the specimens when compared with clay-cement treated samples with an increase in ductility index of the specimens. In the perspective of structural materials, Jo et al. [95] defined ductility as the ability of a material or a structural system to maintain inelastic deformation prior to collapse without significant loss in resistance In a more recent study, Bekhiti et al. [96] studied unconfined compressive strength and ductility of cement stabilized bentonite clay soil by utilizing 0.5%, 1% and 2% rubber fiber content with 5%, 7.5% and 10% cement content. Lately, Akbarimehr et al. [97] investigated the geotechnical behavior of three different forms of waste tire including granular, fiber and chips by performing various tests including compaction, unconfined compressive strength, direct shear and triaxial. It was reported by the authors that rubber fiber provided higher increase in strength among all other forms of rubber tire used.

Durability studies carried out on tire-cement stabilized soils are mostly done by freeze-thaws cycles. Cokca and Yilmaz [98] investigated effect of freeze-thaws on unconfined compressive strength of fly ash-bentonite-rubber mixture. The authors reported that an unconfined compressive strength of mix was reduced by 50% after freeze–thaw cycles. In another study, Roustaei and Ghazavi [99] investigated the impact of freeze/thaw cycles on strength properties by incorporation of rubber and steel fibers to high-plastic clays. The authors concluded that the rate of strength reduction during freeze and thaw cycles is much lower for rubber fibers when compared with those of steel fibers. In a later study, Jafari and Esna-ashari [100] investigated the strength performance of clayey soil stabilized with lime and waste tire cord subjected to freeze and thaws. The authors found that incorporation of tires in lime-stabilized clay reduces the strength and stiffness reduction rate. In one of the few studies on wetting and drying cycles, Yadav and Tiwari [101] analyzed the durability of crumb rubber stabilized artificially cemented clay soils. The authors reported that specimens treated with 3% cement and more than 5% of rubber disaggregated before reaching twelve wet/dry cycles. It was also reported that, with increase of rubber content, the mass loss was observed to also increase. The authors believed that such increase in mass loss is due to thermal expansion differences between rubber and soil–cement matrix, which causes reduction in bond strength and further void formations.

As mentioned, durability is required, as environmental conditions and climate cycles affect the stabilized soil, which will deteriorate under such conditions, including wetting/drying, freezing/thawing cycles, and erosion. The influence of such conditions includes a drop in the strength and stiffness values of the improved soils. Regarding the way of studying durability, analysis declared that stabilized soil durability could be investigated in terms of loss of mass, strength change, or swelling [102]. In Cyprus, the climate is mainly continental, subtropical semi-arid, and the northern regions have a Mediterranean climate [103]. In general, Cyprus has hot and dry summers, wet and cool winters [104]. Therefore, in Cyprus, the wetting/drying cycles rule over strength-control mechanisms. Furthermore, wetting/drying

weathering has been declared to be more aggressive than freezing/thawing weathering [105]. There are a couple of standards that state the loss of the topmost permitted mass after 12 wetting/drying cycles for clays; a number of such specifications are presented in Table 2.2.

Table 2.2. Standards about Wetting/Drying for Clay Soils.

Standard/Research	**Aplication**	**ALM after 12 wet/dry cycles**	**Referance**
US Army Corps of Engineers technical manual (USACE)	Subgrade Layer	≤ 6%	[106]
Unified Facilities Criteria (UFC)	Bases and sub-bases	≤ 6%	[107]
Unified Facilities Guide Specifications (UFGS).	Subgrade	≤ 6%	[108]
Federal Highway Administration (FHWA)	Base, subbase, and subgrade	≤ 6%	[32]
J. Paul Guyer, An Introduction to Soil Stabilization for Pavements	Bases and sub-bases	≤ 6%	[109]
EOAC Student Workbook	General	≤ 6%	[110]
Portland Cement Association (PCA)	Road construction	≤ 7%	[111]
Alaska Soil Stabilization Design Guide	Road construction	≤ 7%	[112]
Highway Research Record	Subgrade	≤ 7%	[113]
Manual on stabilized soil construction for housing	Soil Blocks in Permanent Buildings	≤ 5%	[114]
	Soil Blocks in Rural Buildings	≤ 10%	
Indian Roads Congress (IRC)	Base layer	≤ 14%	[115]
Indian Standard (IS)	Road construction	≤ 14%	[116]

2.4 Environmental Assessment of Ground Improvement Techniques

In an ever-growing population, both waste production and construction activities show a continuous increase. Additionally, global warming, waste management, and energy consumption are considered major challenges facing the world [117,118]. Therefore, sustainable development has become a key issue in several sectors, including the construction sector. Geotechnical engineering, which is a main step in the construction industry, that involves a considerable change in soil characteristics, and the earth's surface is one of the main components of construction projects, thus consuming a considerable amount of energy and could result in serious environmental damage [119]. Nevertheless, limited studies have considered the environmental impact of geotechnical work in construction projects. Due to the lack of data, sustainable evaluation of various geotechnical engineering projects have not been investigated[119–121].

Geotechnical engineering activities could have long-term damage to the environment, which includes but is not limited to global warming, ozone depletion, water and land use, and acidification. Information on such impacts is crucial for decision-makers [122]. As mentioned earlier, one of the key contributors to climate change is cement production as it accounts for around 1.5% of the carbon dioxide produced by humans. Therefore, cement substitution with carbon-efficient materials in soil stabilization as an alternative for shallow foundation and paving purposes has been the focus of several studies [123]. For instance, the use of nonhazardous agricultural waste like rice husk ash [124] to reduce cement consumption in soil stabilization or the use of other wastes, as discussed earlier, to replace high energy consumption binders (cement and lime).

Geotechnical engineering applications, including soil stabilization, are responsible for a significant amount of energy consumption and are resources intensive, hence they have a substantial environmental impact [125]. Additionally, significant changes in landform and the usage of manufactured materials including cement are involved in those applications. Thus, quantifying the potential environmental

impacts of different geotechnical processes and materials alternatives is required to create guidelines to realize their technical goals in the light of sustainable development [125–127].

Life Cycle Assessment (LCA) is a method used to provide a comprehensive evaluation of the potential environmental impact throughout the product's life. Commonly ISO 14040:2006 and 14044:2006 standards are followed in LCA studies. LCA is commonly used in environmentally responsible decision making as it facilitates the comparisons between different materials and processes [122]. However, a lack of guidelines, benchmarks and studies in the geotechnical engineering field is reported in the several studies [126,128,129].

One of the limited studies on assessing the environmental impact of soil stabilization evaluated the emissions flow of five different ground improvement methods, which are considered to be applied in the redevelopment project in Treasure Island, California [125]. Similarly, in Shillaber et al. [130], three alternatives for ground improvement in a levee section in New Orleans have been compared. Other geotechnical systems' environmental impact including retaining walls have been evaluated in the literature. The impact of retaining wall types of commercial buildings in London has been analyzed by Chau et al. [131]. Furthermore, a sustainability and performance comparison of conventional retaining walls made by reinforced concrete and bioengineered slopes has been conducted by Storesund et al. [132] in California. The study results showed a significant reduction in the environmental impact when bioengineered slopes are used. Another study has been conducted to determine an environmental impact baseline for mechanically stabilized earth walls as a sustainable alternative to conventional retaining walls [133]. An additional case study has been conducted in China to evaluate the greenhouse emissions of the construction steps of residential buildings [134].

Moreover, the environmental impact of different tire recovery scenarios of several end-of-life materials has been evaluated in many studies. A case in this point is the study done by Bressi et al. [135] where the environmental impact of using reclaimed

asphalt and tire rubber in railway sub ballast mixture were investigated. The results suggest that the small percentage of the added rubber doesn't justify its use as it affects the properties of the final product. An additional step, that has a negative impact on the environment, is needed to create the required rubber. On the other hand, the use of reclaimed asphalt led to a significant decrease in all of the environmental impact categories. In another research, the use of marble dust in cement production as alternative for the limestone has been investigated [136]. It has been found that this replacement noticeably decreases the environmental impact of the cement life cycle. Similarly the performance and the socio environmental impact of the conventional pavement material have been compared with two different ecofriendly alternatives materials namely fly ash-carbide lime and fly ash-carbide lime salt [137]. The study concluded that fly ash-carbide lime pavement has the least damaging environmental impact compared with the other two options. Likewise, another paper in Italy has compared the life cycle of using crumb rubber from used tyres in roads' wearing course, and thermal energy recovery of the crumb rubber. The results showed that the implementing used tyers in civil work has a greater environmental benefits oppose to incinerate the tyers for energy recovery [138]. A similar conclusion has been driven in [139], in other words, the study results indicated that used tires material use and recycling have more potential for environmental impact reduction.

Nevertheless, LCA studies of soil stabilization using different additives are very limited. The life cycle assessment of different ratios of lime and clay for soil enforcement has been studied by Da Rocha et al. [119]. The results showed lower environmental impact in high density dosage and low binder. Additionally, a significant relation between the binder content and the environmental impact has been established by the authors.

CHAPTER 3

EXPERIMENTAL PROGRAM AND METHODOLOGY

In this chapter, a description of the utilized material properties acquired by several experimental tests is presented. Then, the experimental methods from samples' preparation to testing, data gathering, and analysis are explained. Moreover, the methodology adopted for the environmental assessment of the soil stabilization method proposed by this study is explained.

3.1 Materials

3.1.1 Clay

Disturbed samples were obtained with the help of an excavator from the dig up of a basement, at a depth of around 3 m, situated in the Iskele District, Long Beach region of Cyprus, at grid reference 33°54'14.94"E, 35°15'47.38"N.

The land unit at the examined location is Holocene Aged Alluviums with rock sand-soil and sediment content, showing a wide distribution in the region. Visual assessments revealed that it has an organic matter substance. The units were shaped during the Quaternary-Holocene time because of the sedimentation of the material from Beşparmak mountain to the basin by rivers. The bedrock on the basin floor is the Pliocene Marl, which belongs to the Nicosia Formation. Therefore, the inspected and used material are Holocene aged alluvial deposits comprising of silt and clay content [140].

Atterberg limits (ASTM D4318-17e1) [141], sieve analysis (ASTM D6913-17)[142], and specific gravity (ASTM D854-14) [143] tests were performed to evaluate the basic characteristics of studied soil. Table 3.1 presents the physical

characteristics of the clay. As per information found in Table 3.1, the clay utilized in this examination is classified as inorganic clay with low to medium plasticity (CL) (ASTM D2487 - 17e1) [141]. Moreover, the grain size distribution of clay is shown in Figure 3.1. This is a well-graded fine soil with a D_{50} particle diameter of 0.005 mm, and its specific gravity is 2.66.

Table 3.1. Physical properties of alluvium clay and tire rubber powder (TRP).

Properties	**Clay**	**Tire Rubber Powder**
Liquid limit (%)	46	-
Plastic limit (%)	20	-
Plasticity index (%)	26	-
Specific gravity	2.66	1.13
Fine gravel (4.75 mm < diameter < 20 mm) (%)	-	-
Coarse sand (2.00 mm < diameter < 4.75 mm) (%)	-	-
Medium sand (0.425 < diameter < 2.00 mm) (%)	-	32
Fine sand (0.075 mm < diameter < 0.425 mm) (%)	6	68
Silt (0.002 mm < diameter < 0.075 mm) (%)	54	-
Clay (diameter < 0.002 mm) (%)	40	-
D_{50} particle diameter (mm)	0.005	0.3
USCS class	CL	-

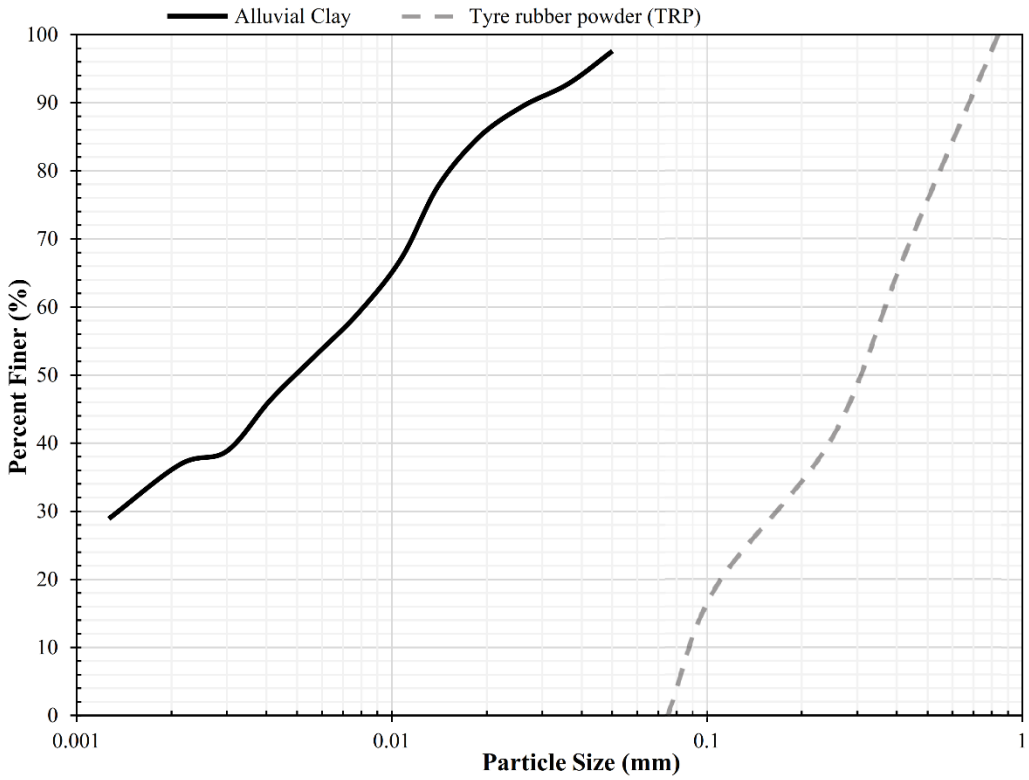

Figure 3.1. The grain size distribution (%) of studied clay and tire rubber powder.

The chemical analysis of the alluvium clay can be found in Table 3.2, supported by x-ray fluorescence spectrometry, which shows that clay is extremely rich in silica (36 %), calcium (17.3 %), and alumina (11.7 %).

Table 3.2. Chemical analysis of both Clay and Cement.

Oxides (%)	Cement (Type I)	Clay
CaO	63.6	17.3
SiO2	21.7	36
AL2O3	4.8	11.7
Fe2O3	3.9	6.67
SO3	1.4	1.13
MgO	0.3	6.38
K2O	0.3	1.81
LOI	2.1	16.4
Others	1.9	2.61

3.1.2 Waste Tire Rubber

The waste rubber tire employed in this study was shredded into two types: i) Tire rubber powder (TRP) (with grain sizes varies between 0.84 to 0.1 mm, Figure 3.1) and ii) Tire rubber fiber (TRF) (with lengths ranging from 5 to 20 mm, Figure 3.2). The shredded tires were collected from a local recycling plant in Nicosia, Cyprus. Before using it in the mixtures, it was washed to remove any dust and impurities covering the surface and air-dried to eliminate the moisture. The specific gravity of tire rubber powder was found, using water pycnometer test (ASTM D854-14) [143], as 1.13. Moreover, the chemical composition of the tire was determined through energy-dispersive X-ray spectroscopy. The primary chemical element forming the tire is the carbon with 88.1% (embodied in a form of natural rubber hydrocarbon composition and carbon black filler) while oxygen (8·6%), zinc (1·8%), sulfur (1·1%), silicon (0·3%), magnesium (0.11%) and aluminum (0.05%).

Figure 3.2. The utilized shredded waste rubber tire (TRP) and (TRF).

3.1.3 Cement

The cement utilized in this study was conventional Portland cement Class I, as determined by the standard ASTM C150/C150M-20 [144]. The specific gravity of

this cement was 3.15, with a Blaine fineness of 305 m^2/kg. Its loss on ignition was 2.1. Table 3.2 shows the percentages of various chemical compounds of this cement.

Ordinary tap water at room temperature was used in this study.

3.2 Methods

3.2.1 Molding and Curing Specimens

A total of 480 specimens were prepared to study the effect of tire rubber as a cement replacement material in this cemented clay. The maximum dry density and the clay's optimum moisture content were determined as 1810 kg/m^3, and 17.35%, following the standard compaction test (ASTM D698 - 12e2) [145]. With the inclusion of cement, the maximum dry density slightly decreases where the optimum moisture content marginally increases. However, adding the tire rubber to the blend slightly decreases both maximum dry density and optimum moisture content. The specimens were compacted inside a cylindrical split mold with a height of 100mm and 50mm diameter (Figure 3.3) at two different and preselected dry densities (1800 kg/m^3 and 1600 kg/m^3). Two different dry densities were used to highlight the effect of compaction on these binders under full degree of saturation condition. After determining the dry mass of clay soil (M_S) based on the predefined dry density (ρ_d), the proportion of cement content (M_c) was measured as a percentage of the dry mass of soil where the tire rubber ($M_{TRP\ or\ TRF}$) was determined as a partial replacement of the mass of cement content. The minimum cement content was determined as 7% where below disaggregation of specimens occurs submerged in water before testing. Additionally, It is stated in USACE [106] that, initial estimated cement content for stabilization of CL type soils is 9 % dry weight of soil.

The dry components of the blend were mixed until homogeneity and the specified amount of water was gradually added while mixing until a uniform paste was attained. The mixture was statically compacted inside the mold in three layers to the

desired density following the method proposed by Ladd [146]. Altogether, not to form a weak surface, the top surface of each layer was slightly scarified. After the sample was shaped, it was taken out from the mold, and the mass and dimensions were measured (Figure 3.4). All the samples were cured inside a humidity chamber with a relative humidity of about 95% at 24° ± 2°C following ASTM C 511-19 [147]. When performing UCS, ultrasonic pulse velocity (UPV) and durability for the samples, the maximum errors were considered: for sample dimensions (diameter ±0.5 mm, and height ±1 mm), molding dry unit weight (γ_d) of ±1%, and water content (ω) of ±0.5% [148,149].

Figure 3.3. Tire-Cement stabilized lightly compacted clay specimens before curing.

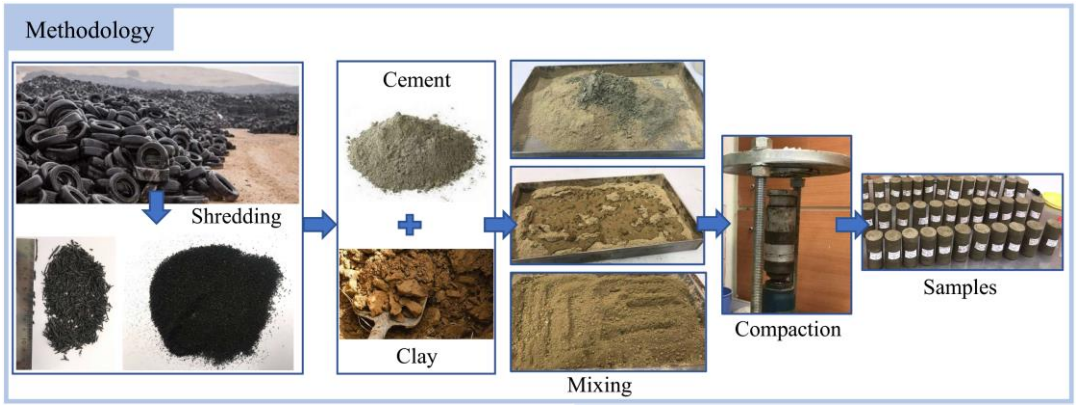

Figure 3.4. Schematic diagram of sample preparation.

According to Consoli *et al*. [150], porosity (η) is a function of the dry density (ρ_d) and solid mass of the blend [i.e., soil mass (M_S), cement mass (M_c) and tire rubber mass ($M_{TRP\ or\ TRF}$)], taking into consideration the specific gravity of each component [i.e., soil (Gs_S), cement (Gs_c), tire rubber ($Gs_{TRF\ or\ TRP}$)]. Therefore, Eq. (1) a modified form of the one proposed by Ekinci *et al.* [151], was utilized to determine porosity(η).

$$\eta = 100 - 100[\left(\frac{\rho_d}{total\ mass\ of\ solid}\right)\left(\frac{M_S}{Gs_S} + \frac{M_c}{Gs_c} + \frac{M_{TRP\ or\ TRF}}{Gs_{TRP\ or\ TRF}}\right)] \quad (1)$$

The cement content highly controls the mechanical properties of the cement-treated soils. The porosity/cement index (η/C_{iv}), proposed by Consoli *et al*. [67] to describe the behavior soils treated with binders, was later modified by Ekinci *et al*. [73] to cover the effect of multiple additives (TRP or TRF in this case). X_{iv} is the porosity/binders index that considers the impact of cement and tire rubber additives on the treated soils' strength, stiffness, and durability properties, and it is calculated using Eq.(2):

$$X_{iv} = \frac{V_C + V_{TRP\ or\ TRF}}{V}, \quad (2)$$

where V_C , V_{TRF} , and V are the volumes of cement, tire rubber powder (TRP), or fiber (TRF) and the total volume of the specimen, respectively.

Tables (Table 3.3, Table 3.4, Table 3.5) show the blends' proportions, the curing periods, as well as the tests conducted for each mix's specimens. Consoli *et al*. [67] suggested modifying the porosity/cement index exponentially to give a better assessment of the strength of granular soils treated with cement. In this study, X_{iv} is modified by an exponent of 0.32, found to be the best fit for all the mixes; such exponent also has been adopted in similar studies using different soil types and various binders [70,73,81,152]. The range of η/X_{iv}^{exp} or η/C_{iv}^{exp} found to be between 20 – 40 % for copper slag–hydrated lime–Portland cement stabilized marine-deposited clay [73] and 20 – 45 % for fiber-reinforced cemented soils [77].

Nevertheless, in this study, the porosity/binder index (η/X_{iv}) was found to better represent the ALM results without any exponent.

Table 3.3. Details of molding, curing, and normalization parameters for strength and stiffness of TRP blends.

Soil Type	Cement content (%)	TRP (%)	Molding dry density (kg/m^3)	Curing Period (Days)	Test Type	Normalization Index (∇)	q_u for normalization (kPa)	G_0 for normalization (MPa)	E for normalization (MPa)
Clay	7, 10, and 13	0	1600 and 1800	7	UCS, G_0, SEM, XRF, XRD,	$\eta/(X_{iv})^{0.32}$ =25	2380.33	4524.16	299.89
				28			3988.55	5551.43	513.31
				60			4521.74	5986.27	560.42
	7, 10, and 13	2.5	1600 and 1800	7	UCS, G_0, SEM, XRF, XRD,	$\eta/(X_{iv})^{0.32}$ =25	2382.88	4762.19	288.81
				28			4723.65	5986.35	442.65
				60			4207.31	6498.51	438.93
	7, 10, and 13	5	1600 and 1800	7	UCS, G_0, SEM, XRF, XRD	$\eta/(X_{iv})^{0.32}$ =25	2316.94	4555.66	276.78
				28			4430.35	5399.84	420.81
				60			4054.44	6149.15	526.01
	7, 10, and 13	10	1600 and 1800	7	UCS, G_0, SEM, XRF, XRD	$\eta/(X_{iv})^{0.32}$ =25	2202.80	4339.70	258.41
				18			4266.73	5398.10	419.08
				60			3468.95	5862.15	401.60
	7, 10, and 13	20	1600 and 1800	7	UCS, G_0, SEM, XRF, XRD	$\eta/(X_{iv})^{0.32}$ =25	1742.26	3749.03	184.36
				28			2951.10	4154.40	294.23
				60			2764.03	4531.68	316.73

Table 3.4. Details of molding, curing, and normalization parameters for strength and stiffness of TRF blends.

Soil Type	Cement content (%)	TRF (%)	Molding dry density (kg/m^3)	Curing Period (Days)	Test Type	Normalization Index (∇)	q_u for normalization (kPa)	G_0 for normalization (MPa)	E for normalization (MPa)
Clay	7, 10, and 13	0	1600 and 1800	7	UCS, G_0, and SEM	$\eta/(X_{iv})^{0.32}$= 25	2380.33	4524.16	312.90
				28			3988.55	5551.43	510.01
				60			4542.32	6030.50	591.12
	7, 10, and 13	2.5	1600 and 1800	7	UCS, G_0, and SEM	$\eta/(X_{iv})^{0.32}$= 25	2984.58	4716.09	302.67
				28			4702.49	5830.56	465.04
				60			5242.88	6509.94	529.92
	7, 10, and 13	5	1600 and 1800	7	UCS, G_0, and SEM	$\eta/(X_{iv})^{0.32}$= 25	2726.23	4601.76	269.39
				28			4222.97	5839.10	433.33
				60			4821.76	6415.76	491.89
	7, 10, and 13	10	1600 and 1800	7	UCS, G_0, and SEM	$\eta/(X_{iv})^{0.32}$= 25	2787.40	4473.83	281.22
				18			3711.04	5506.36	405.81
				60			4116.92	6096.10	466.70
	7, 10, and 13	20	1600 and 1800	7	UCS, G_0, and SEM	$\eta/(X_{iv})^{0.32}$= 25	2328.02	4169.00	240.83
				28			3424.05	5075.68	330.93
				60			3761.03	5590.22	407.87

Table 3.5. Details of molding, curing, and normalization parameters for ALM of TRF and TRP blends.

Soil Type	Cement content (%)	Tire rubber content (%)	Molding dry density (kg/m^3)	Tire Rubber Type	Curing Period (Days)	Test Type	Normalization Index (∇)	ALM for normalization (%)
Clay	7, 10, and 13	0%	1600 and 1800	NA	28	W/D Cycles	NA	NA
				NA	60			NA
	7, 10, and 13	2.5%	1600 and 1800	TRP	28	W/D Cycles	$\eta/(X_{iv})=10$	2.200
				TRP	60			1.462
				TRF	28		$\eta/(X_{iv})=10$	1.090
				TRF	60			2.157
	7, 10, and 13	5%	1600 and 1800	TRP	28	W/D Cycles	$\eta/(X_{iv})=10$	2.644
				TRP	60			1.826
				TRF	28		$\eta/(X_{iv})=10$	1.522
				TRF	60			2.665
	7, 10, and 13	10%	1600 and 1800	TRP	28	W/D Cycles	$\eta/(X_{iv})=10$	2.880
				TRP	60			2.058
				TRF	28		$\eta/(X_{iv})=10$	1.735
				TRF	60			3.227
	7, 10, and 13	20%	1600 and 1800	TRP	28	W/D Cycles	$\eta/(X_{iv})=10$	3.349
				TRP	60			2.560
				TRF	28		$\eta/(X_{iv})=10$	2.203
				TRF	60			3.935

Moreover, the strength, stiffness and durability outcomes have been normalized following a model developed by Consoli *et al.* [71], inspired by Diambra *et al.* [153]. The researchers utilized a method of dividing the formed powered equations by a specific value of strength obtained at a particular value of η/X_{iv}^{exp}. This approach has proven effective in evaluating the mechanical properties of cement-treated soils cured at various ages. Tables (Table 3.3, Table 3.4, Table 3.5) show the determined values of q_u, G_0, and E at $\eta/X_{iv}^{0.32} = \nabla = 25$ applied to normalize all the different blends where $\nabla = 10$ was applied for ALM results. The ∇ values were explicitly selected for normalization because it divides the blends' range of ∇ values [154].

3.2.2 Unconfined Compressive Strength

To evaluate the influence of tire rubber partial cement replacement on the compressive strength of cement-treated soil blends, the unconfined compressive

strength (UCS) test was performed following the ASTM D1633-17 standard [67]. Three samples of each mix were tested for this purpose, where all the samples had been soaked in water for 24 hours to ensure full saturation prior to testing. The UCS test was carried out using a 23 kN PC-controlled load frame (Figure 3.5(a)) with an accuracy of 5 N and a displacement transducer to measure the axial deformation up to 0.001 mm significant digit. The compaction rate was set as 1% axial strain/ minute in accordance with ASTM D1633-17 [155]. The mass and dimensions of the specimens were collected again, before performing the UCS test.

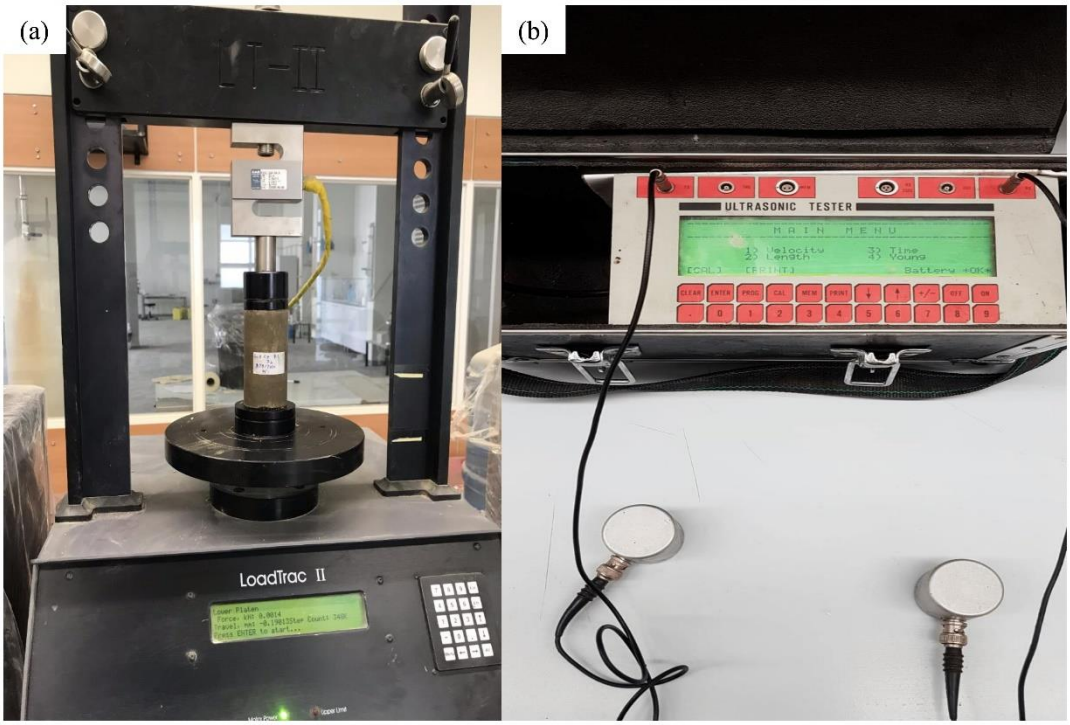

Figure 3.5. Tests' setups; (a) load Frame for UCS and (b) Pundit for Ultrasonic Pulse Velocity (UPV).

After adjusting the sample in the loading frame and setting the displacement indicator at zero reading, the loading phase initiated and proceeded until the sample's failure. The whole process was repeated for the other specimens. The load and displacement data were collected and analyzed to assess the compressive strength at failure and the Young modulus of elastic (E) of each sample, determined by Eq. (3) at the linear portion of the vertical stress-strain diagram (Figure 3.6).

$$E = \frac{\Delta\sigma}{\Delta\varepsilon}, \tag{3}$$

Where, $\Delta\sigma$ is the change in the vertical stress, and $\Delta\varepsilon$ is the change in the vertical displacement.

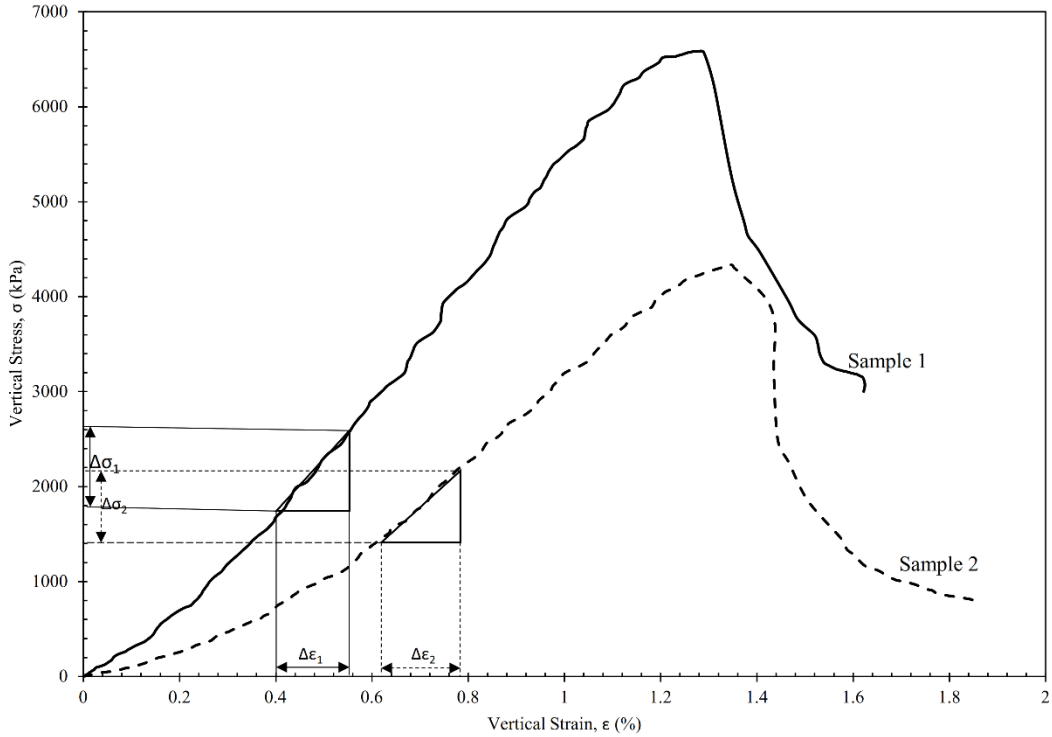

Figure 3.6. Typical stress strain diagrams showing the determination of elastic modulus.

3.2.3 Pulse Velocity Test (Pundit)

UPV test was performed according to ASTM C597-02 standard [156] to acquire the elastic properties of the clay-cement tire rubber powder blend. A Pundit device (MATEST Ultrasonic Tester Model C368) was used (Figure 3.5(b)). The apparatus is associated with two transducers, one of which sends the shear wave and the other receives it, computing the time needed to go through the sample. The two transducers are appended on the two sides of the sample by utilizing silicon grease. Adequate pressure was applied to guarantee a stable transit time, as described in the ASTM

C597-02 standard [156]. In this setting, the device can estimate the shear wave speed (V_s), and this way, the maximum shear modulus (G_0) can be determined using the apparent density of the sample (ρ) as indicated by Eq. (4).

$$G_0 = \rho * V_s^2, \quad (4)$$

where G_0 is the maximum shear modulus, and ρ is the density of the specimen.

Moreover, during durability studies, the test was conducted on the samples at the dry condition at cycles 1, 6, and 12 in order not to disturb the samples. However, before the first cycle (i.e., at zero cycles), the pundit test was conducted on the samples at saturation condition.

3.2.4 Durability Test (Wet/Dry Cycles)

The blends' durability performance was evaluated by carrying out 12 wet/dry cycles on the samples following the ASTM D559 [157] standard. After curing, the samples were soaked in water for 5 h; then, they were dried in an oven for 42 h at 74°C ± 2°C. Subsequently, the sides of the samples, including the top and base, were brushed with a pressure equivalent to 15 N. The pressure was measured by applying brushing stroke to a scale until 13 N force was registered as specified in ASTM D559 [157] standard. The masses after each wetting-drying-brushing cycle were recorded to calculate the mass loss of each cycle and eventually the accumulated loss of mass (ALM) after the twelfth cycle.

3.2.5 Microstructural Tests

Microstructural investigations were performed to differentiate the progress of the pozzolanic reaction, cement hydration, just as the tire rubber powder substitution effect. Scanning Electron Microscopy (SEM), X-ray diffraction analysis (XRD), and X-ray fluorescence spectrometry (XRF) studies were performed at Middle East Technical University, Central Laboratories.

The QUANTA 400F Field Emission SEM testing system was used for SEM analysis, with a resolution of 1.2 nm, alongside an Energy Dispersive System (EDS). Samples broken down to around 10 mm were stuck to aluminum stubs. A layer of gold/platinum was utilized to reduce charging under the electron pillar. The SEM pictures were taken at various degrees of amplification of 1K to 10K.

The crystalline phase composition of the tire rubber powder was determined with the X-ray powder diffraction (XRD) analysis utilizing a Bruker AXS D8 Advance Model X-ray Diffractometer joined with a Cu-Kα X-ray source and a super speed PSD: Vantec-1 locator. Patterns were procured by scanning at 2-theta range 2–90° with a scan speed of 2° per min and at steps of 0.02°. The voltage utilized in the XRD examination was set at 40 kV and 30 mA, respectively. The peaks were identified using Crystal Impact Match Software, Version 3.11.1, with PDF-2 database from International Center for Diffraction Data (ICDD). A Rigaku ZSX Primus II X-ray fluorescence spectrometer (XRF) was used to identify the chemical composition of various blends to determine the oxide fractions.

3.2.6 Life Cycle Assessment (LCA) Method

The life cycle assessment was performed on OpenLCA software v1.10.3 [158] following the guidelines and principles outlined by ISO 14040 and 14044 [159,160] involving four phases: i) goal and scope definition, ii) life cycle inventory, iii) impact assessment and iv) result interpretation.

3.2.6.1 Goal and scope definition

This study aims to evaluate the environmental impacts associated with utilizing cement and waste rubber tire (TRP, or TRF) in soft soil stabilization. The functional unit used in the LCA analysis is 1 m^3 of waste-cement-clay blends.

The system boundaries of this study are illustrated in Figure 3.7, which include the processes and activities related to material production, transportation, and site application of the mixtures. The maintenance and disposal are not considered in this study due to the extended service lifespan of such projects. Nonetheless, this technique is regarded as a disposal method for the waste tire. Therefore, the life cycle method is cradle-to-gate.

The process of producing crumb rubber tires from the end-of-life tires starts from the collection of the ELTs, transporting them to the shredding factory where three different materials are being produced from the shredding and sieving processes of ELTs (i.e., crumb rubber, steel wires, and textile fiber). The steel and textile fiber components of the ELTs are being regarded as avoided materials where the primary end product is crumb tire rubber. Such product is collected, packed then transferred to be used in the blends (Figure 3.7). The production process of TRP and TRF are assumed to be similar, although there might be a slight difference when producing fiber and powder forms of the shredded tires.

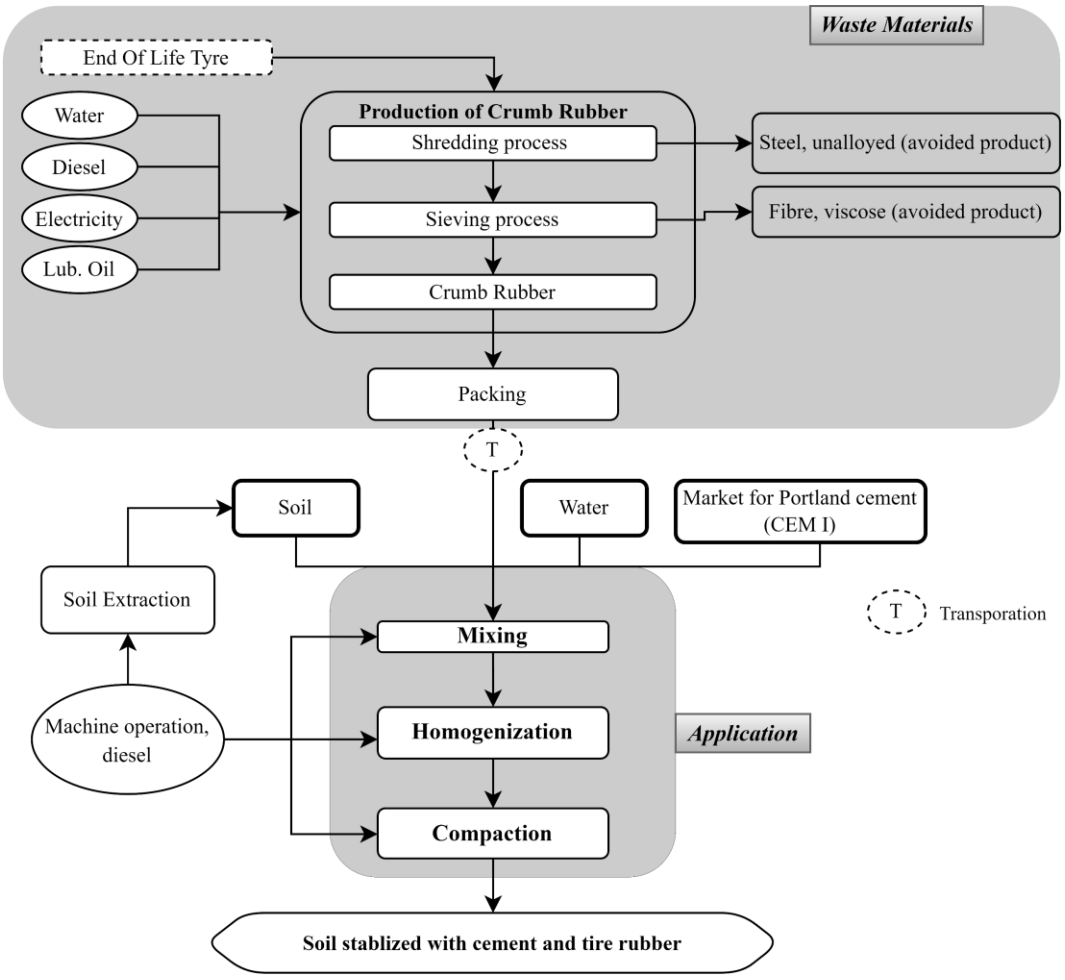

Figure 3.7. Schematic diagram of the process of stabilized soil with cement and tire rubber.

The application process starts with soil excavation and dumping the excavated soil nearby to be brought back and used in the blends. When reaching the desired depth, all the blend components (i.e., soil, cement, and clay) are dryly mixed and spread over then water is mixed with the dry component until homogeneity. Eventually, the material is compacted, creating a stabilized soil layer that can serve its engineering purpose.

3.2.6.2 Life cycle inventory

The data used in the LCA analysis were obtained from the Ecoinvent v3.7 database [161] and several sources from the literature ([135,138]). “Allocation at the point of substitution (APOS)” is the system model from the Ecoinvent database used in this study. In this approach, waste material producers and subsequent users share the environmental burden; thus, treating such material considers the burden as benefit.

The inventory data of the production of 1 ton of tire rubber is tabulated in Table 3.6. The data were obtained from ([135,138]). The primary input of the process is the end-of-life tires, and the main output is the crumb rubber. The process inventory also includes the production of packing bags for TRP/TRF products.

Table 3.6. Life cycle inventory of the production of 1 ton of crumb rubber tire.

Input Flow	**Amount**	**Unit**	**Comment**
used tyre	1000	kg	
diesel, burned in building machine	111	MJ	
electricity, medium voltage	384	kW/h	
lubricating oil	0.04	kg	
tap water	220	kg	
packaging film, low density polyethylene	0.185	kg	Production of packing bag
polymer foaming	0.185	kg	
polypropylene, granulate	1.667	kg	
hot rolling, steel	0.29	kg	Steel bade production for shredding
sheet rolling, steel	0.29	kg	
steel, unalloyed	0.29	kg	
Output Flow	**Amount**	**Unit**	
Crumb Rubber after shredding	695	kg	
steel, unalloyed (avoided product)	199	kg	
fibre, viscose (avoided product)	106	kg	

The quantities of each material were calculated based on their percentages and the density of the mixture, as shown in supplementary Table D.1. Inventory data for the

application processes were considered by the time needed for each machinery to produce stabilized soil from the blends (Table 3.7). The environmental impacts of machinery were considered through each machinery's diesel and oil consumption during the time needed to apply 1 m^3 of each combination. The quantities were obtained from [119], where they investigated a similar technique of soil stabilization.

Table 3.7. Machinery working hours of the application of 1m^3 of the blends.

Equipment	**Power (HP)**	**Time (hours/m^3)**
Soil Excavation	150	0.0105
Dumping Truck	220	0.069
Pad-foot Roller	115	0.0092
Water Spreader Truck	220	0.0039
Cement/lime spreader	115	0.0042
Motor Grader	185	0.0133
Total		0.1101

The material transportation processes in this study were assumed to follow the average global transportation distances for each material in Ecoinvent database. The words “market for” in the inventory data indicate that the average transportation distances are included in the process[162].

3.2.6.3 Impact Assessment

The method used for environmental impact analysis in this study was ReCiPe Midpoint (H). The method considers 18 environmental impacts (Table D.2). However, in this study, only five of them were considered in the analysis (i.e., climate change - GWP100, fossil depletion - FDP, freshwater ecotoxicity - FETPinf, freshwater eutrophication - FEP, human toxicity - HTPinf, ionising radiation - IRP_HE, marine eutrophication - MEP, marine ecotoxicity - METPinf, metal depletion - MDP, natural land transformation - NLTP). The reason of selecting the specific five environmental impacts for the analysis is the significant of such impacts compared to the others, considering the activities and processes in this study. Furthermore, those selected impacts are generally considered in similar studies in the

literature thus choosing them in this study would provide comparable results to the same processes and activities in the other research.

OpenCLA was used to estimate the LCA impact quantities for all the upstream activities (i.e., from the material production to application)

CHAPTER 4

RESULTS AND DISCUSSION

In this chapter, the results of the data analysis are presented and discussed. This chapter starts by discussing the mechanical properties of the blends (i.e., strength and stiffness properties) based on the statistical analysis of variance, then by using the porosity/binder index and correlating the strength and stiffness parameters. Following that, the results of the durability performance of the blends are presented and discussed. Then, the microstructure findings of the mixtures were analyzed and discussed. Finally, this chapter ends with the environmental assessment through the interpretation of life assessment results.

4.1 Effect of Tire Replacement on the Mechanical Behavior

4.1.1 Statistical Analysis of the Investigated Variables

To evaluate the effect of the factors [i.e., Tire Rubber Powder (TRP) content, cement content, curing periods, and the dry density] on the strength and stiffness properties of the mix samples, the analysis of variance (ANOVA) was performed on the data for each mechanical property. Scholars such as Ahmed [163] adopted a similar statistical analysis to evaluate the strength of stabilized soils.

Table A.1 and Table A.2 present the ANOVA analysis parameters for up to three-order interactions of both sample groups (i.e., TRP and TRF, respectively). The statistical analysis of variances showed that all the main factors, two-factor and three-factor interactions are statistically significant as the corresponding p-value is less than 5% which means that it can be claimed with 95% confidence. The relative importance of each factor affecting the coefficient of determination (R^2) of the obtained model was assessed to determine the most relevant factor. The degree of

freedom (DF) indicates the number of independent variables which can be estimated by the statistical analysis whereas the mean squares is the sum of the squares over the degree of freedom. Table A.1 and Table A.2 shows the relationship between controllable factors (dry density, curing period, cement content and tire rubber content) and q_u, G_0 and E. The higher the sum of square value the higher is the deviation from the mean. Therefore, high divergency of controllable factors results in more effect on the q_u, G_0 and E. Moreover, the null hypothesis assumes that the mean of all the values in all the groups is the same. F-test is the ratio between the variation inside each group to the variation of the mean of each group. Therefore, having a higher number of F-ratio means, the variation is significant, and the null hypothesis is not applicable. For example, the dry density variable has two groups (1600 and 1800 kg/m^3), and the variation inside each group's q_u values is less than the variation in the mean between both groups which results in a high F-ratio and gives the density higher dominancy compared to the F-value of the other factors. For q_u, the most important factors were in order of dry density curing period, cement content, and TRF content. For the G_0 the affecting factors were in the order of dry density, curing period, cement content and TRP/TRF content. For the E, the affecting factors were in the order of curing period, dry density, cement content and TRP or TRF content. It can be summarized that the since the TRP or TRF addition is a replacement to cement it is least to affect the measured parameters where in return density and curing periods are highly dominant in controlling measured parameters.

Figure 4.1 shows three outputs showing variables' interaction diagrams from ANOVA. The dry density (1800 and 1600 kg/m^3), cement content (7, 10, 13%), TRP rate as a substitution for cement (2.5, 5, 10, 20%), and curing periods (7, 28, 60 days) were statistically analyzed to show the individual effect of each factor on the unconfined compressive strength (UCS), Figure 4.1(a), modulus of elasticity (E), Figure 4.1(b), and initial shear modulus (G_0), Figure 4.1(c). Nevertheless, the effect of the other factors, the strength (UCS) and stiffness (E and G_0) showed a significant increment as the prepared samples compacted to higher dry density, which can be identified with the lower porosity and higher interaction between soil particles and

cementitious material in denser samples. It can likewise be seen from Figure 4.1 that the strength and stiffness increased significantly with increasing cement amount, notwithstanding the effect of different variables, as the cement plays a primary role in improving the mechanical properties of the cemented soils.

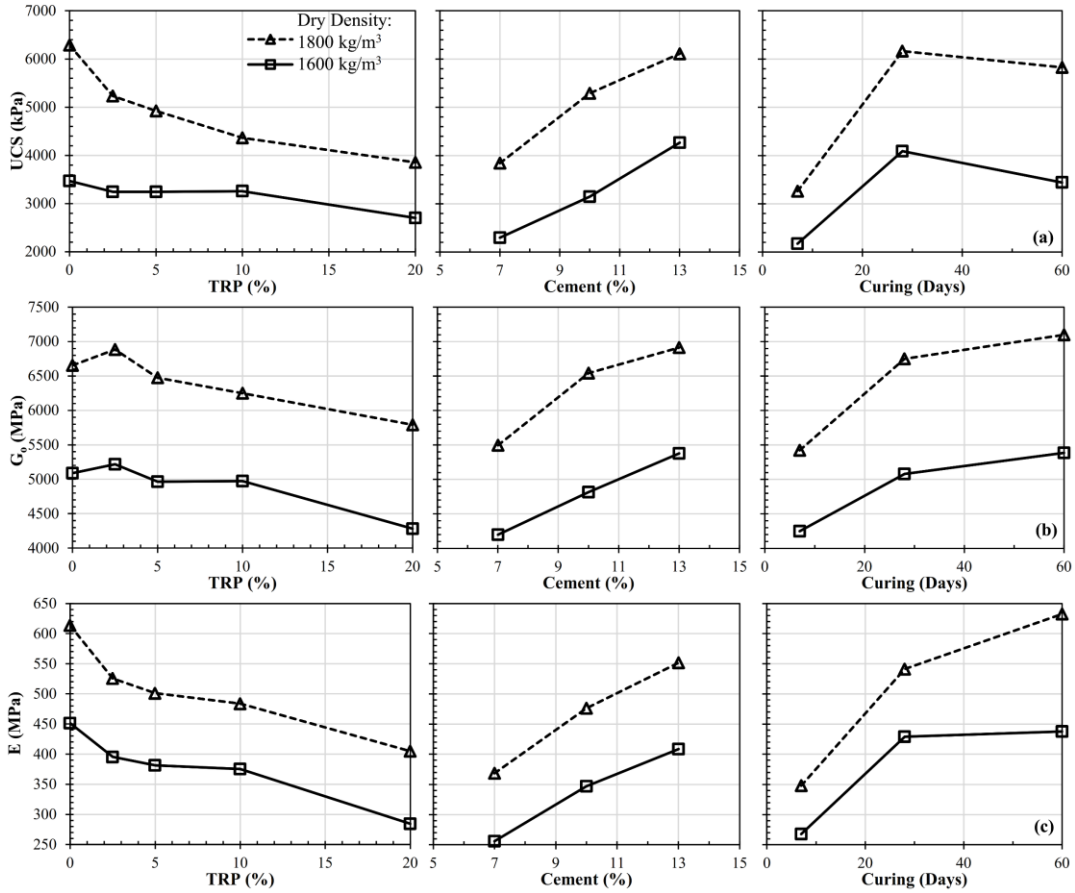

Figure 4.1. The individual effect of TRP percentage, cement content and curing days on (a) the unconfined compressive strength (UCS), (b) The shear modulus (G_o), and (c) The modulus of elasticity (E) of 1600 and 1800 kg/m^3 dry density specimens.

Figure 4.2 show the main effects plot for all the strength and stiffness tests conducted on TRF group samples herein (i.e. curing periods, cement content, tire content and combined analysis). Similar to TRP results, all graphs in Figure 4.2 show that specimens prepared at a density of 1800 kg/m^3 have the highest performance in terms of cementation, mobilization of fibers and encouraging soil-fiber interactions, given

the higher results in terms of UCS, G_0 and E values in comparison to the specimens molded at 1600 kg/m^3 density. It is also evident that the increase in curing period and cement content results in an increase in UCS, G_0 and E where one looking at the curing period (Figure 4.2(a), Figure 4.2(d) and Figure 4.2(g)) can realize that, in contrary to TRP results, an increase on all parameters is witnessed between 28 to 60 days. However, when considering the effect of cement content (Figure 4.2(b), Figure 4.2(e) and Figure 4.2(h)), there is a clear linear increase in all three parameters for the lower density samples but not for the high density samples. It can be seen from Figure 4.2(c) that, at higher density, the addition of TRF gradually reduces the compressive strength. The same can be seen for the lower density mixtures when the percentage us higher than 2.5% as in this percentage, an increase in UCS was seen with respect to the 0%. Similarly, in Figure 4.2(f), it is clear that the initial shear modulus is at peak value when mixing 2.5% of TRF for both densities of specimens and reduces afterwards. It is also monitored in Figure 4.2(i) that the addition of fiber degrades the elastic modulus with the increase of TRF content at both densities. However, at 2.5 % of TRF inclusion and 1600 kg/m^3 density, there is evidential contribution of TRF replacement on all parameters when compared to unreinforced specimens.

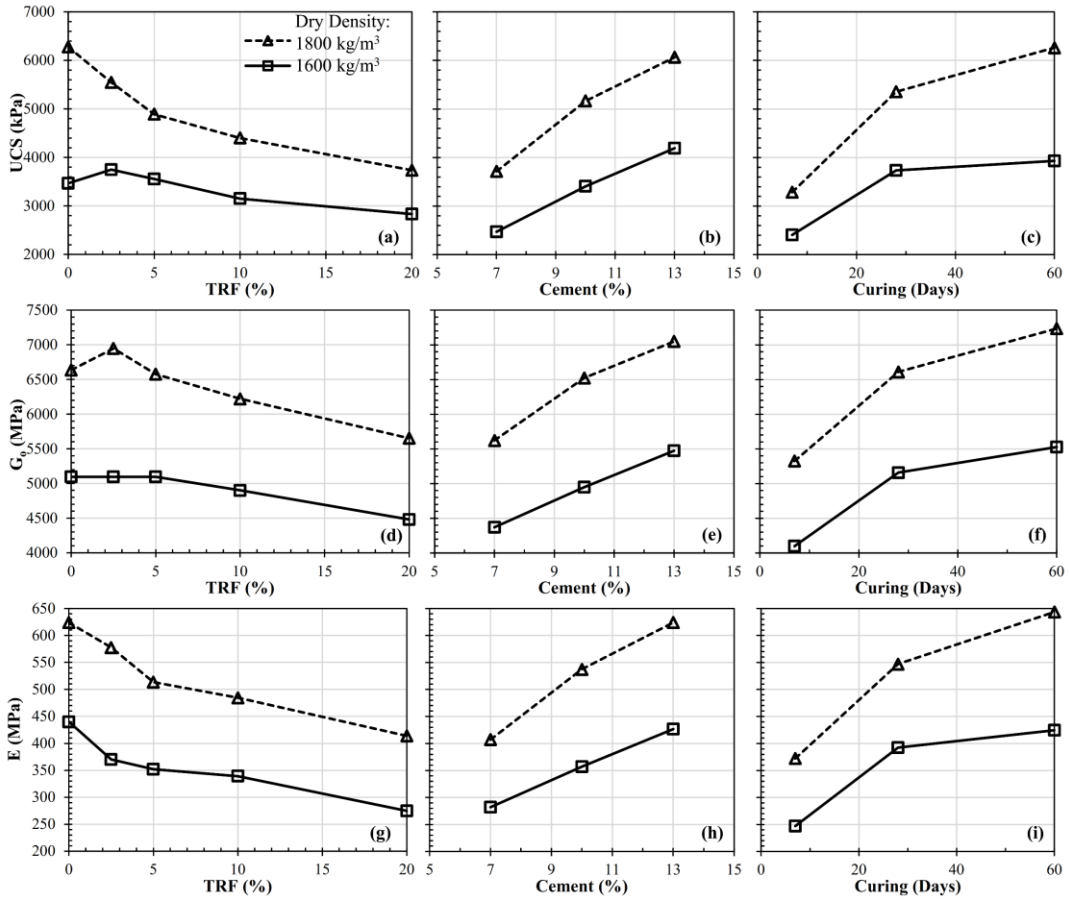

Figure 4.2. The interaction between controllable factors curing period, cement content, TRF content and density for q_u, G_0 and E.

Overall, very slight variation in the TRF and TRP results, except for the noticeable strength drop of TRP samples between 28 to 60 days of curing. Nevertheless, an increase in TRP/TRF content had little effect on UCS, G_0, and E parameters at 1600 kg/m^3 density samples up to 10% substitution when a sharp decrease was observed in further inclusion of tire content. Notably, a TRP/TRF of 20% for any addition of cement percent (7, 10, and 13%) can lead to a significant decrease in mechanical performance. This observation could have been due to the use of tire as a replacement of cement rather than additive. For instance, replacing 13 % of cement with 20% of TRP in volume decreased the actual cement amount to 10.4%. Moreover, for all 1800 kg/m^3 samples, the UCS and E decreased with an increased level of tire, aside from the G_0 of the two densities, and increased up to 2.5% cement substitution of

TRP/TRF. The elastic and shear moduli values increased with curing time as the pozzolanic reaction of the cement improved the strength and stiffness properties over time, particularly at early ages. The rate of increase was approximately 50-60 % from day 7 to day 28 of the curing period and 20-30% in the curing period of 28 and 60 days. Likewise, the UCS increased with the curing times (7 and 28 days) of the samples for all blend groups. Besides, following 60 days of curing, the cement TRP stabilized, the strength of clay encountered dropped significantly in contrast with cemented clay blends, and this level of drop increased with increasing the percentage of TRP and cement levels.

In any case, the lowest UCS can be achieved at the lowest density, lowest cement amount, shortest curing period, and highest tire substitution rate. This can be used satisfactorily to achieve the minimum UCS requirement, as stated in for rammed earth, base, and sub-base layers of roads.

4.1.2 Porosity/Binder Index Influence on the Mechanical Behavior of the Blends

Figure 4.3 and Figure 4.4 show the relationship between the UCS (q_u) and the adjusted porosity/binder ratio ($\eta/X_{iv}^{0.32}$) for every TRP, and TRF composite binder, respectively. Figure 4.3 shows the clay stabilized with 7, 10, 13% Portland cement, compacted to 1600 and 1800 kg/m^3 density, and cured for 7, 28, and 60 days. Moreover, Figure 4.3(a), (b), (c), (d), and (e) contain 0, 2.5, 5, 10, 20% substitution of cement as TRP, respectively. Similarly, the Figure 4.4(a) to (e) show the clay mixed with 7, 10, and 13% of Portland cement, compacted at 1600, and 1800 kg/m^3, cured for 7, 28, and 60 days, and a partial replacement of the cement by 0, 2.5, 5, 10, and 20% TRF (Figure 4.4(a), (b), (c), (d), and (e), respectively).

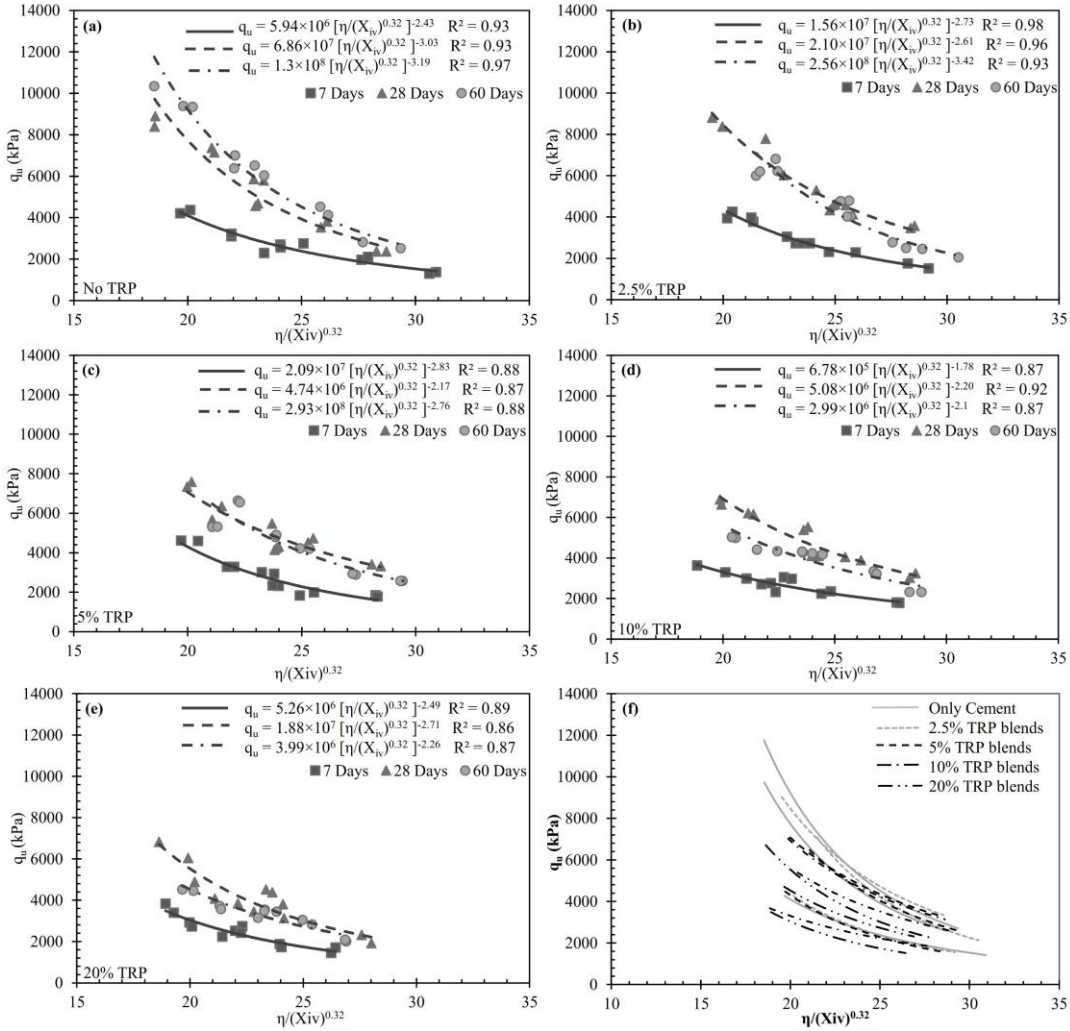

Figure 4.3. The unconfined compressive strength (q_u) and adjusted porosity/binder index correlations for all curing days and cement percentages in both dry density specimens with (a) 0% TRP, (b) 2.5% TRP, (c) 5% TRP, (d) 10% TRP, (e) 20% TRP cement replacements, and (f) All the correlations.

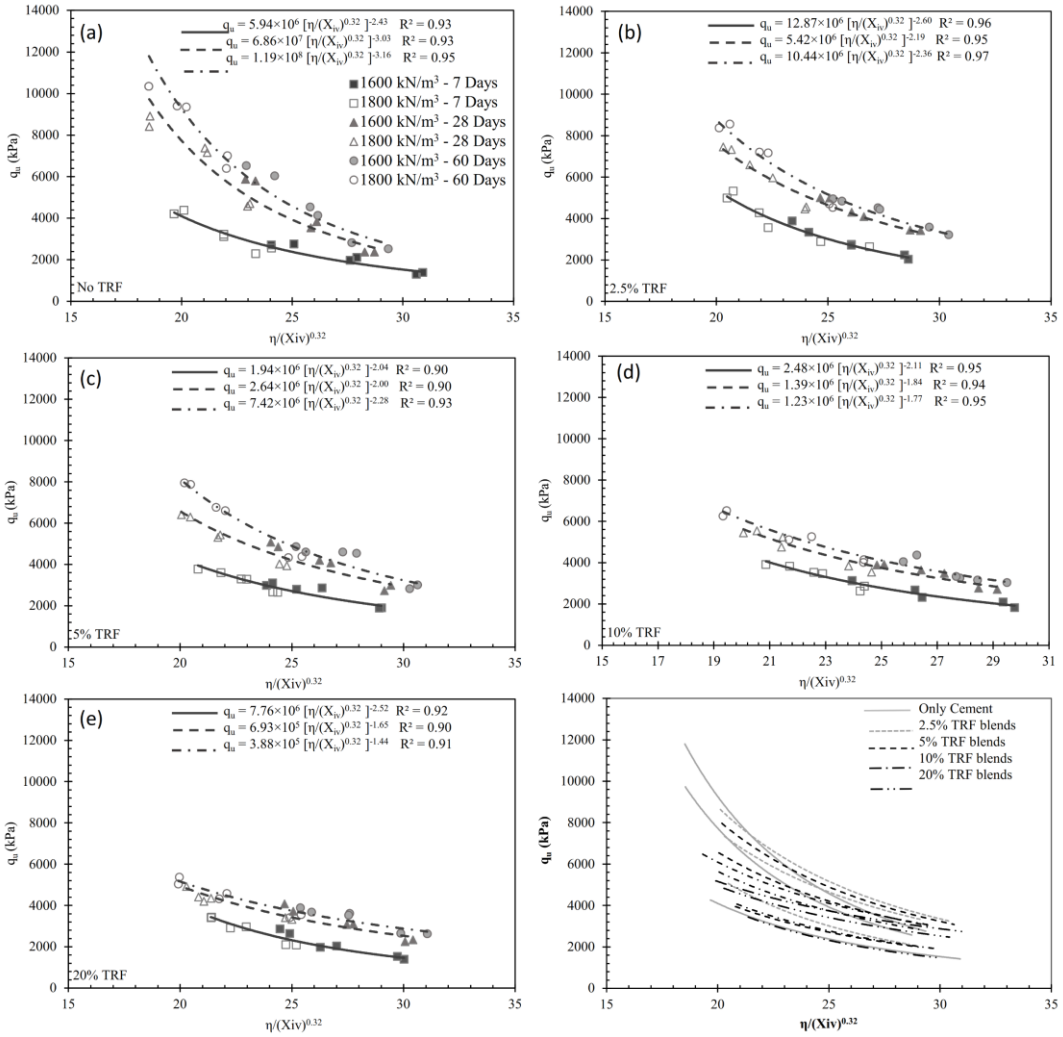

Figure 4.4. The unconfined compressive strength (q_u) and adjusted porosity/binder index ($\eta/(X_{iv})^{0.32}$) correlations for all curing days and cement percentages in both dry density specimens with (a) 0% TRF, (b) 2.5% TRF, (c) 5% TRF, (d) 10% TRF, (e) 20% TRF cement replacements, and (f) All the correlations.

Every level of TRP or TRF was fitted with a power curve that shows the effect of the curing period. A good agreement was found between q_u and $\eta/X_{iv}^{0.32}$ for all the blends. It is clear from Figure 4.3, Figure 4.4 and recent studies (Consoli *et al.* [67], Ekinci *et al.* [73], Ekinci *et al.* [151]) that increase in porosity and increase in mixture content decrease q_u in the long run. In other words, Samples compacted at 1800

kg/m^3 dry density have less porosity thus exhibit higher compressive strength than 1600 kg/m^3 because of the increase of particle contacts through compaction. In Figure 4.3(a), curing periods of 7 and 28 days affect the compressive strength, while 60 days of curing decreases q_u compared with the cement-only mix, and this decrease becomes more pronounced with increased TRP content. The increase in TRP substitution above 5% results in a significant drop in q_u due to replacing cement, a pozzolanic material, with TRP. Furthermore, Figure 4.4(f) shows that at 7 days of curing, the strength was improved by replacing cement with 2.5 to 10% TRF, which can be referred to the contribution of the fiber overcoming the influence of the cement replaced at early ages. However, at 28 and 60 day curing periods, only 2.5% and 5% TRF, at low porosity (1600 kg/m^3), showed an improvement on the strength compared to 0% TRF blends and further substitutions significantly decrease the strength of the cement-treated soils. The reduction in the pozzolanicity of the bulk sample and existence of the carbon element in tire powder weakened the composites. Alignment of all TRP regression curves in Figure 4.3(f) revealed that replacing cement with 2.5 % TRP increased the strength of higher porosity samples (1600 kg/m^3) at all curing periods compared to pure cement mix. In any case, the low porosity samples (1800 kg/m^3) replaced at 2.5% TRP appeared to yield marginally less compressive strength at all curing periods in contrast to samples with only cement. This could be because a chemical reaction accruing in pore spaces is impossible with decreased porosity (i.e., increased density). This phenomenon has been additionally supported by the microstructural analyzes performed in this work.

Figure 4.5 and Figure 4.6 presents the relationship between the initial shear modulus (G_0) and the adjusted porosity/binder index ($\eta/X_{iv}^{0.32}$) of TRP and TRF blends, respectively. Fitted power curves have a higher regression coefficient compared to UCS test results. Conversely, with the UCS results, all samples cured up to 60 days critically increased initial shear modulus. Nonetheless, the increase in shear modulus was substantially lower following 28 days compared to the period between 7 and 28 days for all blends. It can be seen in Figure 4.5(f) that samples prepared with up to 2.5% TRP replacement showed higher initial shear modulus compared to control

samples without containing tire. Consistent with the UCS results, such findings were noted in lower porosities (higher density) mixture groups. However, such a decrease in UCS was not observed in initial shear modulus measurements. In this manner, a weak bond was formed (for example, pores and unreacted particles appeared in SEM images), which is likely the result of chemical reactions rather than physical mechanisms, as in non-destructive tests, the expected increase is monitored. Moreover, Figure 4.6(f) contains all the curves together, allowing a comparison of the effect of TRF on G_0 of all the blends. It can be observed that G_o followed more or less the same behavior of the q_u results when concerned with the impact of TRF contents. The replacement of 2.5% and 5% TRF showed improvement along all the blends' porosities and at almost all the curing ages, compared to 0% TRF. However, more than 10% cement replacement of TRF, considerably decrease the initial shear modulus (G_0).

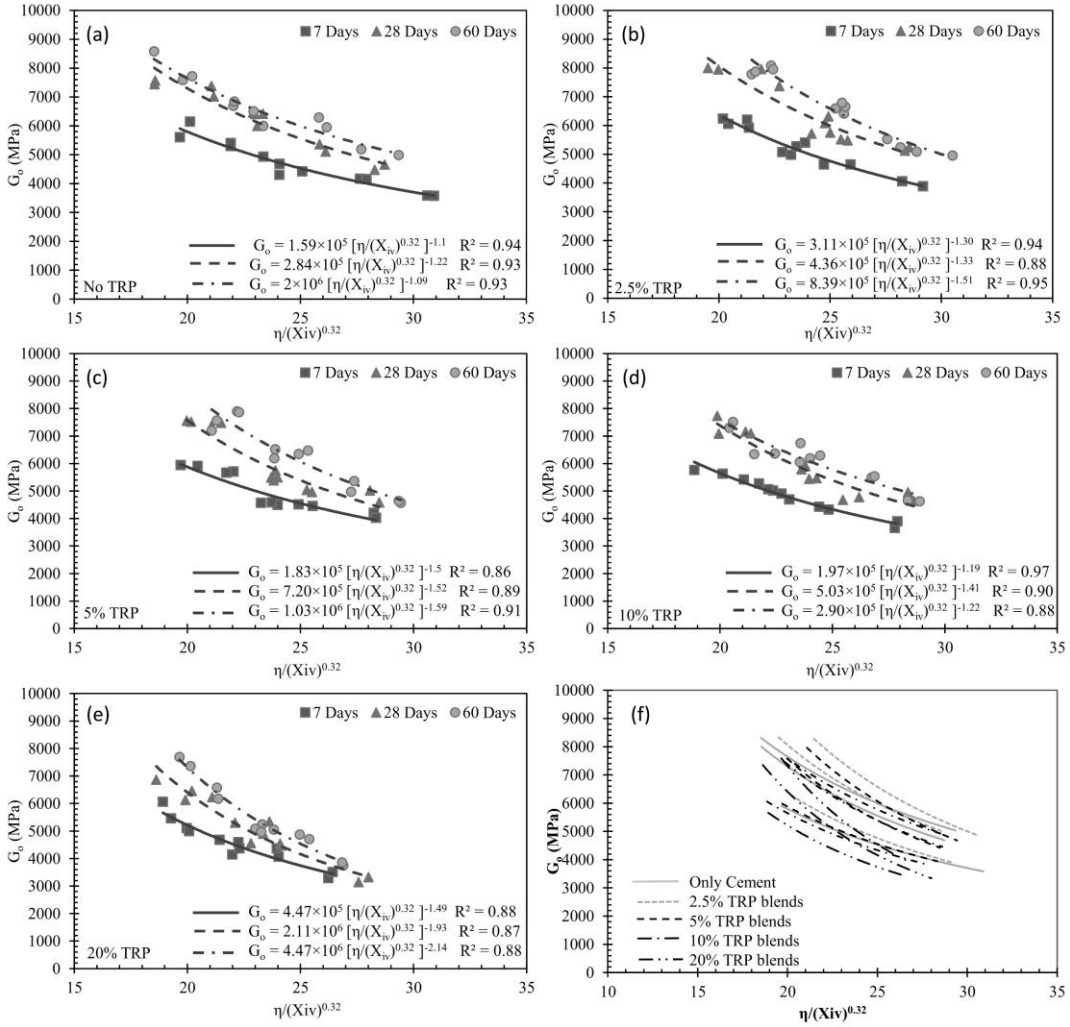

Figure 4.5. The shear modulus (G_o) and adjusted porosity/binder index correlations for all curing days and cement percentages in both dry density specimens with (a) 0% TRP, (b) 2.5% TRP, (c) 5% TRP, (d) 10% TRP, (e) 20% TRP cement replacements, and (f) All the correlations.

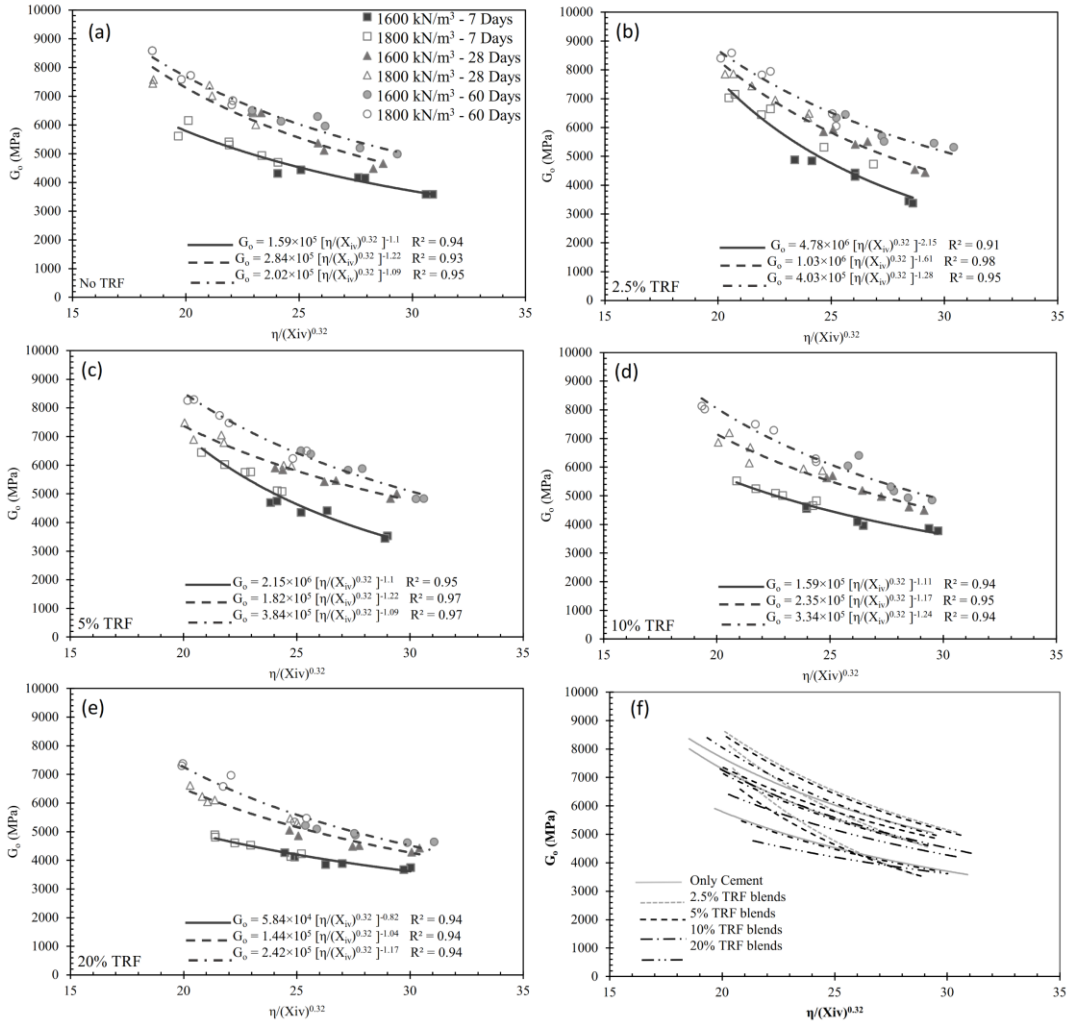

Figure 4.6. The shear modulus (G_o) and adjusted porosity/binder index ($\eta/(X_{iv})^{0.32}$) correlations for all curing days and cement percentages in both dry density specimens with (a) 0% TRF, (b) 2.5% TRF, (c) 5% TRF, (d) 10% TRF, (e) 20% TRF cement replacements, and (f) All the correlations.

The modulus of elasticity (E) of each (TRP and TRF) mix at the two densities and three different curing ages were determined from stress-strain graphs. Figure 4.7(a), (b), (c), (d), and (e) show the cement only, 2.5%, 5%, 10%, and 20% cement replacement with TRP, respectively, by curing periods. Similarly, Figure 4.8 (a), (b), (c), (d), and (e) show the cement only, 2.5%, 5%, 10%, and 20% cement replacement with TRF, respectively, by curing periods. All regression coefficients were high and varied between 0.82-0.96. The modulus of elasticity results appear to be in alignment

with the UCS and G_0 results. The elastic modulus increased with the increase in the curing period. Such observation is much clearer at 2.5% and 5% substitution levels of TRP or TRF. Above 5% TRP and cement-only blends appear to decrease the effect for the 28 to 60 days period. It can be seen in Figure 4.7 (f) and Figure 4.8(f) that substituting with 2.5% TRP or TRF yielded a sharp decrease in elasticity, as 2.5 to 10% tires less reduction of E was noticed, and a comparable sharp decrease above 10% was reported. A marginal change in the trend might be caused by the method of obtaining E when compared to q_u and G_o.

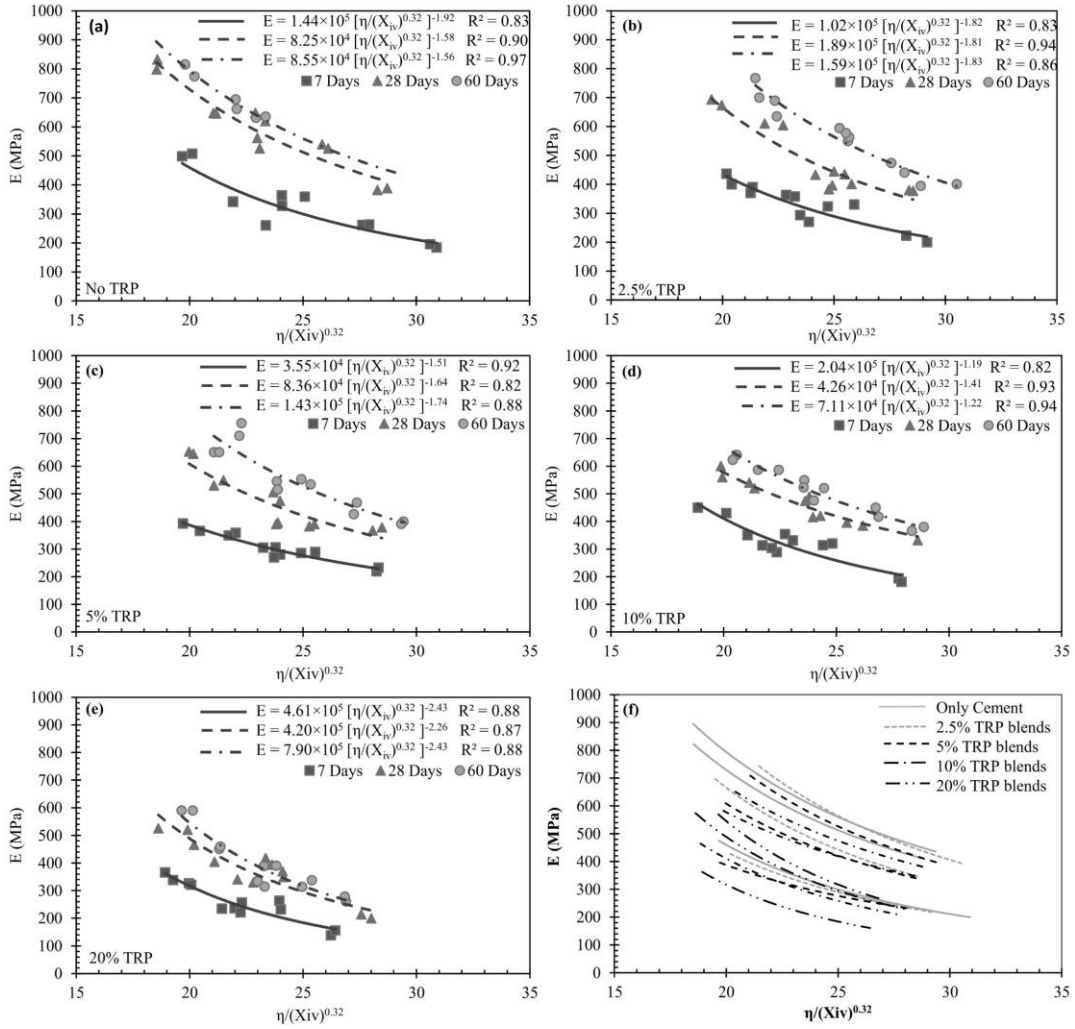

Figure 4.7. The modulus of elasticity (E) and adjusted porosity/binder index correlations for all curing days and cement percentages in both dry density

specimens with (a) 0% TRP, (b) 2.5% TRP, (c) 5% TRP, (d) 10% TRP, (e) 20% TRP cement replacements, and (f) All the correlation.

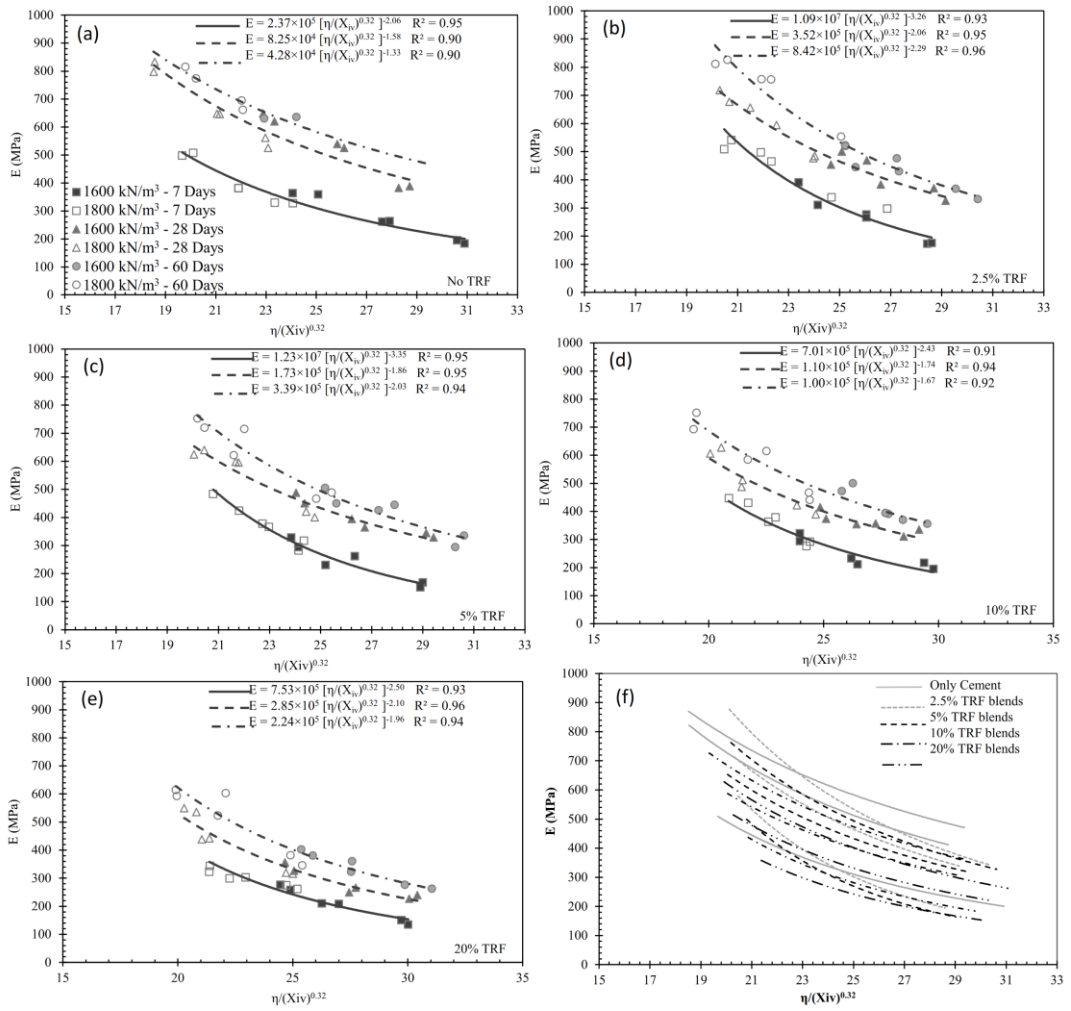

Figure 4.8. The modulus of elasticity and adjusted porosity/binder index $(\eta/(X_{iv})^{0.32})$ correlations for all curing days and cement percentages in both dry density specimens with (a) 0% TRF, (b) 2.5% TRF, (c) 5% TRF, (d) 10% TRF, (e) 20% TRF cement replacements, and (f) All the correlations.

Considering the previous discussion, it can be settled that replacing cement with TRP/TRF up to 2.5% can effectively improve the cemented clay's compressive strength (q_u), which also has been observed by Yadav and Tiwari [94]. Furthermore, an increased substitution rate of TRP or TRF might bring about more ductile blends. A decrease in elasticity can be an option to reduce pavement reflective cracking

because of the cement stabilized base. It can remove the necessity of adding a chip seal, geotextile, or unbound granular layer between the stabilized base and surface to provide stress relaxation [164,165]. Additionally, at small strains (G_0), cement replacement of TRP/TRF up to 2.5 % seems feasible. However, as the deformation continues to large strains (UCS), the TRP samples cured for as long as 60 days appear to have reduced strength (this does not apply to 28-days blends as they show increase in UCS up to 5% substitution). Consequently, a formation of weak bonds or chemical reactions appeared to develop at 60 days, affecting only the large strain behavior of the TRP composites. This phenomenon was also explained in the microstructure section for the blends that showed better performance (at 2.5% TRP replacement level). Nevertheless, such behavior was not observed in TRF samples at 60 days of curing which might be referred to the large contact area between the TRP particles and the clay, compared to TRF threads. Such surface area allows more chemical reaction to happen and create distributed weak bonds along the samples.

The parameters (q_u, G_0, and E) are essential parameters in many geotechnical engineering designs such as the calculations of bearing capacity, shallow foundation settlement and pile capacity. Moreover, q_u parameter is used to check slope stability of cohesive soils and G_0 is used in dynamic design of geotechnical projects.

4.1.3 Normalization of Strength and Stiffness Results

As expressed in the methodology section, Figure 4.9 combines the TRP replacement and just cement' blends for unconfined compressive strength (q_u), initial shear modulus (G_o), and elastic modulus (E) outcomes normalized with the adjusted porosity/binder index. It can be seen that Eqs. (5) and (6) have a high coefficient of regression (R^2= 0.89), and Eq. (7) has a moderate coefficient level (R^2= 0.77). Those relationships contribute significantly to determine the q_u, G_0, and E for specific blends of the type of clay used at any level of TRP replacement cured for a specific period, as determined by a single test. If possible, this test should be performed using three identical specimens to obtain a representative value of the strength for the

selected value of $\eta/X_{iv}^{0.32} = \nabla$. In light of the recent studies on other types of materials (Consoli *et al.* [67], Ekinci *et al.* [73], Ekinci *et al.* [151]), it is recommended to utilize ∇ values close to 25. Moreover, the mix is suggested to have a predetermined value of ($\eta/X_{iv}^{0.32} = \nabla$) close to 25 at which the graphs have been normalized and it divides the range of the porosity/binder index values.

$$q_u = q_{u_{(\eta/X_{iv^{0.32}}=25)}} \cdot 4339.4(\eta/X_{iv^{0.32}})^{-2.60} \quad R^2 = 0.89 \tag{5}$$

$$G_o = G_{0_{(\eta/X_{iv^{0.32}}=25)}} \cdot 88.6(\eta/X_{iv^{0.32}})^{-1.39} \quad R^2 = 0.89 \tag{6}$$

$$E = E_{(\eta/X_{iv^{0.32}}=25)} \cdot 308(\eta/X_{iv^{0.32}})^{-1.77} \quad R^2 = 0.77 \tag{7}$$

Eqs. (5), (6), and (7) can be used to obtain unconfined compressive strength, initial shear modulus, and elastic modulus for the blends of cemented clays blended with 0, 2.5, 5, 10, and 20% TRP as a cement replacement with one single test.

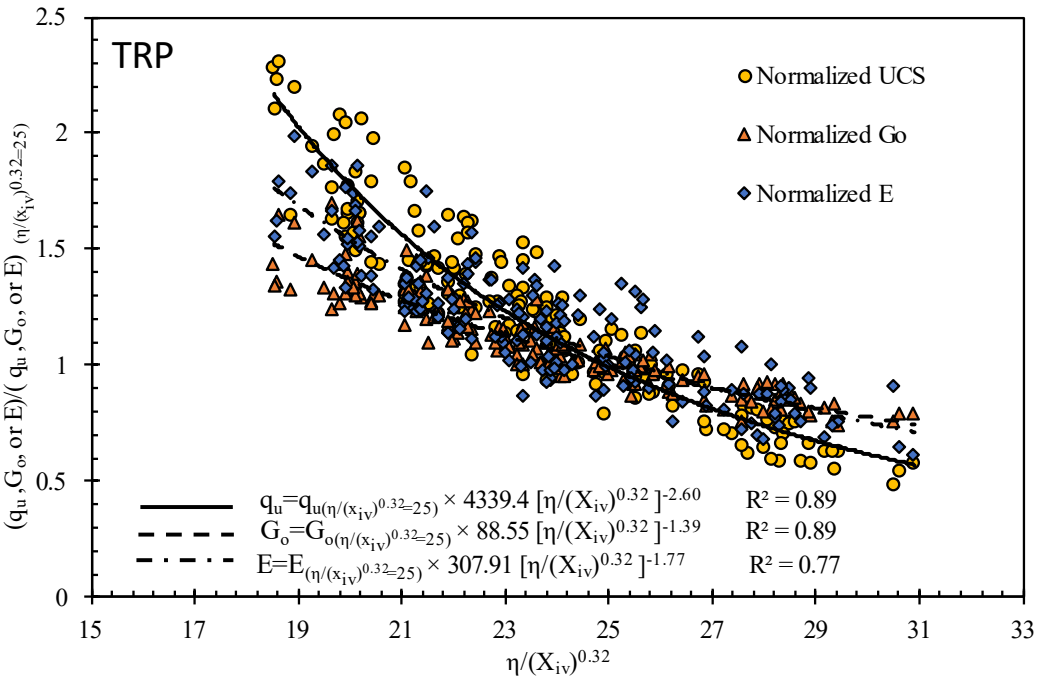

Figure 4.9. The unconfined compressive strength (q_u), the initial shear modulus (G_o), and elastic modulus (E) normalized with porosity/binder index for all the TRP tested samples.

Similarly, the results of the unconfined compressive strength (q_u), initial shear modulus (G_o), and elastic modulus (E) of TRF samples were normalized as mentioned in the methods section. The results of the normalization of all the blends against the porosity/binder index ($\eta/X_{iv}^{0.32}$) is shown in Figure 4.10. The power curves representing the relationship trends show a high degree of significance (R^2= 88 and 89%). The resulting correlations significantly contribute to estimating the unconfined compressive strength, the initial shear modulus, and the elastic modulus of cement-treated soils with any replacement proportion of TRF, cured for a specific time through conducting the tests for one blend. Eq. (8), (9), and (10) can be used to find q_u, G_o, and E of TRF-cement-clay mix having a predetermined porosity/binder index (∇) and knowing the parameters ($q_{u_{(\eta/X_{iv}^{0.32}=25)}}, G_{0_{(\eta/X_{iv}^{0.32}=25)}}, \mathrm{E}_{(\eta/X_{iv}^{0.32}=25)}$) from a tested sample having ∇=25.

$$q_u = q_{u_{(\eta/X_{iv}^{0.32}=25)}} . 1405.9(\eta/X_{iv}^{0.32})^{-2.25} \quad R^2 = 0.89 \tag{8}$$

$$G_o = G_{0_{(\eta/X_{iv}^{0.32}=25)}} . 55.48(\eta/X_{iv}^{0.32})^{-1.25} \quad R^2 = 0.89 \tag{9}$$

$$\mathrm{E} = \mathrm{E}_{(\eta/X_{iv}^{0.32}=25)} . 798.28(\eta/X_{iv}^{0.32})^{-2.08} \quad R^2 = 0.89 \tag{10}$$

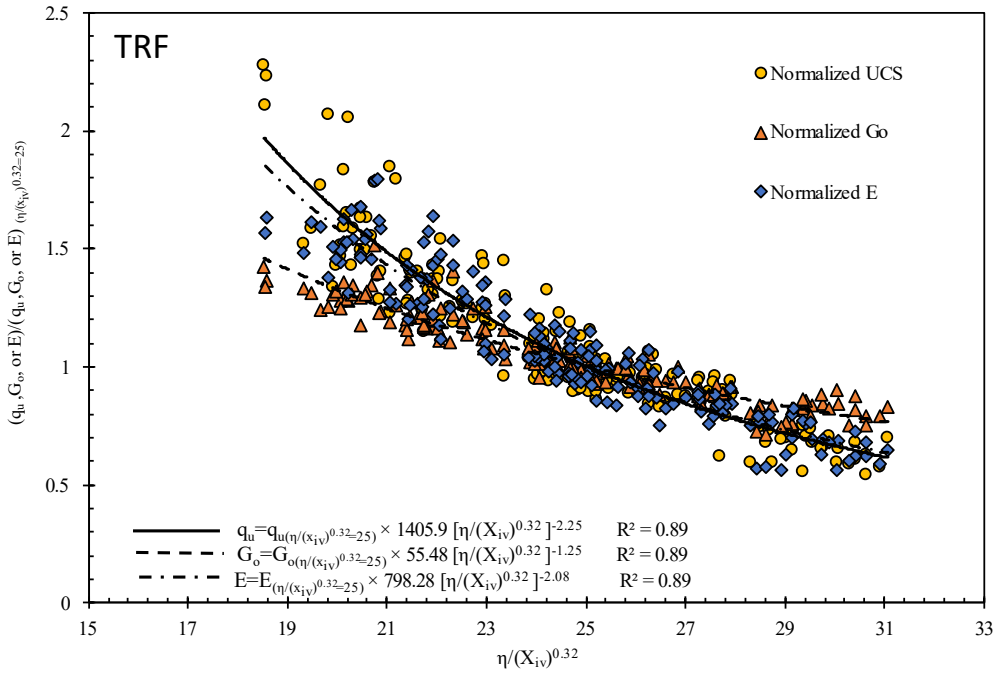

Figure 4.10. The unconfined compressive strength (q_u), initial shear modulus (G_o), and elastic modulus (E) normalized with the modified porosity/binder index ($\eta/(X_{iv})^{0.32}$) for all the TRF blends.

The correlations in Figure 4.9 and Figure 4.10 were fitted in a power curve as the best model to express the relationships. It has been chosen based on a statistical evaluation of the correlations using different models and their resulted R-square as presented in Table A.3. Moreover, the curves have been validated through an error estimation of the actual and predicted value from the equation; the error estimation of the normalized equations concluded in this section is presented in Table B.1 (TRP) and Table B.2 (TRF). The average error estimated for the TRP proposed equations are: 9.16% for UCS, 5.13% for G_0 and 10.04% for E, and for TRF proposed equations are: 13.9% for UCS, 4.2% for G_0 and 7.64% for E.

4.1.4 Acquiring Strength and Stiffness Parameters via Non-Destructive Testing

Non-destructive tests are widely used in geotechnical works; such techniques are convenient, economical, and efficient to be applied. In this study, an ultrasonic pulse velocity (UPV) test has been utilized as a non-destructive test to determine the initial shear modulus of all the blends. The q_u versus G_0 for 1600 kg/m^3 and 1800 kg/m^3 compacted clay TRP blends, considering 2.5% to 20% substitution cured at 7, 28, and 60 days, are shown in Figure 4.11. A good power curve with a good coefficient of correlation (R^2=0.81) was fitted to represent the relationship (Eq.(11)). Moreover, Figure 4.12 shows the E versus G_0 for all examined TRP mixes. Eq. (12) presents a power curve relationship with a high coefficient of correlation (R^2=0.84). Eqs. (11) and (12) serve to obtain the underlying shear modulus of samples prepared at the selected value of $\eta/(X_{iv})^{0.32}$ = 25 and correlates of the appropriate parameter of unconfined compressive strength and elastic modulus in Eqs. (5), (6), and (7). Besides, Eqs. (11) and (12) can be used to acquire q_u and E for specific blends of the

clay with any level of TRP replacement cured for a specific period simply by assessing G_0 utilizing non-destructive tests (i.e., ultrasonic pulse velocity test).

$$q_u = 0.0006{G_0}^{1.81} \quad R^2 = 0.81 \tag{11}$$

$$E = 0.00071{G_0}^{1.54} \quad R^2 = 0.84 \tag{12}$$

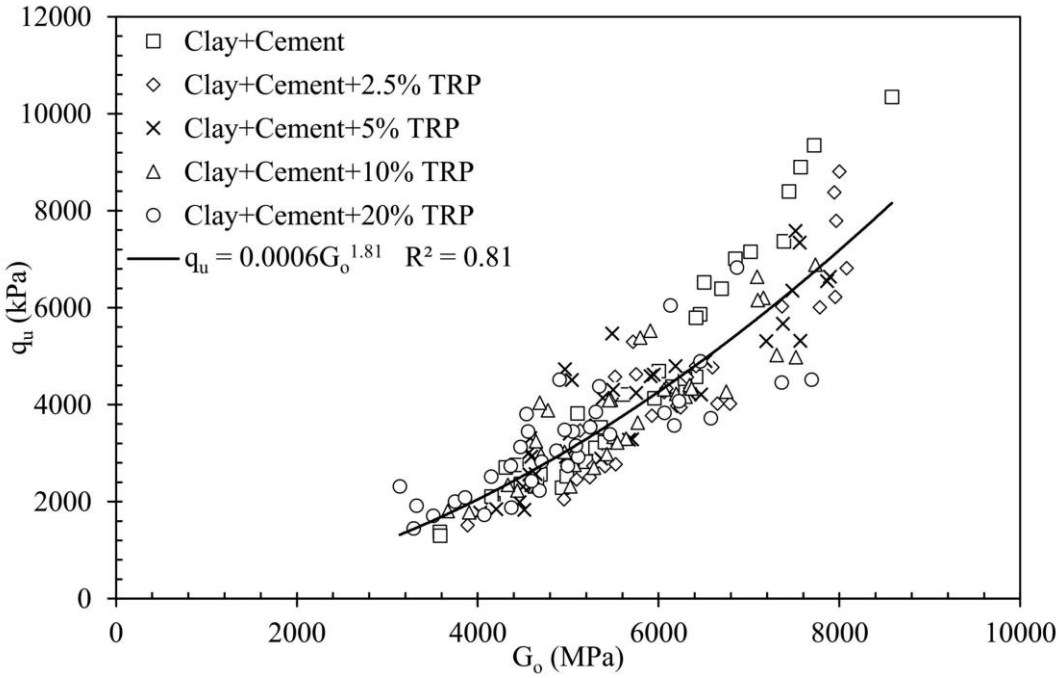

Figure 4.11. The unconfined compressive strength (q_u) as a function of the initial shear modulus (G_o) for all the blends considering the cement replacement percentages of TRP (0, 2.5, 5, 10, and 20%).

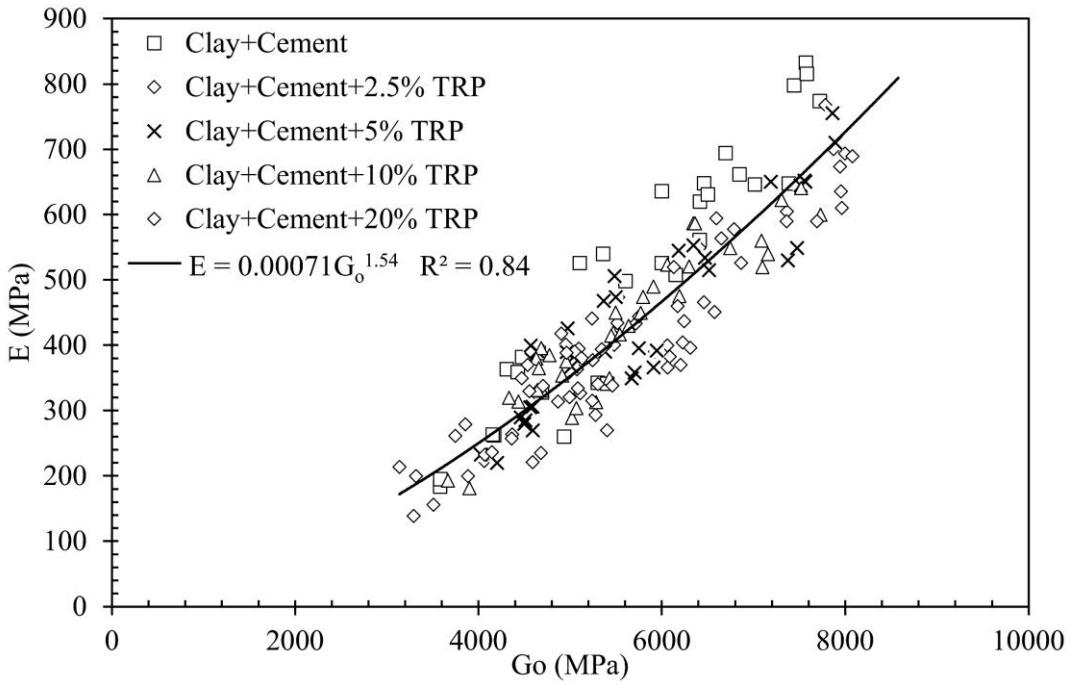

Figure 4.12. The elastic modulus (E) a function of the initial shear modulus (G_o) for all the blends considering the cement replacement percentages of TRP (0, 2.5, 5, 10, and 20%)

Moreover, the resulting unconfined compressive strength (q_u) and modulus of elasticity (E) as a function of the initial shear modulus (G_o) of TRF blends are presented in Figure 4.13 and Figure 4.14, respectively. Figure 4.13 and Figure 4.14 consider all the blends containing 7, 10, and 13% cement partially replaced by 0, 2.5, 5, 10, 20% TRF, cured for 7, 28, 60 days, and compacted at 1600 and 1800 kg/m^3 dry densities. Both relationships are illustrated by powered curves that have high significance rate of 87% and 91% (Figure 4.13 and Figure 4.14, respectively). Eqs. (13) and (14) can be used to obtain the strength q_u and elastic modulus E of any TRF-cemented-clay blend cured for a specific time by performing only one non-destructive (UPV) test. G_o in both equations can be determined following Eq. (6) described in the previous section.

$$q_u = 0.00124{G_0}^{1.73} \quad R^2 = 0.87 \tag{13}$$

$$E = 0.00021{G_0}^{1.68} \quad R^2 = 0.91 \tag{14}$$

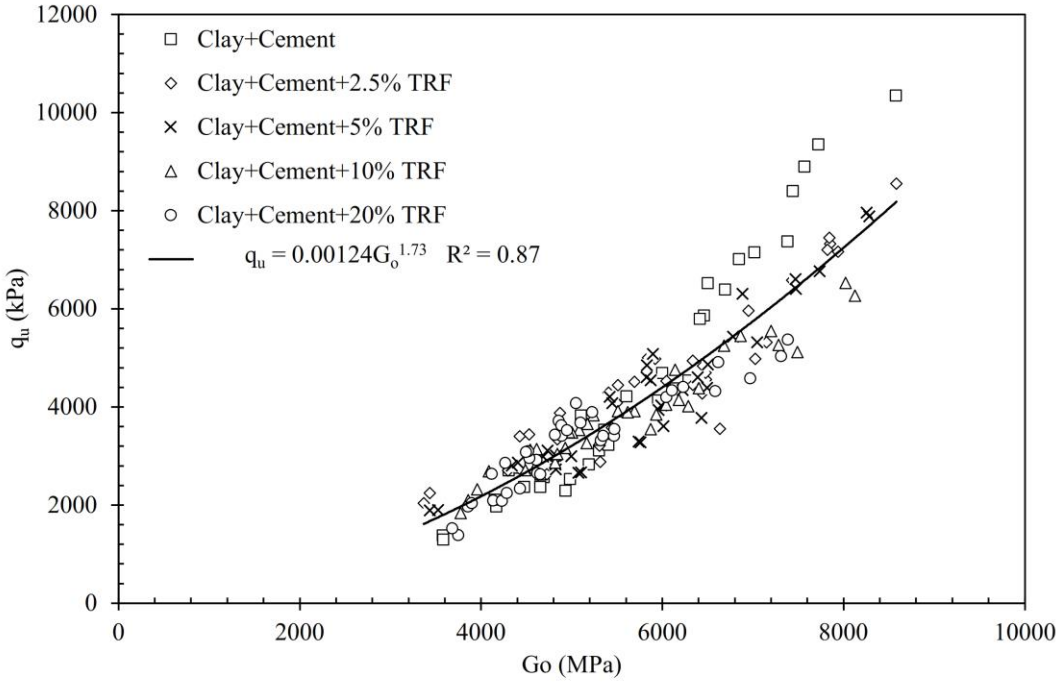

Figure 4.13. The unconfined compressive strength (q_u) as a function of the initial shear modulus (G_o) for all the blends considering the cement replacement percentages of TRF (0, 2.5, 5, 10, and 20%).

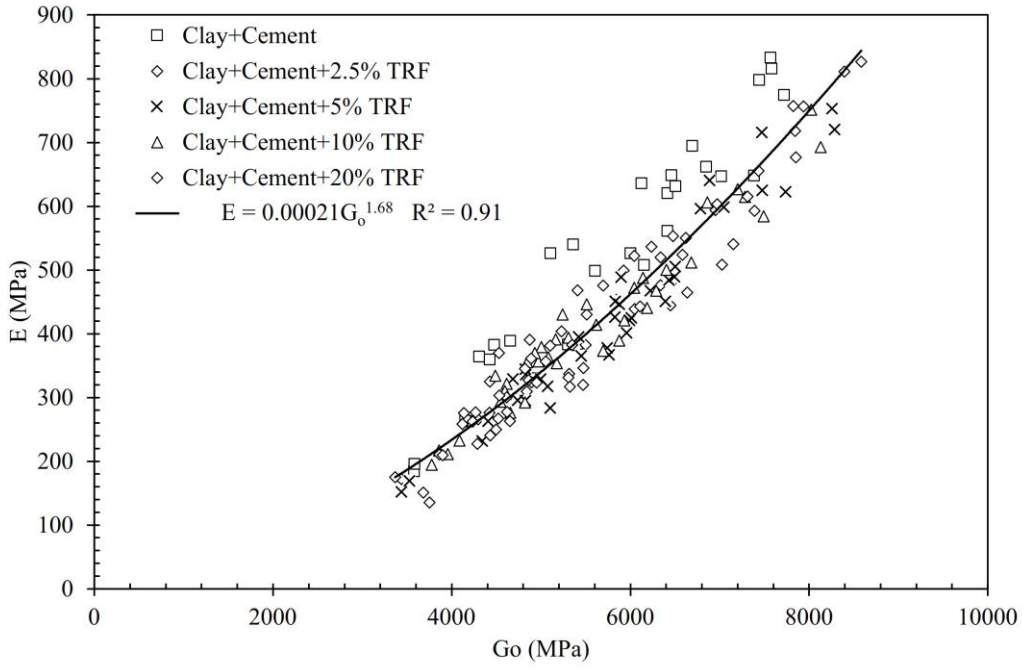

Figure 4.14 The elastic modulus (E) a function of the initial shear modulus (G_o) for all the blends considering the cement replacement percentages of TRP (0, 2.5, 5, 10, and 20%).

4.2 Durability of Blends

4.2.1 Influence of Tire Replacement on Durability of Blends

To assess durability performance of artificially cemented clay stabilized with TRP and TRF, wet/dry cycles were performed. Figure 4.15 and Figure 4.16 show artificially cemented clays stabilized with waste rubber tire (i.e., powdered and fibers) at four tire contents of 2.5% to 20% (as a replacement of cement), three cement content (7%, 10%, 13%), (1600 and 1800 kg/m^3) dry densities and (28 and 60 days) curing ages (7 days curing samples were not use to assess the durability due to the degradation of the samples at the first several cycles). It is clear that, regardless of cement and tire content, the accumulated loss of mass (ALM) of all samples is well below the reported standard requirements (such as 6% for base and subbase and 10% for soil locks in rural buildings), as listed in Table 3.5. Additionally, all specimens at the extended curing period reduce the ALM regardless of all other factors. Looking closely at the results in Figure 4.15, one can realize that, for TRP stabilized samples, an increase in ALM is seen with increasing tire content. Further, the rate of increase seems to vanish with the increase of cement content. However, Figure 4.16 shows that the inclusion of 2.5% TRF in all low-density cement contents and 7% cement content of high-density samples results in a slight reduction in ALM, which is consistent with the UCS results.

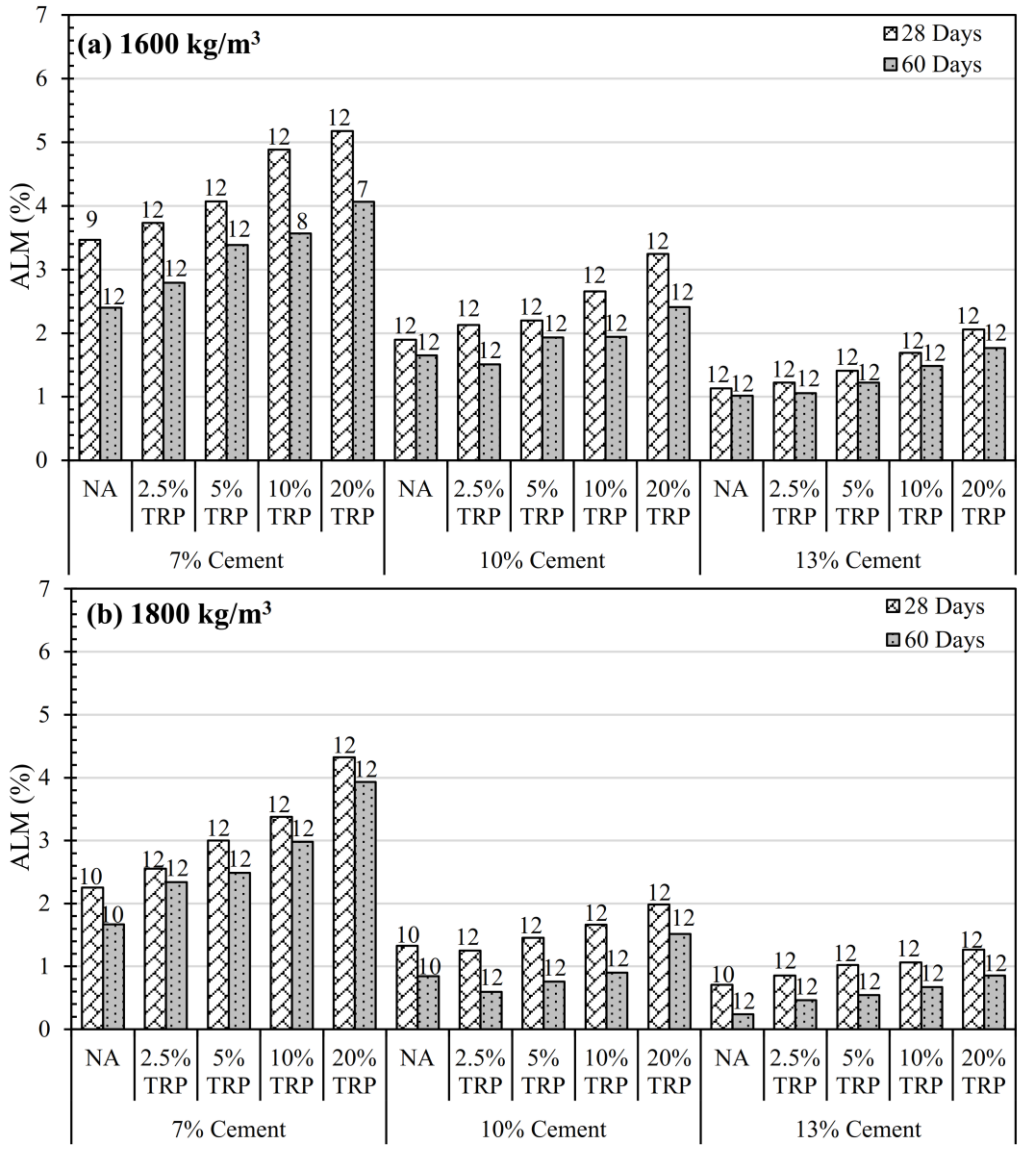

Figure 4.15. The Accumulated Loss of Mass (ALM) of TRP-cemented clay composites cured for 28 and 60 days and compacted at two dry densities: (a) 1600 kg/m^3 and (b) 1800 kg/m^3.

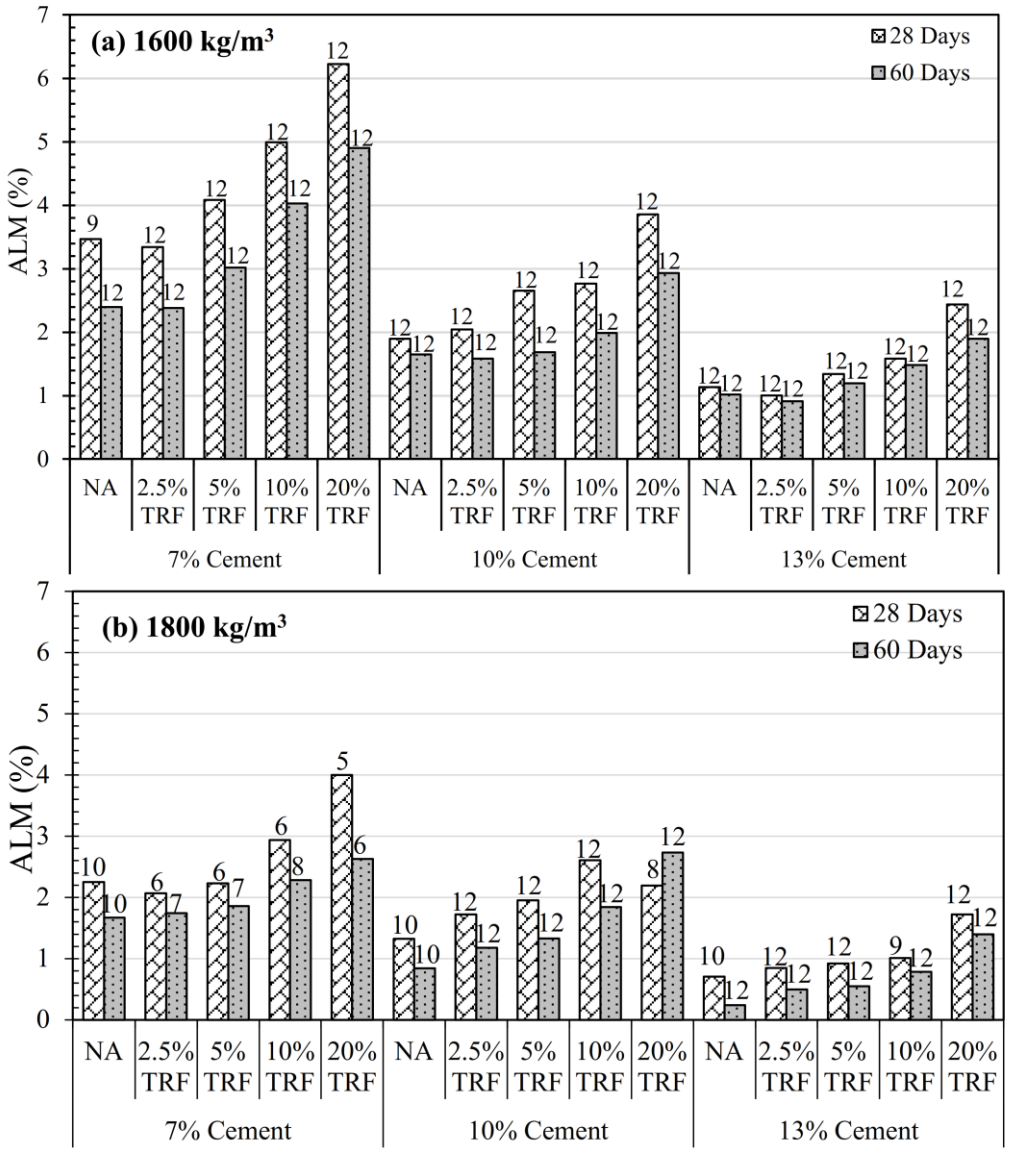

Figure 4.16. The Accumulated Loss of Mass (ALM) of TRF-cemented clay composites cured for 28 and 60 days and compacted at two dry densities: (a) 1600 kg/m^3 and (b) 1800 kg/m^3.

Figure C.1 and Figure C.2 show variation of accumulated loss of mass (ALM) of all prepared specimens at each cycle for curing periods of 28 and 60 days, respectively. In general, a linear trend can be established between the ALM and the wet/dry cycles, as the rate of ALM is particularly constant throughout 12 cycles. It is clear from both graphs that the ALM is reducing with respect to increasing the curing period and in

the sense of using tire fiber type instead of tire powder. The contribution due to the use of TRF instead of TRP might be the result of mechanical influence of the fiber surfaces since a higher percentage of surface particles bonded with the main fiber body. It is also evidential that, in both TRF and TRP samples above the specified 2.5% tire replacement, a more porous structure results in lower resistance against the abrasive processes during with the durability test. Moreover, the amount of cement in the blends is controlling the mass loss because of the substantial improvement in cohesion the cement provides. However, incorporating more rubber tire decreases the impact of the cement on weathering resistivity because of the heterogenous effect of the heat on the rubber tire and cement or clay as well as the tendency of the weak bonds between them to easily break during wetting/drying process [101].

4.2.2 Accumulated Loss of Mass as a Function of Initial Shear Modulus

Figure 4.17 and Figure 4.18 represent the correlations between the accumulated loss of mass (ALM) during 12 complete wet/dry cycles versus the maximum initial shear modulus (G_o) measured at 0, 1, 6, and 12 wet/dry cycles in TRP (Figure 4.17) and TRF (Figure 4.18) samples. Furthermore, the correlations were implemented on the results of the samples cured for two different ages, i.e., 28 days [Figure 4.17(a), Figure 4.18(a)], and 60 days [Figure 4.17(b), Figure 4.18(b)]. Figure 4.17 and Figure 4.18 show a clear powered trend of decreasing ALM as the maximum shear modulus increases. The degree of significance (R^2) of all correlations is more than R^2 =0.92. It must be noted that the specimens that did not reach the 12 cycles were eliminated from this analysis. In general, there were no significant differences between group [TRP] and group [TRF] in terms of shear modulus and ALM relationship. However, the time effect of hydration reaction on the shear modulus and ALM is obvious when comparing Figure 4.17(a) and (b) or Figure 4.18(a) and (b), where 60-day curing samples gained more stiffness and, thus, had less tendency toward degradation under the wet/dry cycles compared with 28-day samples.

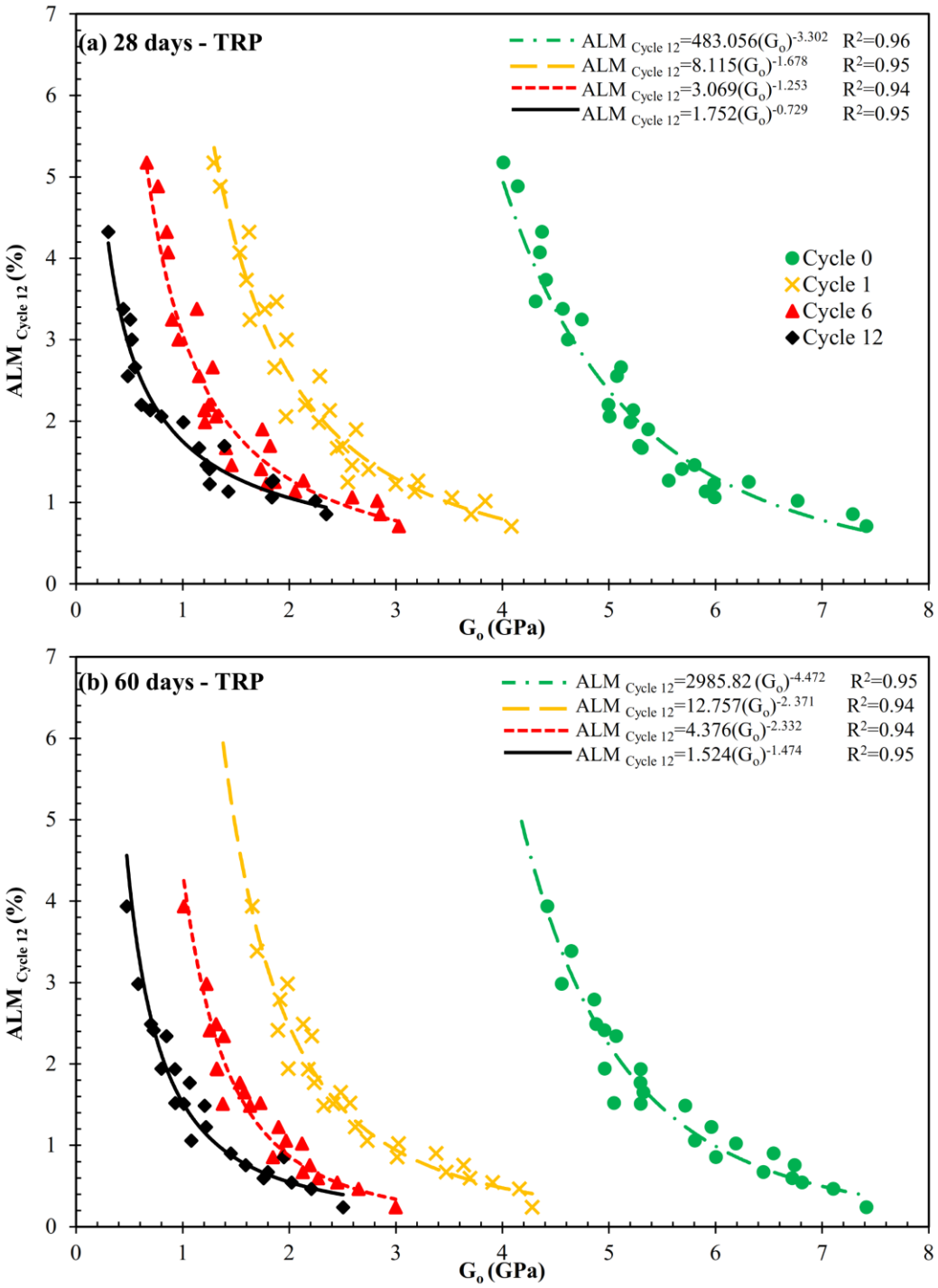

Figure 4.17. The Accumulated Loss of Mass (ALM) after the 12th wet/dry cycle as a function of the maximum initial shear modulus (G_o) measured at 0, 1, 6, 12 cycle on TRP-cemented clay specimens cured for two curing ages: (a) 28 days, and (b) 60 days.

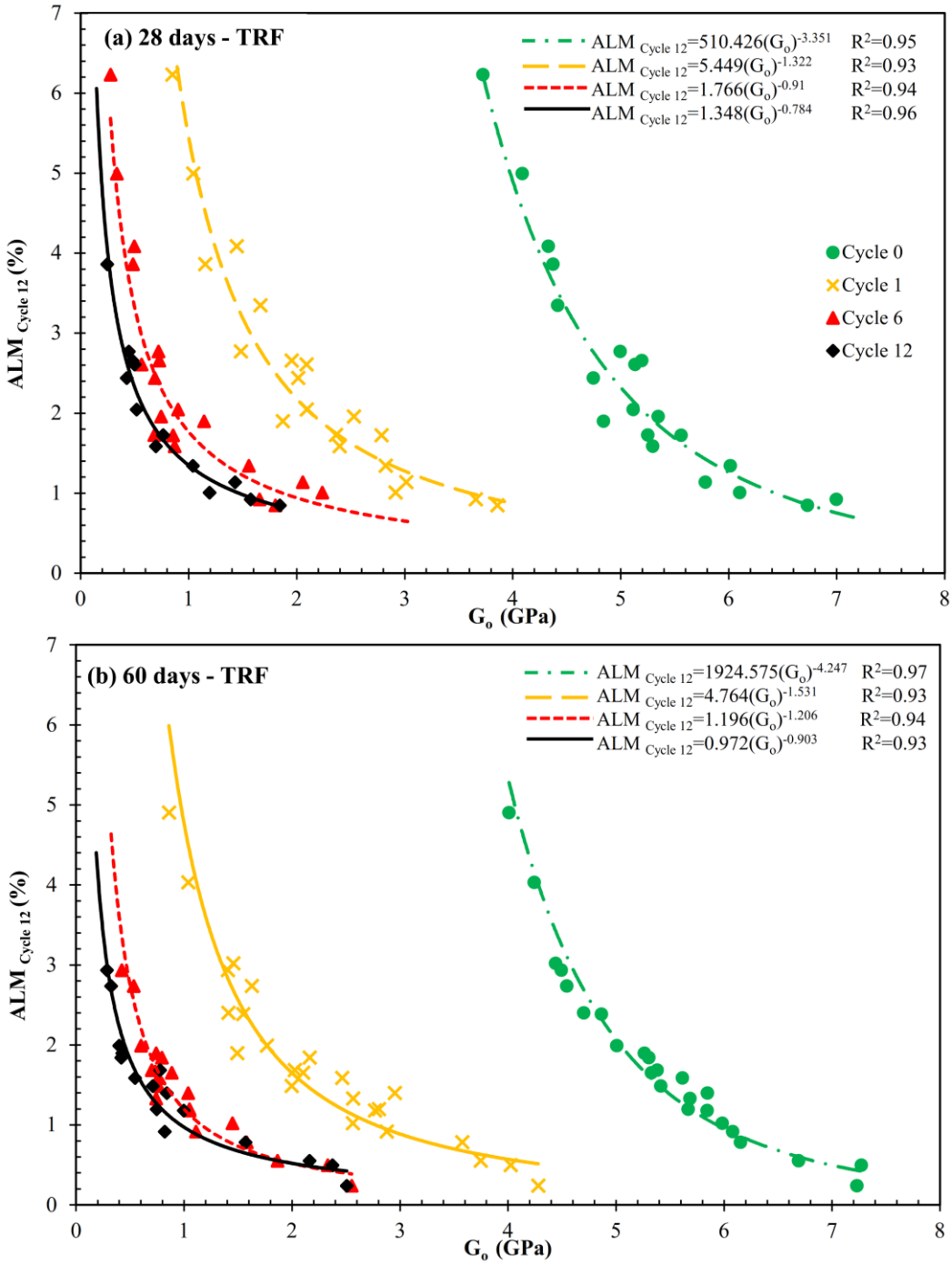

Figure 4.18. The Accumulated Loss of Mass (ALM) at the 12th wet/dry cycle as a function of the maximum initial shear modulus (G_o) measured at 0, 1, 6, 12 cycle on TRF-cemented clay specimens cured for two curing ages: (a) 28 days, and (b) 60 days.

The purpose of correlating the maximum shear velocity at zero cycles (i.e., after curing and 24 h of water soaking for saturation purposes) with the ALM is to express functions to predict the degradation performance of any blend combining a similar type of clay with cement and tire rubber (TRF or TRP) cured for a specific period (i.e., 28 and 60 days) without getting through all the processes of wetting/drying cycles. Nevertheless, the shear modulus results after the first, sixth, and twelfth cycles were also correlated with ALM to check the durability performance of soil with cement and tire rubber blends during seasonal and weathering changes by using an undestructive test (UPV). Therefore, ALM as a percentage can be calculated following Eq. (15), given the initial shear modulus G_o (GPa) at different wet/dry cycles:

$$ALM_{Cycle\ 12}(\%) = \mathrm{A} \times (G_o)^L, \quad (15)$$

where A and L are scalars representing the integer coefficient and the power, respectively. A and L depend on the mix combinations, cycle number, and the wet/dry condition of the samples during performing the UPV test. A, L, and R^2 (coefficient of determination) values for the different blend groups are tabulated in Table 4.1.

Table 4.1. Parameters of the Figure 4.17 and Figure 4.18 correlation functions to be applied on Eq. (15) for ALM determination.

Curing (days)	Cycle No.	TRP group			TRF group		
		A	L	R^2	A	L	R^2
28	0	483.056	-3.302	0.96	510.426	-3.351	0.95
28	1	8.115	-1.678	0.95	5.449	-1.322	0.93
28	6	3.069	-1.253	0.94	1.766	-0.91	0.94
28	12	1.752	-0.729	0.95	1.348	-0.784	0.96
60	0	2985.82	-4.472	0.95	1924.575	-4.247	0.97
60	1	12.757	-2.371	0.94	4.764	-1.531	0.93
60	6	4.376	-2.332	0.94	1.196	-1.206	0.94
60	12	1.524	-1.474	0.95	0.972	-0.903	0.93

Consoli *et al*. [82] proposed the idea of replacing the time-consuming wet/dry cycles test with a simple test (such as UPV), in which the authors correlated the ALM and G_o of different binders with soils. The current study obtains such correlation considering the effect of numerous variables on the same material combination (i.e., alluvial clay, cement, and waste rubber tire).

4.2.3 Porosity/Binder Index Influence on the ALM of the blends

Figure 4.19 represents the correlation between the porosity/binder index and the accumulated loss of mass (ALM) after 12 wet/dry cycles of cemented soil with TRP [Figure 4.19 (a,c,e,g)] and TRF [Figure 4.19(b,d,f,h)] composites. The figures include the results of samples compacted at (1600 and 1800 kg/m^3) dry densities and 28 and 60 days of curing. However, specimens that could not reach the twelfth cycle were eliminated from the analysis. For this reason, and due to that most of the cement–clay samples (without TRP or TRF) did not reach twelfth cycle, the porosity/binder index versus ALM correlation was not applicable. Overall, the ALM increases exponentially as η/X_{iv} increase, while ALM is less in 60-day curing samples compared with 28-day curing ones, as shown in Figure 4.19. All the resulting functions in Figure 4.19 have high coefficients of determination (R^2 > 0.92), except for one with R^2 = 0.84 due to limited data points for such specific correlation. Furthermore, the powered curves in Figure 4.19 were normalized to obtain a single correlation for each cemented clay with the TRF and TRP sample groups. The results were normalized by dividing the powered functions by a specific value of (η/X_{iv}) [i.e., (η/X_i) = 10 in this study]. The (η/X_{iv}) value was explicitly selected for normalization because it divides the blends' range of (η/X_{iv}) values. Table 3.5 shows the determined values of accumulated loss of mass (ALM) after 12 wet/dry cycles at η/X_{iv} = 10 applied to normalize all the different blends.

Strong correlations of normalized ALM at the twelfth cycle and η/X_{iv} were obtained (R^2 = 0.96 for TRP group) and (R^2 = 0.94 for TRF group) as represented in Figure 4.20. Eqs. (16) and (17) would enable the determination of ALM at the twelfth cycle

of wet/dry cycles of any blends containing a similar type of clay treated with cement and either TRP [Eq. (5)] or TRF [Eq. (12)]. Such a process would save time and labor by performing only a single nondestructive test (UPV). Explicitly, two samples can be prepared and cured at $\frac{\eta}{X_{iv}} = 10$, and a UPV test can be performed to obtain the initial shear modulus (G_o). Then, by using the equation established in the previous section [Eq. (15)], ALM $_{\text{cycle } 12}$ at $\frac{\eta}{X_{iv}} = 10$ can be obtained. Finally, Eqs. (16) and (17) can be used to calculate the ALM of any blends containing similar soil type with cement and TRF or TRP based on the mix used to prepare the ($\frac{\eta}{X_{iv}} = 10$) samples:

$$ALM_{TRP\ cycle\ 12}\,(\%) = (ALM_{\left(\frac{\eta}{X_{iv}}=10\right)})_{TRP\ cycle\ 12} \times 0.0067\left(\frac{\eta}{X_{\text{iv}}}\right)^{2.171} \quad R^2 = 0.96, \tag{16}$$

$$ALM_{TRF\ cycle\ 12}\,(\%) = (ALM_{\left(\frac{\eta}{X_{iv}}=10\right)})_{TRF\ cycle\ 12} \times 0.0235\left(\frac{\eta}{X_{\text{iv}}}\right)^{1.626} \quad R^2 = 0.94. \tag{17}$$

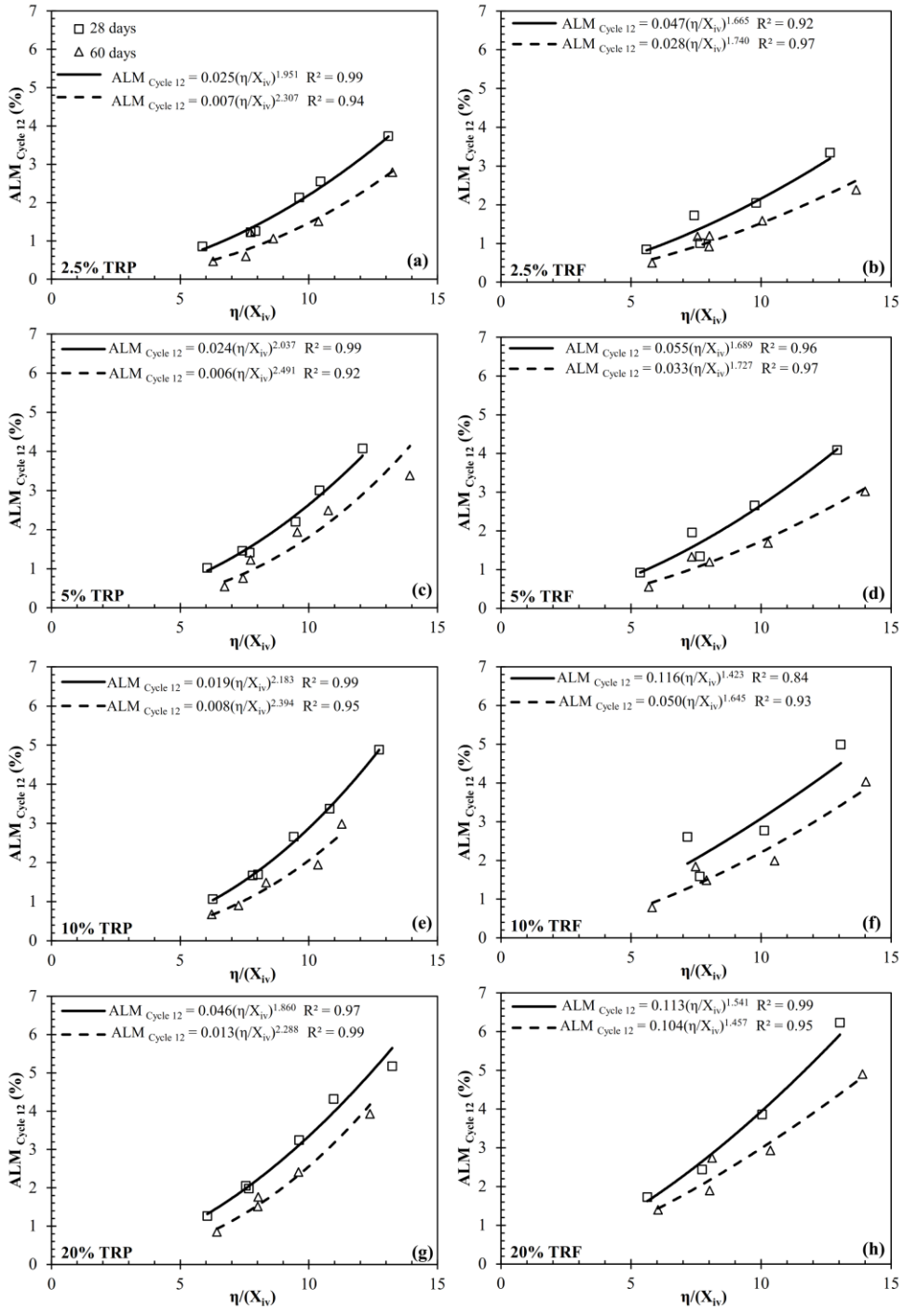

Figure 4.19. The Accumulated Loss of Mass (ALM) and porosity/binder index (η/X_{iv}) relations for both curing periods and cement contents in both dry densities' samples with TRP contents((a) 2.5% TRP, (c) 5% TRP, (e) 10% TRP, (g) 20% TRP), and TRF contents((b) 2.5% TRF, (d) 5% TRF, (f) 10% TRF, (h) 20% TRF).

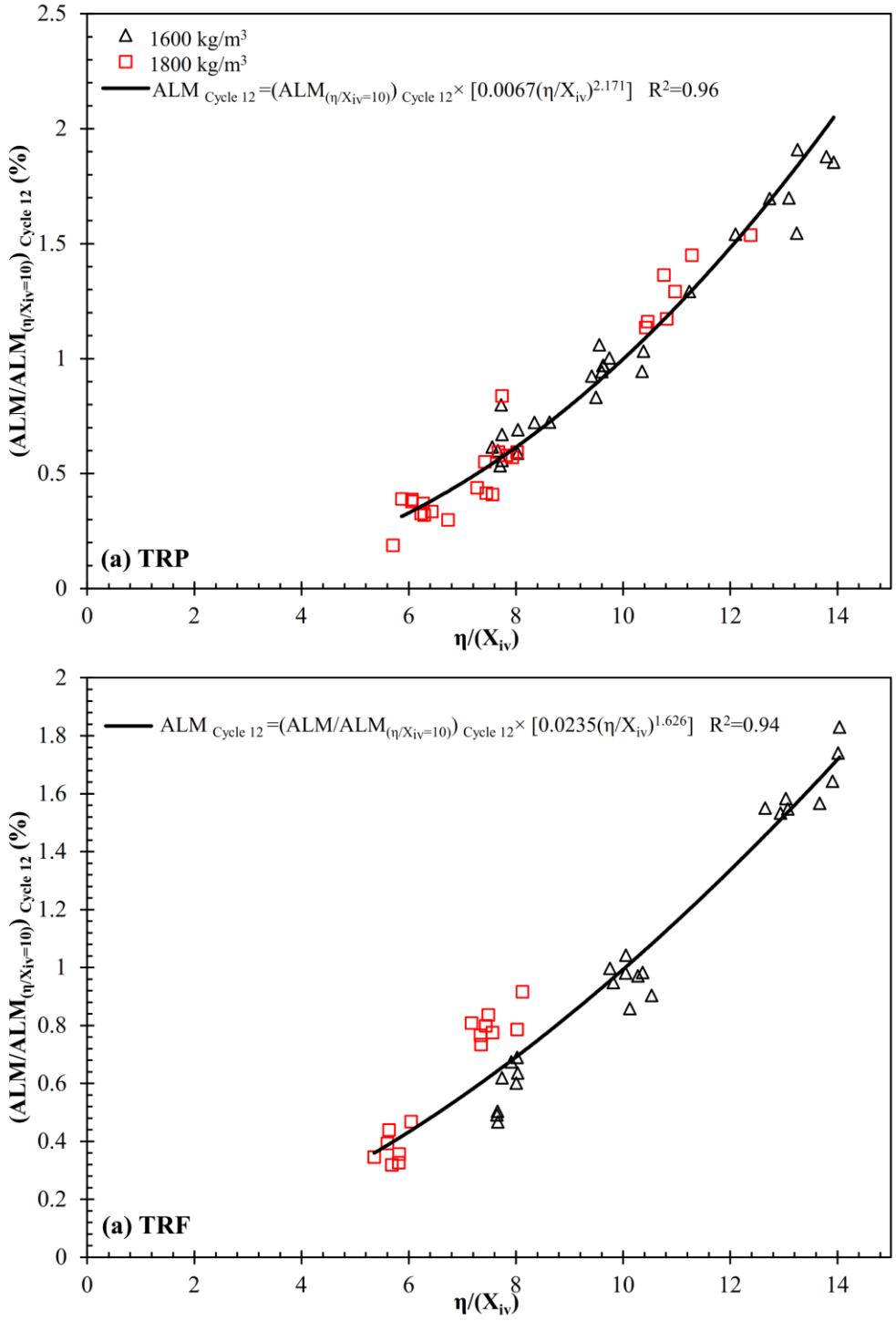

Figure 4.20. The Accumulated Loss of Mass (ALM) normalized with porosity/binder index (η/X_{iv}) for all blends containing (a) TRP and (b) TRF.

4.3 Microstructure

Figure 4.21(a) and Figure 4.21(b) show the XRD results of the composites at 28- and 60-d of curing, respectively. The quartz and calcite were the main phases and contained minor peaks in phyllosilicates, dolomites, and feldspars. The results also showed the availability of Illite, Chlorite-Kaolinite, and Smectite mineral species.

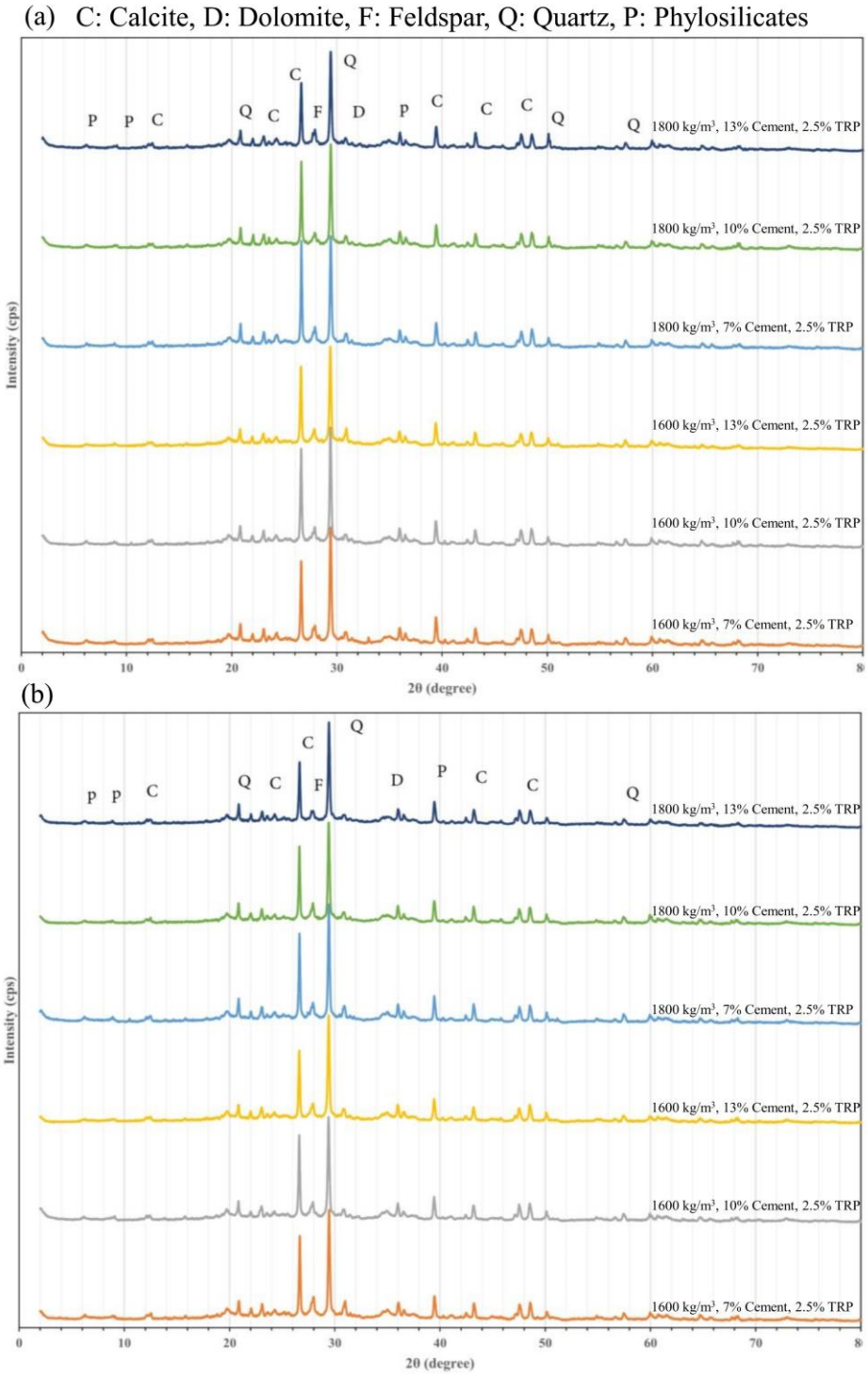

Figure 4.21. XRD results for tested blends at (a) 28-days and (b) 60-days curing periods.

Figure 4.22 (a) to Figure 4.22(f) show the SEM images of the TRP samples prepared for 1600kg/m^3 and 1800kg/m^3 density at 28-days curing and the SEM images in Figure 4.23(a) to Figure 4.23(f) show the samples were prepared under the same conditions but at 60-days curing. The samples tested at 60-days show a reduction in strength, which differs from the samples prepared and cured at 28-days. As cement content increased, a denser and more compacted microstructure was revealed in SEM images. Moreover, as density increased, the pores became less apparent. As the cement content increased from 7 to 13% in SEM images, the number of white deposits designated as the Portlandite phase are more visible. The small cylindrical shape in SEM depicts Portlandite. The pores turned out to be less accessible in whole mixtures with a density of 1600 kg/m^3. Small spheres showed up as tire powder, and these were delegated carbon atoms. Hydrated silicate and aluminum phases classified C-S-H and C-A-S-H were also observed, as demonstrated in Figure 4.22 (a) to Figure 4.22(f).

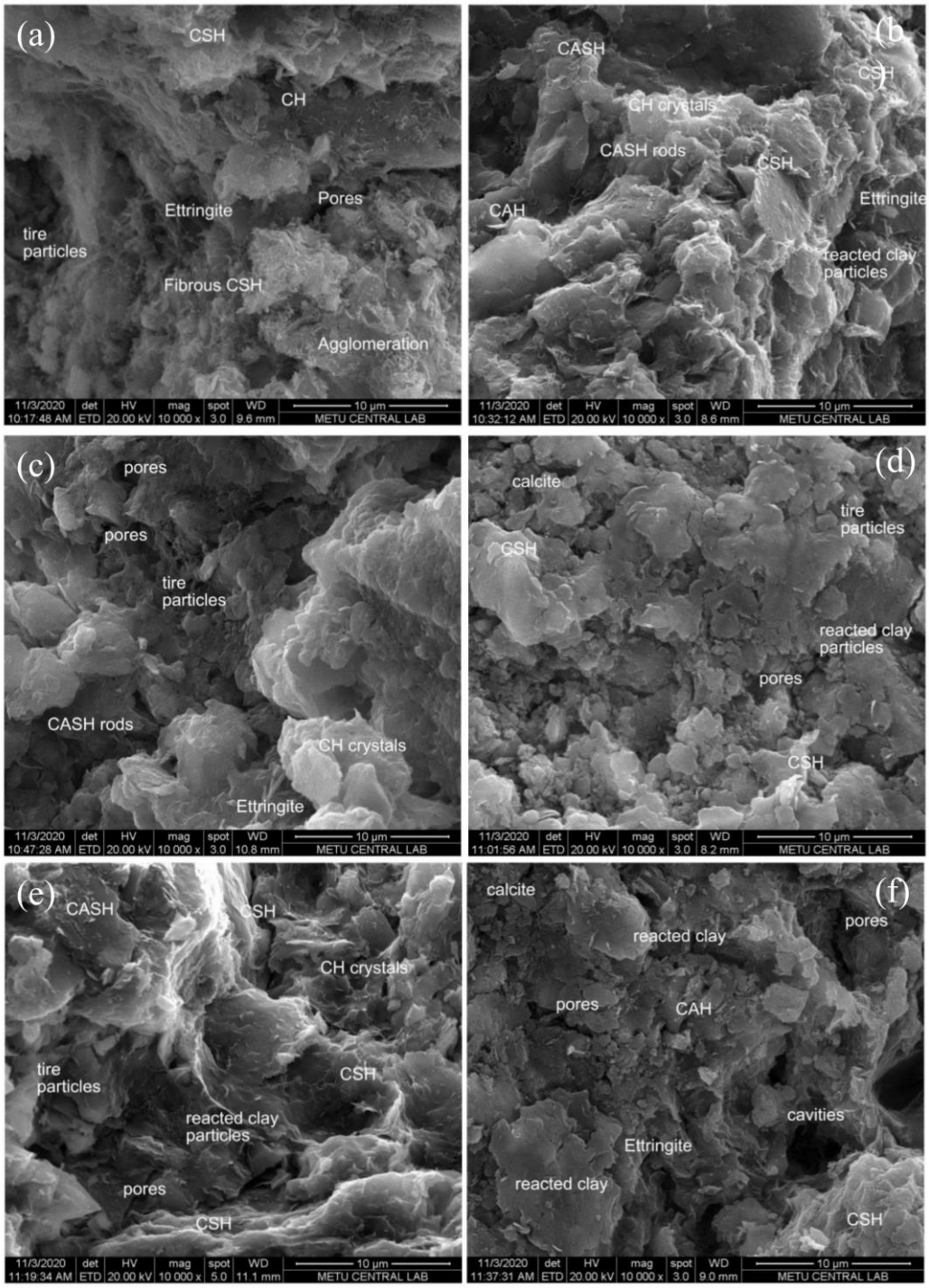

Figure 4.22. SEM micrographs for blends a)1600kg/m^3, 7% Cement and 2.5% TRP, b) 1600kg/m^3, 10% Cement and 2.5% TRP, c) 1600kg/m^3, 13% Cement and 2.5% TRP, d) 1800kg/m^3, 7% Cement and 2.5% TRP, e) 1800kg/m^3, 10% Cement and 2.5% TRP, f) 1800kg/m^3, 13% Cement and 2.5% TRP at 28-days

During the initial curing period (28-d), the tire powder may have acted as a nucleation site and could fill the pores. The pore-filling effect enhanced the strength of the composites. The initial stage of mixing the clay particles with cement contributed to a few changes in bonds. The normal bonds were either debilitated or obliterated. However, the arrangement of new bonds with the cement interaction improved the matrix properties.

More aluminum hydrate arrangements during the early curing period can clarify the porosity refinement of the composites. Hence, Figure 4.22(a) to Figure 4.22(f) account for more hydration products (CSH, CAH). These cementitious products hold the soil particles together. The pores are filled with the fine powder of tires and prompting a denser microstructure. The solidness of the composites can be increased by improving the connections between soil and cement grains as agglomeration, Figure 4.22(a), and reticulate C-S-H formation, Figure 4.23(c) and Figure 4.23(e) in late-stage curing. This can be possible by increasing the cement amount in the mixtures.

At a later age curing period (60-days), when compared to similar mixture groups, more ettringite arrangement is seen as a needle-like and foiled form in SEM images (see Figure 4.23(a) to Figure 4.23(f)). The availability of tire powder particles implies that the hydration was not completed. As the cement amount increased, more gels formed in various phases. The size of the ettringite needles increased, and shapes became larger, as seen in Figure 4.23(b) and Figure 4.23(d). Additionally, larger pores, classified as cavities, were formed. Those formations are believed to be one of the reasons for the composites' strength reduction. The mixture groups containing 13% cement had more C-S-H and fewer pores. When density increased to 1800 kg/m^3, the same pattern was seen in those mixture groups. Curiously, those mixtures had more pores but a more stable and denser arrangement. It is known that the amount of cement produces more hydration products, and those magnesium sulfate hydrates push the pores and make them grow. Because of this process, the distance between the particles increased. Thus, more spaces were accessible for hydration. Since the hydration was not completed (more spaces are readily available as

cavities), the tire powder particles seemed to be inert and act as a filler, not a pozzolan. This is consistent with results pertaining to the strength, which showed a decrease at 60-days.

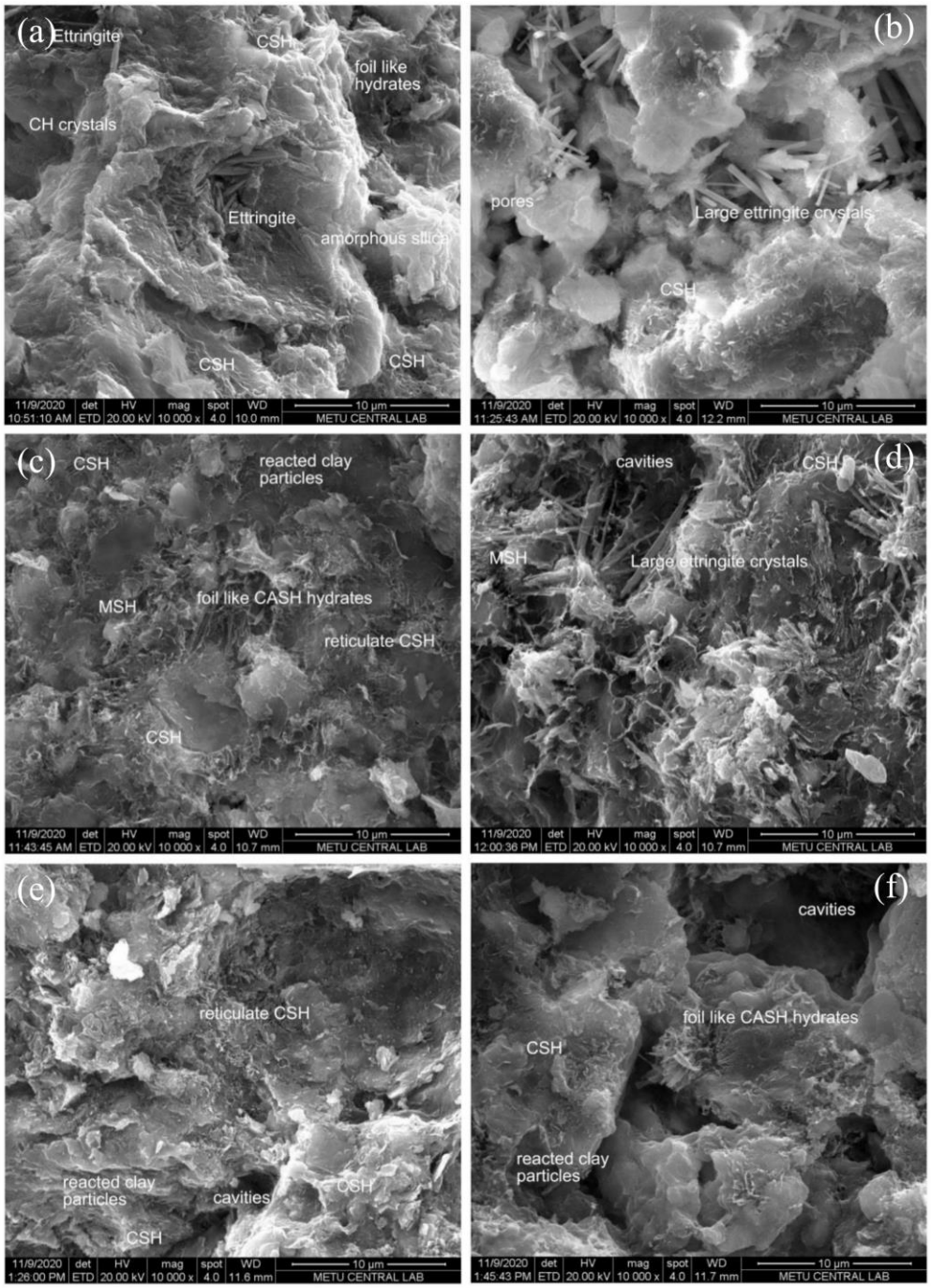

Figure 4.23. SEM micrographs for blends a)1600kg/m^3, 7% Cement and 2.5% TRP, b) 1600kg/m^3, 10% Cement and 2.5% TRP, c) 1600kg/m^3, 13% Cement and 2.5% TRP, d) 1800kg/m^3, 7% Cement and 2.5% TRP, e) 1800kg/m^3, 10% Cement and 2.5% TRP, f) 1800kg/m^3, 13% Cement and 2.5% TRP at 60-days

More gels formed with samples with a density of 1800 kg/m^3. Pores decreased in comparison to similar samples with a density of 1600 kg/m^3. The increment in cement amount led to a better arrangement of the particles. The composites became denser. Notwithstanding, in 1800kg/m^3, 10% Cement, and 2.5% TRP mixture groups, the availability of more obscure areas (dark color) of various sizes seemed to increase. This can be ascribed to other hydration products that need more curing time to be steady. These observations are consistent with the porosity and strength values accounted for in this investigation at 28-days.

Because of the interaction between positive charges of the cem’nt's components and negative charges of the s’il's component, an all-around improved flocculated and solidified mixture was formed, as shown in Figure 4.23(c) and Figure 4.23(e). Positive charges of the calcium absorbed negative charges of the clay. Consequently, the clay particles formed clusters, improving bonds among soil particles, thereby increasing strength. At that point, a hydration reaction was principally liable for the short-term gain in strength since it produced the primary bonds and reduced the mixt’re's water content. Interestingly, the pozzolanic reactions initiated when a sufficient concentration of hydroxide particles was produced, and a specific degree of alkalinity was reached in the pore fluid. The secondary reactions were extensively slower than the hydration reaction and lasted for quite a while. The high measure of ettringite and Portlandite crystals, as seen in SEM pictures, supported this phenomenon.

The more splendid color shows the magnesium silicate hydrate development (Figure 4.23(c) and Figure 4.23(d)). Curiously, these phases were by all accounts not weakening the bonds at the beginning of the hydration at early ages (before 28-d). Instead, a chemical reaction occurred between the calcium, silica, and alumina that

were promptly accessible in the soil to deliver complex aluminates and silicates, as seen in Figure 4.23(c) and Figure 4.23(f) at later ages (60-days). Because of flocculation, solid aggregation of soil particles that impeded the finer partic’es' pores restricted the entrance of water molecules into it. Thus, at this phase, hydration products could not be created. Along these lines, mature products were susceptible to any attack during wetting-drying cycles, with the resulting load causing a drop in strength.

During loading, non-uniform stress distribution may be created, and the strains in the matrix can cause a strength decrease at 60-days because of the absence of sufficient bonding between the rubber tire powder and the clay particles. This is obvious in Figure 4.23(d) to Figure 4.23(f). More Portlandite was observed at 60-days, showing slower hydration. The needle-like shape structure, which showed up on SEM images, demonstrated that hydration was not completed. The carbon particles appeared unreacted and became less available when the cement content increased. The tire contained an unreasonable measure of carbon particles. In this investigation, the tire was utilized as a powder form. Therefore, the surface area increased, and more carbon particles were promptly accessible for the mixtures. Carbon particles destroyed C-’-H's structure, forming a flimsier type of ettringite gels, which hampered the bonds between the cement and soil particles.

Moreover, these fine tire powder particles absorbed more water and consumed the water to be used for the reaction. The arrangement of the enormous amount of hydration products upheld this hypothesis. Notwithstanding, the weakening of the C-S-H structure and more unstable ettringite development destroyed the matrix. When the load was applied, it attained at the critical stage, and the sample failed at a low strain level. The sudden drop in peak load of soil-cement tire powder mixture demonstrated the brittle behavior of the material at 60-days. The strength reduction might have been due to the existing rubber tire acting as a barrier and cement not being available for reaction to produce proper bonds. Thus, upon loading, the developed bonds cracked and became weaker, as supported by Ahmed and El-Naggar’s study [166]. The pores were well-connected with each other, and this

phenomenon can cause unexpected failure during loading. Moreover, as bonding improved, the load at which the clay is produced increased. At higher cement content, the samples became more brittle.

Tire powder occupied unfilled spaces inside the matrix during the early hydration period, leading to the increment in the shear modulus. The hydration products could not develop because tire powder particles block the pores. More ettringite needles were available at 60-days. This shows that additional time was required for complete hydration. The availability of Portlandite likewise showed that the hydration was not at the desired level. The unreacted particles observed in Figure 4.23(d) and Figure 4.23(f) in the form of cavities showed that more water is necessary for the development of hydration products. The loads could be effectively transferred to all composite parts if the pores are well-connected with one another. As the density of composites increased, their porosity reduced, and less water entered. When the water content declined, the water could not lubricate the point of contact between the clay-tire powder-cement grains, and the particle friction between them increased. More pressure could be applied to composites during loading, and the non-uniform pressure distribution on the contact points could cause a decrease in mechanical properties.

Furthermore, the strength could have been reduced due to the high amount of magnesium in clay, which could expand the bonds between the soil and cement. Thus, this process weakens the bond structures, decreasing the strength of the composites. As a result, the tire powder showed less Portlandite consumption at early ages. The white appearance on the SEM pictures shows the Portlandite crystals at early stages. Montmorillonite and Illite soil groups showed lower pozzolanic reactivity at lower cement dosages. Magnesium enrichment occurred because of the glasslike magnesium silicate hydrated (MSH) phases with a brighter color at the interface of the ettringite needles. Moreover, MSH had a lower binding capacity compared to the C-S-H. The expanding initiated the micro-crack concentrations, and when the stress surpassed the strength of the composites, micro-cracks were created

inside the matrix, and weak bonding between the clay-cement particles then decreased in strength.

Figure 4.24(a) to Figure 4.24(f) shows the SEM images of the samples prepared at the densities of 1600kg/m^3 and 1800kg/m^3 and 60-days curing with 2.5% TRF content and 7, 10 and 13% cement content. As cement content increases, a denser and more compacted microstructure was reported and reviewed with the help of SEM images. Moreover, as density increases, the pores become smaller, and a denser structure is formed. In SEM images, as the cement content increased from 7 to 13%, the quantity of white deposits designated as the Portlandite phase were reported. The small cylindrical shape in SEM is Portlandite. The pores turn out to be less yet accessible on the whole mixtures having a density of 1600 kg/m^3. There are likewise hydrated silicate and aluminum phases classified as C-S-H and C-A-S-H as demonstrated in Figure 4.24(a) to Figure 4.24(f).

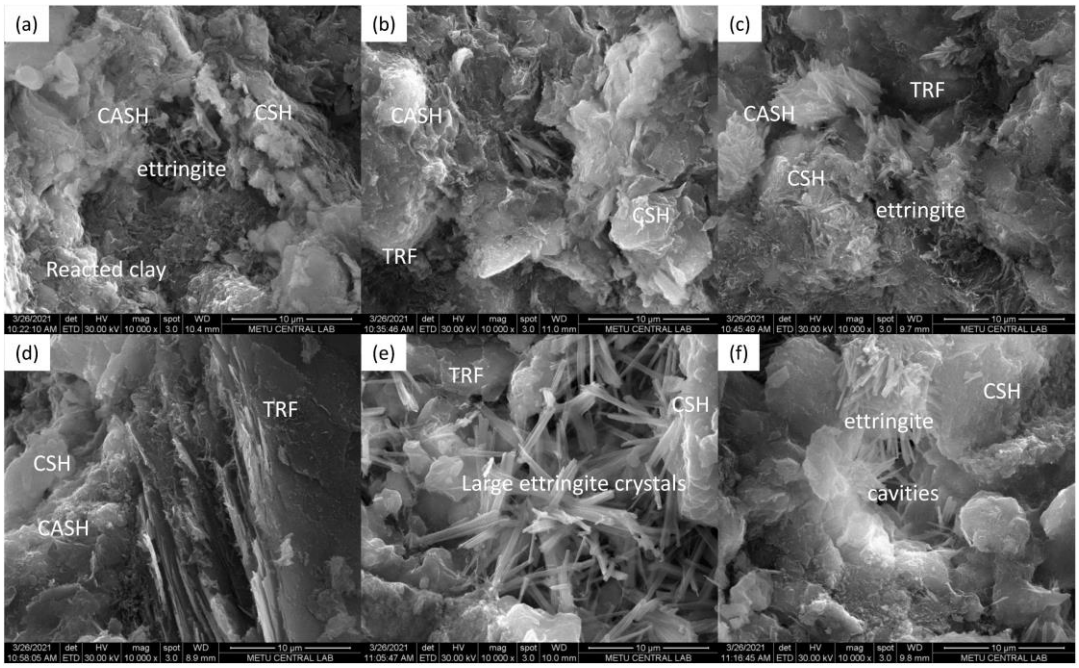

Figure 4.24. SEM micrographs for blends (a)1600kg/m^3, 7% Cement and 2.5% TRF, (b) 1600kg/m^3, 10% Cement and 2.5% TRF, (c) 1600kg/m^3, 13% Cement and 2.5% TRF, (d) 1800kg/m^3, 7% Cement and 2.5% TRF, (e) 1800kg/m^3, 10% Cement and 2.5% TRF, (f) 1800kg/m^3, 13% Cement and 2.5% TRF at 60-days.

Similar to TRP samples, because of the interaction between positive charges of the cem’nt's components and negative charges of the s’il's component, an all-around improved flocculated and solidified mixture was formed as shown in Figure 4.24(a) to Figure 4.24(f). Positive charges from calcium absorb negative charges from clay, making the clay particles to be clustered and along these lines improving bonds amongst soil particles and thereby increasing strength. At that point, the hydration reaction is the cause of the short-term gain of strength since it produces the primary bonds and reduces the water content of the mixture. Interestingly, the pozzolanic reactions initiate when a sufficient concentration of hydroxide particles is produced, and a specific degree of alkalinity is reached in the pore fluid. The secondary reactions are much slower than the hydration reactions and can continue for quite a while.

It can be seen in Figure 4.25(a) and Figure 4.25(b) that a hard shell developed around the rubber particles through the cement hydration, which increases the compatibility in stiffness between rubber and clay. However, as seen in Figure 4.25(c) and Figure 4.25(d), the cavity and microcracks on the surface of rubber fibers may also cause poor adhesion between the cemented clay and rubber fibers, which may lead to the generation of gaps in the interface. The weak interfacial interaction between the cemented clay and rubber fiber may be responsible for the reduction in unconfined compressive strength, with increase of fiber content above 2.5 %.

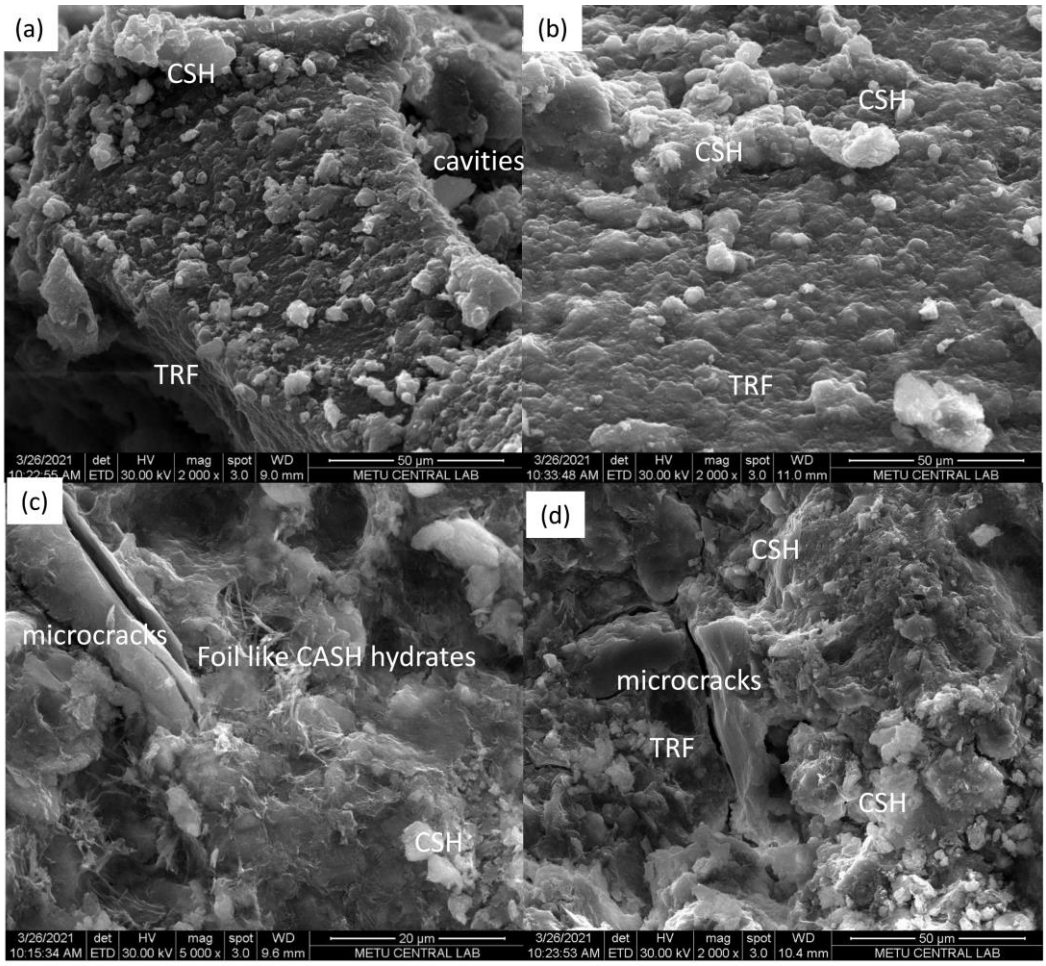

Figure 4.25. SEM micrographs for (a-b) hard shell development around the rubber (c) cavity and (d) microcracks on the clay rubber interface.

4.4 Environmental Assessment

The environmental assessments of treating problematic soil with cement and waste rubber tire (TRP and TRF) has been conducted through life cycle assessment (LCA). The LCA results have been interpreted and presented as follows:

4.4.1 Environmental Impacts of cemented clay with tire rubber inclusion.

The results of the environmental impact assessment containing 18 categories for each blend are given in Table D.2. However, the selected five categories' results have been interpreted in this section. The selection of the specific categories was based on their significance of evaluating the environmental impacts of this project. Figure 4.26(a) and Figure 4.26(b) show the five impact categories, namely GWP100, FDP, ODPinf, PMFP, ULOP, and WDP, from the tire rubber blends, all with a density of 1600 kg/m^3 and 1800 kg/m^3, respectively. Moreover, for each group, cement percentage and waste tire rubber (TRP, and TRF) percentage are shown in the graphs. Additionally, to include all impact categories in one graph to allow comparisons between the different densities and materials, the scale of each impact has been adjusted using the values and units shown in the figures' legend. Therefore, the Y-axis in Figure 4.26 was kept constant.

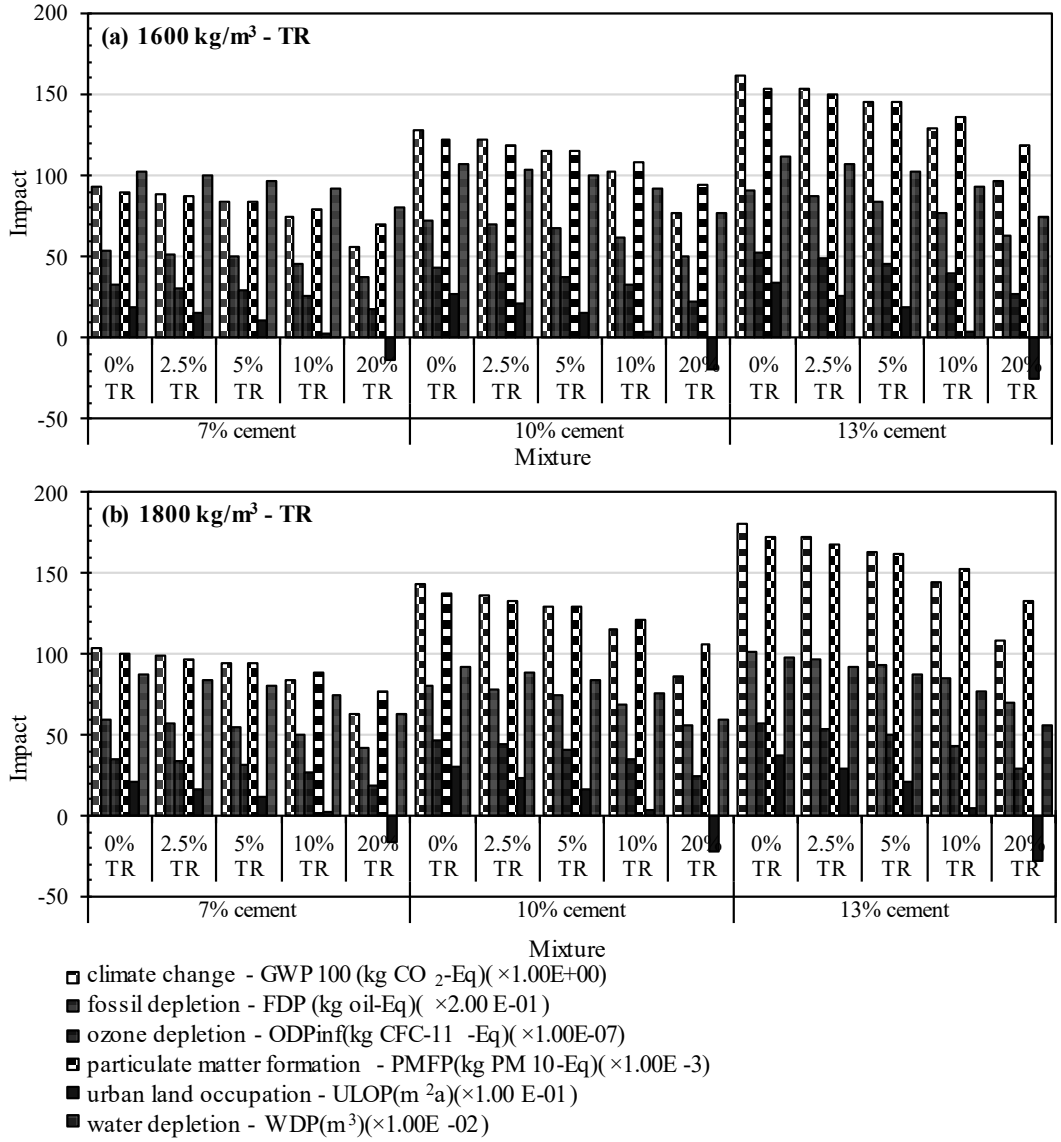

Figure 4.26. The five potential environmental impact categories of waste rubber tire cemented-soil blends compacted at two dry densities: (a) 1600 kg/m^3, (b) 1800 kg/m^3.

In Figure 4.26, two patterns can be observed, which are the change in environmental impact influenced by the cement percentage, and the second pattern is created by the effect of percentages of the TR used. Firstly, the results suggest that a higher percentage of cement results in higher environmental damage potential in all categories, as illustrated in Figure 4.26. Furthermore, a decrease in the environmental

impact with the increase in tire waste percentage can be monitored in both dry densities blends. On the other hand, a considerable rise in environmental impact associated with density increase can be witnessed when comparing Figure 4.26(a) and Figure 4.26(b). Thus, the highest potential for environmental damage occurred, as expected, at the highest cement percentage (13%) with no replacing material. Additionally, this point has a higher impact at a higher density, namely 1800 kg/m^3.

In general, all the environmental impact categories have the same pattern. However, water depletion slightly increases when replacing cement with waste tires because the production of waste material requires the use of water; for instance, shredding the tires consumes water. Nevertheless, the urban land occupation impact category decreased significantly by the addition of waste rubber tires, reaching a negative value at 20% tire replacement of cement. The use of waste tires in this method is regarded as a waste disposing technique; thus, any environmental burden of such wastes is accounted as a benefit. Therefore, at 20% tire, the urban land occupation is negative because of gaining the benefit of the traditional disposal methods such as landfills. The global warming potential (GWP 100) is decreased with the inclusion of waste tires as a replacement for cement due to the decrease of GHGs the activities of such method provide. Fossil depletion indicates the usage of fossil fuels in the processes; the results showed a decrease in this category when replacing cement because of cement production's significant consumption of energy. Similarly, particulate matter formation and ozone depletion dropped because of the reduction in the processes that generates particles and chlorofluorocarbons to the atmosphere.

As mentioned earlier, cement production consumes a large share of raw material and considerably contributes to GHGs emissions [167], thus justifying the high environmental impacts in high cement content blends. Such impacts drop when partially replacing cement with waste tire rubber because this technique not only reduces cement consumption but also incorporates harmful waste (i.e., waste tire) in the process, which positively impacts the environment. The slight increase in the environmental impacts in the higher density blends is mainly due to the higher amount of material utilized in the same blend compared to the lower density samples.

4.4.2 Normalized environmental impacts per unit (Strength, Stiffness, or Accumulated Loss of Mass)

As discussed earlier, the blends in this study have different variables that affect their mechanical and durability performances. Similarly, such variables affect the outcomes of the environmental impacts. Therefore, to show the environmental contribution of each blend linked to an objective engineering property of the blend, normalization of each environmental impact per unit strength, stiffness and ALM were evaluated. The results of samples cured for 28 days were selected in this analysis as a mid-age of the curing interval. The normalized environmental impact of each mixture per unit of UCS, G_0, and ALM is shown in Figure 4.27, Figure 4.28, and Figure 4.29, respectively. Each contains two subgraphs in which each represents one of the waste tires rubber (i.e., TRP, TRF). Additionally, the right side of each figure represents the density of 1600 kg/m^3, while 1800 kg/m^3 density is shown on the left side.

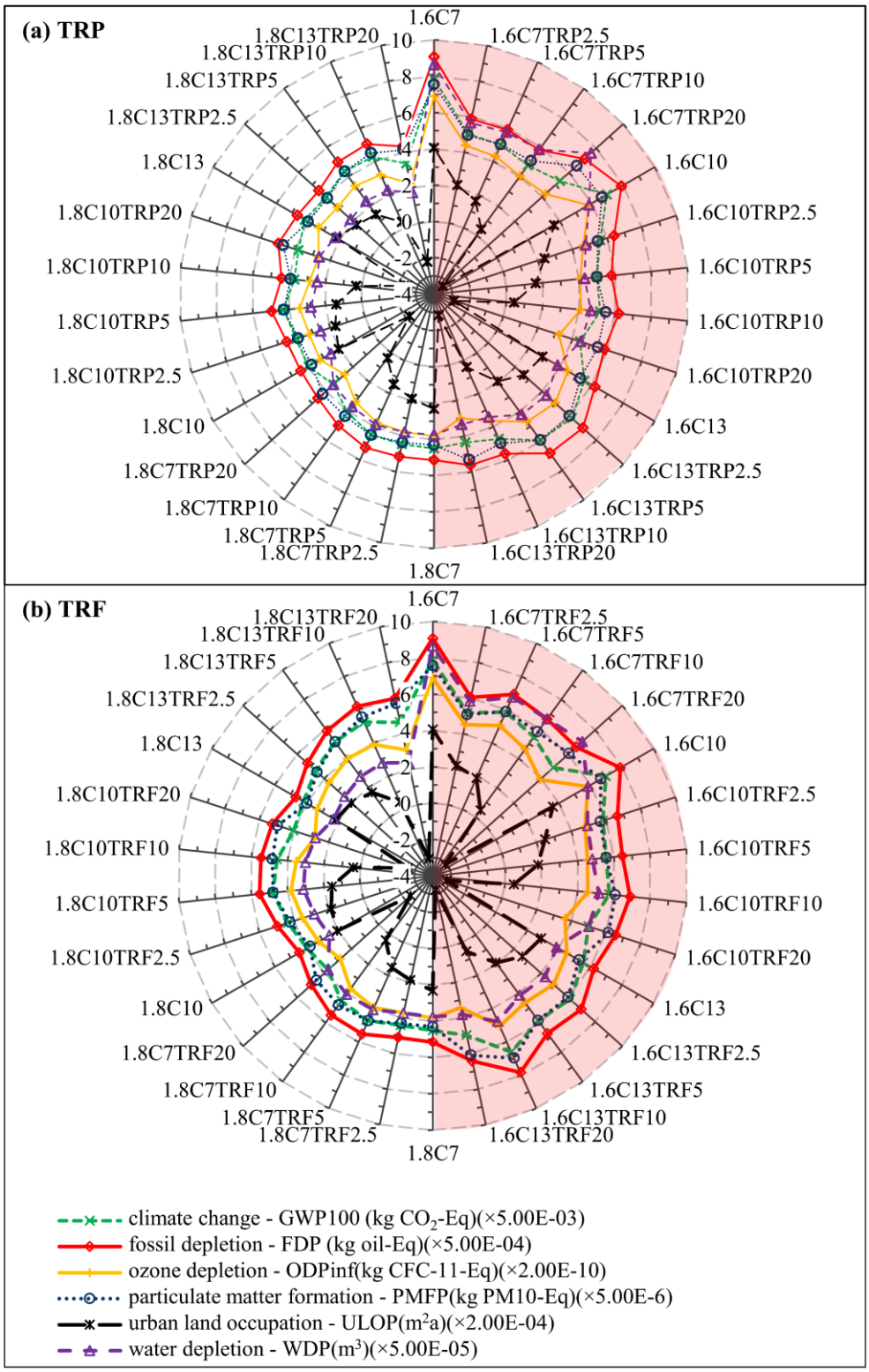

Figure 4.27. Normalized five environmental impact categories per unit UCS for different cemented soils with two waste tire forms: (a) TRP, and (b) TRF.

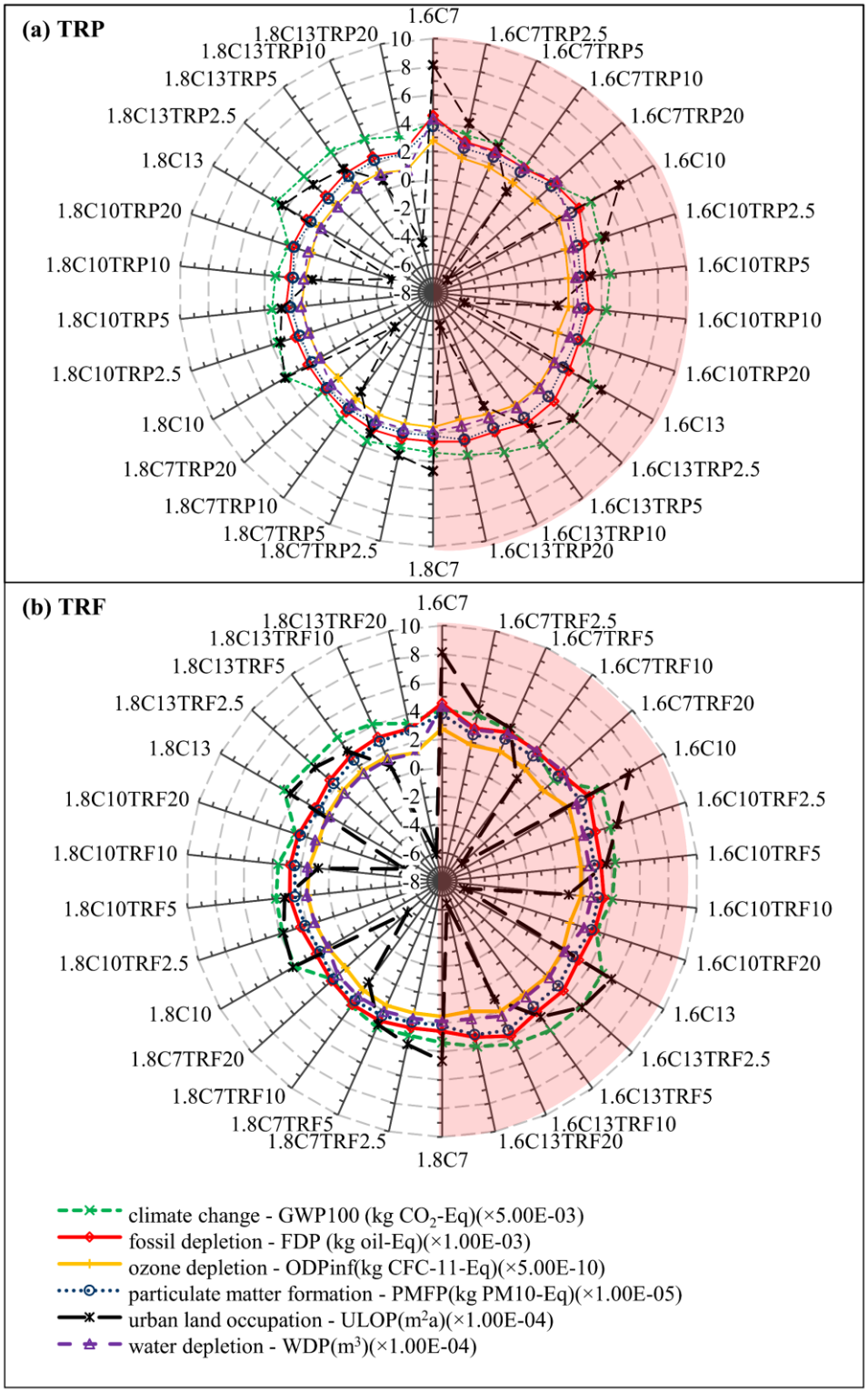

Figure 4.28. Normalized five environmental impact categories per unit G_o for different cemented soils with two waste tire forms: (a) TRP, and (b) TRF.

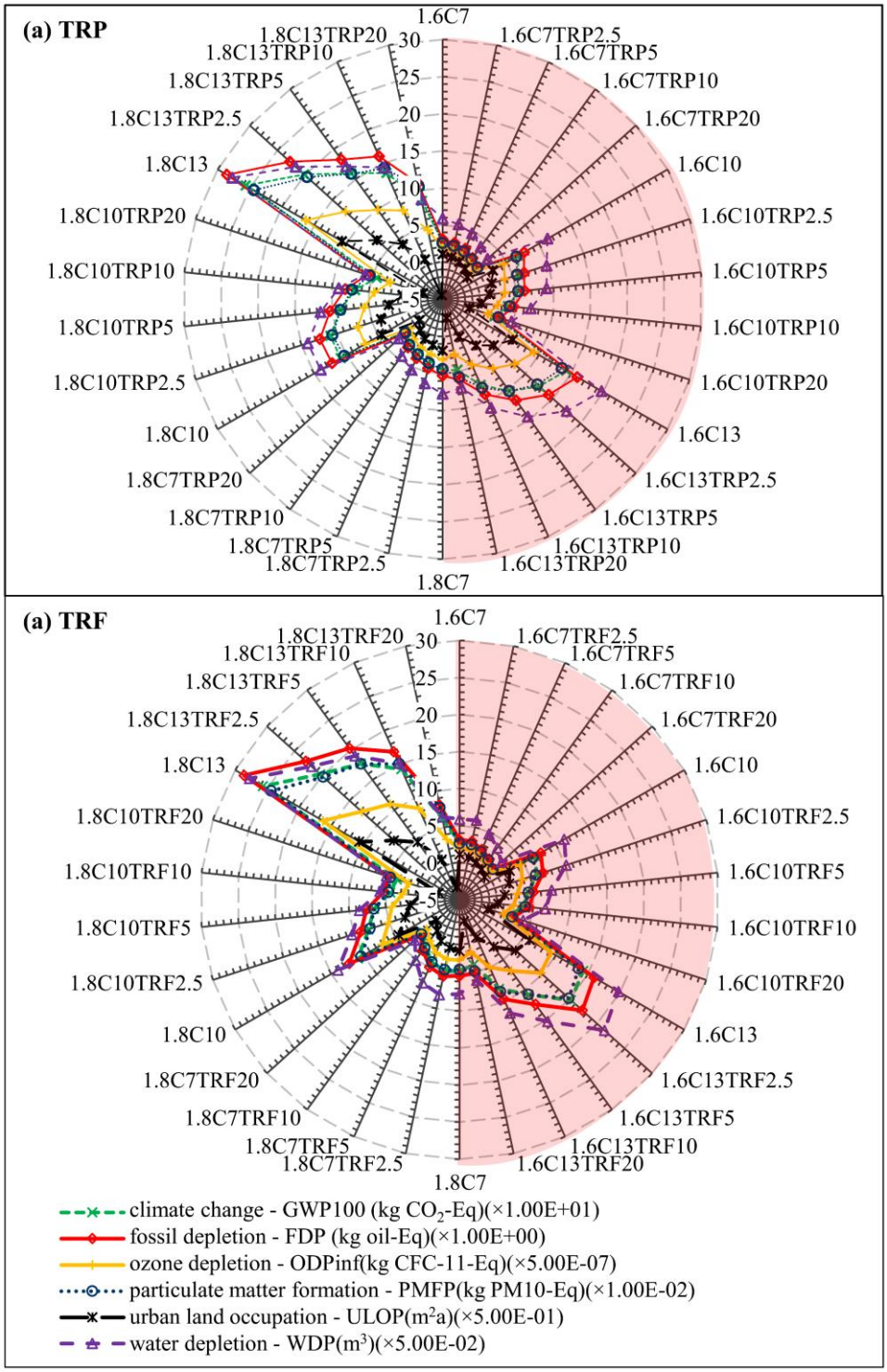

Figure 4.29. Normalized five environmental impact categories per unit ALM for different cemented soils with two waste tire forms: (a) TRP, and (b) TRF.

The results indicate that the highest environmental impact per unit strength for both TRP and TRF is observed in the lower density and when zero tire rubber content is used to replace the cement content, as indicated in Figure 4.29 (a) and (b). Additionally, similar trends can be observed for the waste material, including a noticeable decrease in the normalized impact as a higher waste percentage is utilized for the same cement percentage. Furthermore, a higher percentage of used cement for the same density decreases the normalized environmental impact. Moreover, it can be observed from Figure 4.27 that higher density results in lower environmental impact per unit strength. Moreover, when comparing the strength normalized impact of both TRP and TRF in Figure 4.27(a) and (b), nonobvious variation is witnessed due to the assumption that both mixtures have the same environmental impacts and as explained earlier, slight variation in the strength of TRP and TRF was reported.

Similarly, the normalized impact per unit G_0 in Figure 4.28 acquires the same patterns as the normalized strength patterns. This includes the increase in the normalized G_o impact in the groups with the lower density. Also, a similar inverse relationship between the normalized impact and both the cement percentage and the replacement percentage is observed in Figure 4.28. However, those trends have a slighter change in Figure 4.27 compared to Figure 4.28.

Figure 4.29 (a), (b), and (c) show the environmental impact per unit ALM for TRP, and TRF mixture groups. As the value of impact/ALM increases, it indicates more environmental affect. Overall, all the environmental impacts/ALM in Figure 4.29 follow the same pattern. Although higher density blends have higher impact/ALM contrary to the impact per UCS or G_o, the cement content is the most dominant factor influencing the impact/ALM of the blends. Samples treated with only cement have the highest environmental impact per unit ALM. Nonetheless, partial replacement of cement causes a significant drop in the impact/ALM, and it continues to decrease with the increase of the waste tire rubber content.

Higher density corresponds to higher materials usage including cement in the mix which result in higher values of environmental impact. However, when considering

the normalized impact per unit strength (UCS), the density increase resulted in lower normalized impact values as shown in Figure 4.27. The decrease in the normalized impact is due to the substantial increase in the strength values with the increase in the density (i.e., the environmental cost of one unit strength increase is significantly lower in the blends with density of 1800 kg/m^3 comparing to the mixes with lower density that is 1600 kg/m^3).

The same pattern is less prominent when considering impact per unit stiffness (G_0) because of the lower variation in the G_0 values between both densities compare to the variation in UCS results. Moreover, similar pattern in normalized ALM results exist. However, the dominant variable in determining the normalized environmental impact/ALM is the cement content thus controlling the pattern where a significant drop in the values happens when replacing cement with waste tires material.

Overall, the environmental impact per UCS or G_0 decrease by increasing the cement content and the dry density reaching the optimum at 1800 kg/m^3 and 13% cement. However, the incorporation of waste tire initially increases the impact/UCS, G_0 whilst such values decrease at higher replacement percentages. Moreover, impact/ALM rises when increasing the cement content and the density whereas the inclusion of waste tire decreases such ratio. The control of cement content over impact/ALM values shows that any replacement of cement drops such values. To sum up, the inclusion of waste tires provides environmental benefits when impact/performance is used for evaluation.

CHAPTER 5

CONCLUSIONS

The world has been under the influence of global warming for a long time, and the world's natural resources continue to be consumed rapidly. For this reason, alternative wastes should be evaluated with various laboratory tests to check their appropriateness and produce environmentally friendly performance-based materials. This research evaluated the use of tire wastes in artificially cemented clay, such as geotechnical building materials and pavement applications. Utilization of significant amounts of such wastes can help address the global sustainability situation. Physical, mechanical, long-term durability, and environmental performances of laboratory-produced materials were evaluated. A series of UCS, UPV, and wet/dry cycles tests was conducted on samples consisting of soil, cement (7%, 10%, and 20%) of the soil dry mass, and tire rubber (TRF and TRP) of (0%, 2.5%, 5%, 10%, and 20%) as a partial replacement of cement content. All blends were prepared at (1600 and 1800 kg/m^3) dry densities and (7, 28 and 60 days) curing periods. The physical, mechanical, and durability performance of the final composites was evaluated by analyzing their microstructure using Scanning Electron Microscopy (SEM), x-ray diffraction (XRD), and x-ray fluorescence spectrometry (XRF) tests. Correlations were proposed to determine unconfined compressive strength, shear modulus, modulus of elasticity, and accumulated loss of mass for specific blends of clay with any percentage of waste tire powder replacement cured for a specific period, which can be obtained using only a single test. Finally, environmental evaluation of the blends has been performed through life cycle assessment (LCA) method. The results have been evaluated, and the outcomes of the discussion can be concluded as follows:

5.1 The Mechanical Behavior

From the mechanical properties investigation outcomes presented in this study, the following conclusions were reached:

- Based on the statistical results, the most important variables affecting the UCS, G_0 and the E of a tire-fiber-reinforced clay are the dry density and the curing period, respectively.
- Denser samples showed higher increase in q_u, G_o, and E than less compacted ones considering the significant particle contacts of blends' particles in denser samples.
- 2.5 % TRP or TRF of partial cement replacement can be selected as the optimum dosage that can improve the cemented soils' mechanical properties. 5% to 10% showed a moderate drop in the blends' strength and stiffness, whilst a significant decrease was observed for 20%.
- The TRP stabilized samples experienced a reduction on the UCS after 60 days of curing, compared with 28 days. However, this trend was not observed in the TRF group of samples. However, such phenomenon was not found in G_o and E results.
- Porosity/binders index ($\eta/X_{iv}^{0.32}$) was found to be an effective factor controlling the mechanical response of the tire-reinforced soils.
- The proposed model provides a significant contribution, as it empowers the unconfined compressive strength, initial shear modulus, and elastic modulus for blends of clays with 2.5% and 20% TRP and cement cured for specific periods to be determined by a single test.

- Proposed relationships can assist with deciding the q_u, $G_{0,}$ and E for specific blends of clay with any level of TRP substitution cured for a specific period simply by conducting non-destructive tests, such as ultrasonic pulse velocity.
- The UCS results at the lowest density, minimum cement content, and maximum tire replacement level can be satisfactorily be used in various applications, as recorded in for rammed earth, sub-base, and base for roads.

5.2 Durability

The results of durability assessment through wet/dry cycles have been discussed and the following outcomes can be concluded:

- ALM of TRP or TRF stabilized specimens considerably decreased at denser samples or when the cement content increased, regardless of other factors. However, ALM gradually increased after 2.5% of TRP or TRF inclusion.
- Comparing ALM of TRF and TRP stabilized samples, there is no considerable difference except for 1800 kg/m^3 and 7% cement group of samples, where TRF samples failed (disturbed) in their fifth to eighth wet/dry cycles.
- The ALM of all the tested composites exhibits a linear increase throughout the wet/dry cycles.
- The ALM after the twelfth cycle and the maximum initial shear modulus (G_o) correlations were found to be effective assessment methods to evaluate the durability performance of samples containing similar soil type, cement, and TRF or TRP and cured for a specific period.
- The porosity/binder index (η/X_{iv}) seemed to assess the ALM of the cemented soil stabilized with TRF or TRP considering the curing age. Moreover, normalized correlations were established to minimize the effect of the wide range of factors on the blends.

- The proposed ALM correlations with G_o and η/X_{iv} can be used to predict the ALM of any mix containing similar soil type, cement, and TRP or TRF using a single nondestructive test (UPV).

5.3 Microstructure

Microstructure analysis results of the blends were discussed, and the following outcomes are concluded:

- It is evident in the microstructural examination that a drop in cement TRP stabilized soil' strength at 60 days of curing is due to the weakening of the bonds between the tire-soil-cement interface and the unstable phase formation of magnesium alumina sulfate hydrate. That was more obvious in TRP samples due to the large surface area the tire powder provides compared to tire fibers (TRF).
- The hard shell developed around the rubber particles increases the compatibility in stiffness between rubber and clay. However, the cavity and microcracks on the surface of rubber fiber may also result in weak interfacial interaction between the cemented clay and rubber fiber and may be responsible for the reduction in unconfined compressive strength, with increase of fiber content above 2.5 %.
- The existence of carbon in the tires act as a barrier and prevented further creation of hydration products thus fewer bonding agents between soil particles and less strength of the mixes.

5.4 Environmental Assessment

The concluded outcomes of the life cycle asessments of the blends are presented as follows:

- High cement content samples have more negative environmental impacts and such effects reduces with introducing the waste rubber tire to the blends.
- Denser samples produces less environmental impact per strength or stiffness than low density samples even though denser blends consume more materials.
- Cement content is the domenent factor of environmental impact/ALM thus high cement cotent resulted in a significant increase in such factor.

The use of hazardous wastes and unsuitable soils could decrease project costs and environmental effects. In addition, improving the soil with some wastes would encourage the utilization of the available soil nearby, which does not need high technology. Moreover, waste rubber tires decraeses the brittlness which can be advantageous for reflection cracking on roads because of the cement stabilized base. In addition, it can eliminate the requirement of chip seal, geotextile, or unbound granular layer between the stabilized base and surface to provide stress relaxation. Overall, the utalization of waste in soil stablization provides range of engineering advantages as well as the social, economical, and environmental benefits compared to energy consuming materials.

5.5 Recommendations

- It is recommended to study the physio-chemical and morphological characterization of the proposed mixtures.
- It is also recommended to check the validity of the proposed correlations using the same methodology with various tire gradings as a replacement for cement.
- It is recommended to investigate the use of the idealized mixes in cemented-clay columns as a ground improvement technique. Ultimatelly, in life cycle nassesment, it is suggested to evaluate each environmental impact per unit property of the treated soils for similar projects.

REFERENCES

[1] I. Hosseinpour, M.S.S. Almeida, M. Riccio, M. Baroni, Strength and compressibility characteristics of a soft clay subjected to ground treatment, Geotech. Geol. Eng. 35 (2017) 1051–1066.

[2] M. Rezaei, R. Ajalloeian, M. Ghafoori, Geotechnical Properties of Problematic Soils Emphasis on Collapsible Cases, Int. J. Geosci. 03 (2012) 105–110. https://doi.org/10.4236/ijg.2012.31012.

[3] I. Yilmaz, B. Civelekoglu, Gypsum: An additive for stabilization of swelling clay soils, Appl. Clay Sci. 44 (2009) 166–172. https://doi.org/10.1016/j.clay.2009.01.020.

[4] A.M. Tang, Y.J. Cui, V.N. Trinh, Y. Szerman, G. Marchadier, Analysis of the railway heave induced by soil swelling at a site in southern France, Eng. Geol. 106 (2009) 68–77. https://doi.org/10.1016/j.enggeo.2009.03.002.

[5] M. Ozer, R. Ulusay, N.S. Isik, Evaluation of damage to light structures erected on a fill material rich in expansive soil, Bull. Eng. Geol. Environ. 71 (2012) 21–36. https://doi.org/10.1007/s10064-011-0395-2.

[6] H.F. Winterkorn, S. Pamukcu, Soil stabilization and grouting, in: Found. Eng. Handb., Springer, 1991: pp. 317–378.

[7] O.G. Ingles, J.B. Metcalf, Soil stabilization principles and practice, 1972.

[8] J.K. Mitchell, Soil improvement-state of the art report, in: Proc., 11th Int. Conf. SMFE, 1981: pp. 509–565.

[9] N.C. Consoli, H.C.S. Filho, P. Alegre, N. Cristelo, V. Real, Effect of wet-dry cycles on the durability, strength and stiffness of granite residual soil stabilised with Portland cement, (2019).

[10] D.R. Biswal, U.C. Sahoo, S.R. Dash, Strength and stiffness studies of

cement stabilized granular lateritic soil, in: Int. Congr. Exhib. Sustain. Civ. Infrastructures Innov. Infrastruct. Geotechnol., Springer, 2017: pp. 320–336.

[11] A. Suddeepong, A. Intra, S. Horpibulsuk, C. Suksiripattanapong, A. Arulrajah, J.S. Shen, Durability against wetting-drying cycles for cement-stabilized reclaimed asphalt pavement blended with crushed rock, Soils Found. 58 (2018) 333–343.

[12] Y. Lu, S. Liu, Y. Zhang, Z. Li, L. Xu, Freeze-thaw performance of a cement-treated expansive soil, Cold Reg. Sci. Technol. 170 (2020) 102926.

[13] M.S. Deepak, S. Rohini, B.S. Harini, G.B.G. Ananthi, Influence of fly-ash on the engineering characteristics of stabilised clay soil, Mater. Today Proc. 37 (2021) 2014–2018.

[14] S. Wang, Q. Xue, W. Ma, K. Zhao, Z. Wu, Experimental study on mechanical properties of fiber-reinforced and geopolymer-stabilized clay soil, Constr. Build. Mater. 272 (2021) 121914.

[15] M. Schneider, M. Romer, M. Tschudin, H. Bolio, Sustainable cement production—present and future, Cem. Concr. Res. 41 (2011) 642–650. https://doi.org/https://doi.org/10.1016/j.cemconres.2011.03.019.

[16] K.M. Rahla, R. Mateus, L. Bragança, Comparative sustainability assessment of binary blended concretes using Supplementary Cementitious Materials (SCMs) and Ordinary Portland Cement (OPC), J. Clean. Prod. 220 (2019) 445–459.

[17] M.S. Rafat Siddique and Arpit Kumar Singhal, Use of Unprocessed Wood Ash as Partial Replacement of Sand in Concrete, ACI Mater. J. 116 (n.d.). https://doi.org/10.14359/51718052.

[18] R.M. Andrew, Global \chem{CO_2} emissions from cement production, 1928--2018, Earth Syst. Sci. Data. 11 (2019) 1675–1710. https://doi.org/10.5194/essd-11-1675-2019.

[19] A. Ekinci, Effect of preparation methods on strength and microstructural properties of cemented marine clay, Constr. Build. Mater. 227 (2019) 116690. https://doi.org/https://doi.org/10.1016/j.conbuildmat.2019.116690.

[20] C.B. Cheah, M.H. Samsudin, M. Ramli, W.K. Part, L.E. Tan, The use of high calcium wood ash in the preparation of Ground Granulated Blast Furnace Slag and Pulverized Fly Ash geopolymers: A complete microstructural and mechanical characterization, J. Clean. Prod. 156 (2017) 114–123. https://doi.org/https://doi.org/10.1016/j.jclepro.2017.04.026.

[21] M. Frías, O. Rodríguez, M.I. Sanchez de Rojas, E. Villar-Cociña, M.S. Rodrigues, H. Savastano Junior, Advances on the development of ternary cements elaborated with biomass ashes coming from different activation process, Constr. Build. Mater. 136 (2017) 73–80. https://doi.org/https://doi.org/10.1016/j.conbuildmat.2017.01.018.

[22] R. Siddique, Utilization of wood ash in concrete manufacturing, Resour. Conserv. Recycl. 67 (2012) 27–33. https://doi.org/https://doi.org/10.1016/j.resconrec.2012.07.004.

[23] A. Mohajerani, L. Burnett, J. V Smith, S. Markovski, G. Rodwell, M.T. Rahman, H. Kurmus, M. Mirzababaei, A. Arulrajah, S. Horpibulsuk, F. Maghool, Recycling waste rubber tyres in construction materials and associated environmental considerations: A review, Resour. Conserv. Recycl. 155 (2020) 104679. https://doi.org/10.1016/j.resconrec.2020.104679.

[24] V. Torretta, E.C. Rada, M. Ragazzi, E. Trulli, I.A. Istrate, L.I. Cioca, Treatment and disposal of tyres: Two EU approaches. A review, Waste Manag. 45 (2015) 152–160. https://doi.org/10.1016/j.wasman.2015.04.018.

[25] Geological Survey Department (GSD), The Geology of Cyprus, Nicosia, Cyprus, 2017. http://www.moa.gov.cy/moa/gsd/gsd.nsf/page45_en/page45_en?OpenDocu

ment.

[26] J. Kerisel, Old structures in relation to soil conditions, Geotechnique. 25 (1975) 433–483.

[27] P. Kulanthaivel, B. Soundara, S. Velmurugan, V. Naveenraj, Experimental investigation on stabilization of clay soil using nano-materials and white cement, Mater. Today Proc. 45 (2021) 507–511.

[28] J. Chu, S. Varaksin, U. Klotz, P. Mengé, Construction processes, in: Proc. 17th Int. Conf. Soil Mech. Geotech. Eng. (Volumes 1, 2, 3 4), IOS Press, 2009: pp. 3006–3135.

[29] A. Herzog, J.K. Mitchell, Reactions accompanying stabilization of clay with cement, Highw. Res. Rec. (1963).

[30] P.J. Walker, Strength, durability and shrinkage characteristics of cement stabilised soil blocks, Cem. Concr. Compos. 17 (1995) 301–310.

[31] A.A. Al-Rawas, A.W. Hago, H. Al-Sarmi, Effect of lime, cement and Sarooj (artificial pozzolan) on the swelling potential of an expansive soil from Oman, Build. Environ. 40 (2005) 681–687.

[32] Federal Highway Administration (FHWA), Standard Specifications for Construction of Roads and Bridges on Federal Highway Projects FP-14, (2014).

[33] A. PC, Soil Cement Laboratory Handbook. Portland Cement Association, (1992) 59.

[34] SAPEM, South African Pavement Engineering Manual. South African National Roads Agency Ltd., (2009).

[35] BS 1924, Stabilized Materials for Civil Engineering Purposes. General Requirements, Sampling, Sample Preparation and Tests on Materials Before Stabilization.British Standards Institution: London, UK, (1990).

[36] D.J. Maclean, W.A. Lewis, British practice in the design and specification of cement-stabilized bases and subbases for roads, Highw. Res. Rec. (1963) 56–76.

[37] MRTS08, Plant-mixed stabilised pavements using cement or cementitious blends. Department of Transport and Main Roads Technical Standard, Australia, (2010).

[38] JTJ034, Technical specifications for construction of highway roadbases. Beijing: Ministry of Communications of the People's Republic of China, (2000).

[39] CCANZ, Cement Stabilisation. Cement & Concrete Association of New Zealand. IB89, (2008).

[40] KTŞ, Türkiye Karayolları Teknik Şartnamesi, (Turkish Highway Technical Specification). In: 407–408, ed. Ankara, Turkey: KGM, (2013).

[41] Standards Australia, The Australian earth building handbook. Standards Australia. Sydney, Australia, (2002).

[42] G.F. Middleton, L.M. Schneider, Bulletin 5. Earth-Wall Construction, 4th ed., CSIRO Division of Building, Construction and Engineering, North Ryde, Australia, 1987.

[43] NZS 4297, Engineering Design of Earth Buildings. Standard New Zealand. Wellington, New Zealand, (1998).

[44] General H and CBC, New Mexico Earthen Building Materials Code. CID-GCB-NM. Santa Fe, (2009).

[45] B.J. Dempsey, M.R. Thompson, Durability properties of lime-soil mixtures, 1967.

[46] A.A. Firoozi, C. Guney Olgun, A.A. Firoozi, M.S. Baghini, Fundamentals of soil stabilization, Int. J. Geo-Engineering. 8 (2017) 1–16.

[47] S. Nunes, C. Costa, Self-compacting concrete also standing for sustainable circular concrete, Waste Byprod. Cem. Mater. (2021) 439–480. https://doi.org/10.1016/B978-0-12-820549-5.00015-2.

[48] J. Fink, Cement additives, Pet. Eng. Guid. to Oil F. Chem. Fluids. (2021) 441–492. https://doi.org/10.1016/B978-0-323-85438-2.00010-4.

[49] B. Indraratna, A.S. Balasubramaniam, M.J. Khan, Effect of fly ash with lime and cement on the behaviour of a soft clay, Q. J. Eng. Geol. 28 (1995) 131–142. https://doi.org/10.1144/gsl.qjegh.1995.028.p2.04.

[50] H. Xiao, W. Wang, S.H. Goh, Effectiveness study for fly ash cement improved marine clay, Constr. Build. Mater. 157 (2017) 1053–1064. https://doi.org/10.1016/j.conbuildmat.2017.09.070.

[51] A. Bhurtel, A. Eisazadeh, Strength and Durability of Bottom Ash and Lime Stabilized Bangkok Clay, KSCE J. Civ. Eng. 24 (2020) 404–411. https://doi.org/10.1007/s12205-019-0850-3.

[52] A. Kumar, D. Gupta, Behavior of cement-stabilized fiber-reinforced pond ash, rice husk ash-soil mixtures, Geotext. Geomembranes. 44 (2016) 466–474. https://doi.org/10.1016/j.geotexmem.2015.07.010.

[53] S. Gowthaman, K. Nakashima, S. Kawasaki, A State-of-the-Art Review on Soil Reinforcement Technology Using Natural Plant Fiber Materials: Past Findings, Present Trends and Future Directions, Mater. . 11 (2018). https://doi.org/10.3390/ma11040553.

[54] C. Li, J.G. Zornberg, Validation of discrete framework for fiber-reinforcement, in: Proc., North Am. Conf. Geosynth., Citeseer, 2003.

[55] C. Li, J.G. Zornberg, Interface shear strength in fiber-reinforced soil, in: Proc. Int. Conf. SOIL Mech. Geotech. Eng., Citeseer, 2005: p. 1373.

[56] B.J. Freilich, C. Li, J.G. Zornberg, Effective shear strength of fiber-reinforced clays, in: 9th Int. Conf. Geosynth. Brazil, Citeseer, 2010: pp.

1997–2000.

[57] C. Tang, B. Shi, W. Gao, F. Chen, Y. Cai, Strength and mechanical behavior of short polypropylene fiber reinforced and cement stabilized clayey soil, Geotext. Geomembranes. 25 (2007) 194–202.

[58] Z.H. Özkul, G. Baykal, Shear behavior of compacted rubber fiber-clay composite in drained and undrained loading, J. Geotech. Geoenvironmental Eng. 133 (2007) 767–781.

[59] A. Ekinci, P.M. V Ferreira, The undrained mechanical behaviour of a fibre-reinforced heavily over-consolidated clay, in: ISSMGE TC211 and BBRI, 2012.

[60] M. Mirzababaei, M. Miraftab, M. Mohamed, P. McMahon, Unconfined compression strength of reinforced clays with carpet waste fibers, J. Geotech. Geoenvironmental Eng. 139 (2013) 483–493.

[61] I. Falorca, M.I.M. Pinto, Effect of short, randomly distributed polypropylene microfibres on shear strength behaviour of soils, Geosynth. Int. 18 (2011) 2–11.

[62] M. Mirzababaei, A. Arulrajah, S. Horpibulsuk, M. Aldava, Shear strength of a fibre-reinforced clay at large shear displacement when subjected to different stress histories, Geotext. Geomembranes. 45 (2017) 422–429.

[63] A. Ekinci, P.M.V. Ferreira, M. Rezaeian, The mechanical behaviour of compacted Lambeth-group clays with and without fibre reinforcement, Geotext. Geomembranes. 50 (2022) 1–19.

[64] A. Ekinci, A. Abki, M. Mirzababaei, Parameters Controlling Strength, Stiffness and Durability of a Fibre-Reinforced Clay, Int. J. Geosynth. Gr. Eng. 8 (2022). https://doi.org/10.1007/s40891-022-00352-8.

[65] A. Al-Tabbaa, T. Aravinthan, Natural clay-shredded tire mixtures as landfill barrier materials, Waste Manag. 18 (1998) 9–16.

https://doi.org/10.1016/S0956-053X(98)00002-6.

[66] H.J. Pendola, T.W. Kennedy, W.R. Hudson, Evaluation of factors affecting the tensile properties of cement-treated materials, Center for Highway Research, University of Texas at Austin, 1969.

[67] N.C. Consoli, D. Foppa, L. Festugato, K.S. Heineck, Key Parameters for Strength Control of Artificially Cemented Soils, J. Geotech. Geoenvironmental Eng. 133 (2007) 197–205. https://doi.org/10.1061/(asce)1090-0241(2007)133:2(197).

[68] N.C. Consoli, D.A. Rosa, R.C. Cruz, A.D. Rosa, Water content, porosity and cement content as parameters controlling strength of artificially cemented silty soil, Eng. Geol. 122 (2011) 328–333. https://doi.org/10.1016/j.enggeo.2011.05.017.

[69] N.C. Consoli, R.R. de Moraes, L. Festugato, Variables controlling strength of fibre-reinforced cemented soils, Proc. Inst. Civ. Eng. Gr. Improv. 166 (2013) 221–232. https://doi.org/10.1680/grim.12.00004.

[70] N.C. Consoli, R.A. Quiñónez, L.E. González, R.A. López, Influence of Molding Moisture Content and Porosity/Cement Index on Stiffness, Strength, and Failure Envelopes of Artificially Cemented Fine-Grained Soils, J. Mater. Civ. Eng. 29 (2017) 4016277. https://doi.org/10.1061/(asce)mt.1943-5533.0001819.

[71] N.C. Consoli, S.F.V. Marques, M.F. Floss, L. Festugato, Broad-Spectrum Empirical Correlation Determining Tensile and Compressive Strength of Cement-Bonded Clean Granular Soils, J. Mater. Civ. Eng. 29 (2017) 6017004. https://doi.org/10.1061/(asce)mt.1943-5533.0001858.

[72] C. Henzinger, S.A. Schuhmacher, L. Festugato, Applicability of the Porosity/Binder Index to Nonhomogeneous Mixtures of Fine-Grained Soil with Lignite Fly Ash, J. Mater. Civ. Eng. 30 (2018) 6018013. https://doi.org/10.1061/(asce)mt.1943-5533.0002447.

[73] A. Ekinci, H.C. Scheuermann Filho, N.C. Consoli, Copper Slag-Hydrated Lime-Portland Cement Stabilized Marine Deposited Clay, Proc. Inst. Civ. Eng. Improv. (2019) 1–30.

[74] N.C. Consoli, A. V da Fonseca, S.R. Silva, R.C. Cruz, A. Fonini, Parameters controlling stiffness and strength of artificially cemented soils, Geotechnique. 62 (2012) 177–183. https://doi.org/10.1680/geot.8.P.084.

[75] N.C. Consoli, E.J. Bittar Marin, R.A. Quiñónez Samaniego, K.S. Heineck, A.D.R. Johann, Use of Sustainable Binders in Soil Stabilization, J. Mater. Civ. Eng. 31 (2019) 6018023. https://doi.org/10.1061/(asce)mt.1943-5533.0002571.

[76] L. Festugato, E. Menger, F. Benezra, E.A. Kipper, N.C. Consoli, Fibre-reinforced cemented soils compressive and tensile strength assessment as a function of filament length, Geotext. Geomembranes. 45 (2017) 77–82.

[77] M. Mirzababaei, M. Mohamed, A. Arulrajah, S. Horpibulsuk, V. Anggraini, Practical approach to predict the shear strength of fibre-reinforced clay, Geosynth. Int. 25 (2018) 50–66.

[78] L. Festugato, A.P. da Silva, A. Diambra, N.C. Consoli, E. Ibraim, Modelling tensile/compressive strength ratio of fibre reinforced cemented soils, Geotext. Geomembranes. 46 (2018) 155–165.

[79] N.C. Consoli, L.F. Tomasi, The impact of dry unit weight and cement content on the durability of sand–cement blends, Proc. Inst. Civ. Eng. Improv. 171 (2018) 96–102.

[80] N.C. Consoli, K. da Silva, S. Filho, A.B. Rivoire, Compacted clay-industrial wastes blends: Long term performance under extreme freeze-thaw and wet-dry conditions, Appl. Clay Sci. 146 (2017) 404–410. https://doi.org/https://doi.org/10.1016/j.clay.2017.06.032.

[81] M. Hanafi, A. Ekinci, E. Aydin, Triple-Binder-Stabilized Marine Deposit

Clay for Better Sustainability, Sustainability. 12 (2020) 1–16.

[82] N.C. Consoli, L. Festugato, H.C.S. Filho, G.D. Miguel, A.T. Neto, D. Andreghetto, Durability assessment of soil-pozzolan-lime blends through ultrasonic-pulse velocity test, J. Mater. Civ. Eng. 32 (2020) 4020223.

[83] Y.T. Kim, H.S. Kang, Engineering Characteristics of Rubber-Added Lightweight Soil as a Flowable Backfill Material, J. Mater. Civ. Eng. 23 (2011) 1289–1294. https://doi.org/10.1061/(asce)mt.1943-5533.0000307.

[84] A. Al-Tabbaa, T. Aravinthan, Natural clay-shredded tire mixtures as landfill barrier materials, Waste Manag. 18 (1998) 9–16. https://doi.org/10.1016/S0956-053X(98)00002-6.

[85] C. Hidalgo Signes, J. Garzón-Roca, P. Martínez Fernández, M.E. Garrido de la Torre, R. Insa Franco, Swelling potential reduction of Spanish argillaceous marlstone Facies Tap soil through the addition of crumb rubber particles from scrap tyres, Appl. Clay Sci. 132–133 (2016) 768–773. https://doi.org/10.1016/j.clay.2016.07.027.

[86] A.F. Cabalar, Z. Karabash, W.S. Mustafa, Stabilising a clay using tyre buffings and lime, Road Mater. Pavement Des. 15 (2014) 872–891. https://doi.org/10.1080/14680629.2014.939697.

[87] A. Ahmed, M.H. El Naggar, Effect of cyclic loading on the compressive strength of soil stabilized with bassanite–tire mixture, J. Mater. Cycles Waste Manag. 20 (2018) 525–532. https://doi.org/10.1007/s10163-017-0617-1.

[88] E. Kalkan, Preparation of scrap tire rubber fiber-silica fume mixtures for modification of clayey soils, Appl. Clay Sci. 80–81 (2013) 117–125. https://doi.org/10.1016/j.clay.2013.06.014.

[89] S. Akbulut, S. Arasan, E. Kalkan, Modification of clayey soils using scrap tire rubber and synthetic fibers, Appl. Clay Sci. 38 (2007) 23–32.

https://doi.org/10.1016/j.clay.2007.02.001.

[90] J.S. Yadav, S.K. Tiwari, A study on the potential utilization of crumb rubber in cement treated soft clay, J. Build. Eng. 9 (2017) 177–191. https://doi.org/10.1016/j.jobe.2017.01.001.

[91] M.A. Shahin, L.S. Hong, Utilization of shredded rubber tires for cement-stabilized soft clays, in: Gr. Improv. Geosynth., 2010: pp. 181–186.

[92] M. Ho, C. Chan, I. Bakar, One Dimensional Compressibility Characteristics of Clay Stabilised with Cement-Rubber Chips, Int. J. Sustain. Constr. Eng. Technol. 1 (2010) 91–104.

[93] C.-M. Chan, Strength and stiffness of a cement-stabilised lateritic soil with granulated rubber addition, Proc. Inst. Civ. Eng. Improv. 165 (2012) 41–52.

[94] J.S. Yadav, S.K. Tiwari, Effect of waste rubber fibres on the geotechnical properties of clay stabilized with cement, Appl. Clay Sci. 149 (2017) 97–110. https://doi.org/10.1016/j.clay.2017.07.037.

[95] B.-W. Jo, G.-H. Tae, B.-Y. Kwon, Ductility evaluation of prestressed concrete beams with CFRP tendons, J. Reinf. Plast. Compos. 23 (2004) 843–859.

[96] M. Bekhiti, H. Trouzine, M. Rabehi, Influence of waste tire rubber fibers on swelling behavior, unconfined compressive strength and ductility of cement stabilized bentonite clay soil, Constr. Build. Mater. 208 (2019) 304–313.

[97] D. Akbarimehr, A. Eslami, E. Aflaki, Geotechnical behaviour of clay soil mixed with rubber waste, J. Clean. Prod. 271 (2020) 122632.

[98] E. Cokca, Z. Yilmaz, Use of rubber and bentonite added fly ash as a liner material, Waste Manag. 24 (2004) 153–164.

[99] M. Roustaei, M. Ghazavi, Strength characteristics of clay mixtures with waste materials in freeze-thaw cycles, (2011).

[100] M. Jafari, M. Esna-ashari, Effect of waste tire cord reinforcement on unconfined compressive strength of lime stabilized clayey soil under freeze–thaw condition, Cold Reg. Sci. Technol. 82 (2012) 21–29.

[101] J.S. Yadav, S.K. Tiwari, Effect of inclusion of crumb rubber on the unconfined compressive strength and wet-dry durability of cement stabilized clayey soil, J. Build. Mater. Struct. 3 (2016) 68–84.

[102] J. Bonnot, Semi-rigid pavements, Assoc. Int. Perm. Des Congrès La Route Paris, Fr. (1991).

[103] K. Frenken, Irrigation in the Middle East region in figures AQUASTAT Survey-2008., Water Reports. (2009).

[104] S.A. Salman, S. Shahid, T. Ismail, K. Ahmed, E.-S. Chung, X.-J. Wang, Characteristics of annual and seasonal trends of rainfall and temperature in Iraq, Asia-Pacific J. Atmos. Sci. 55 (2019) 429–438.

[105] G. Li, F. Wang, W. Ma, R. Fortier, Y. Mu, Y. Mao, X. Hou, Variations in strength and deformation of compacted loess exposed to wetting-drying and freeze-thaw cycles, Cold Reg. Sci. Technol. 151 (2018) 159–167.

[106] USACE, Soil Stabilization for Pavements, USACE Tech. Man. No. TM5-822-14. (1994).

[107] Unified Facilities Criteria (UFC), UFC 3-250-11 Soil Stabilization and Modifications for Pavements, Washington, DC, 2020.

[108] Unified Facilities Guide Specifications (UFGS), UFGS 32 11 13.13 Lime Treated Subgrade, Washington, DC, 2019.

[109] J.P. Guyer, An introduction to soil stabilization for pavements, Guyer Partners, 2018.

[110] U.S.A.E. School., Computer literacy: student workbook, class 45C22 (EOAC), class 45C20 (EOBC)., (1986) 41 p.

file://catalog.hathitrust.org/Record/002725478.

[111] Portland Cement Association (PCA), Soil Cement Laboratory Handbook, Engineering Bulletin, Portland Cement Association, Skokie, IL, 1992.

[112] R.G. Hicks, Alaska soil stabilization design guide, Alaska. Department of Transportation and Public Facilities. Research and …, 2002.

[113] J.A. Epps, W.A. Dunlap, B.M. Gallaway, D.D. Currin, Soil stabilization: a mission oriented approach, Highw. Res. Rec. (1971).

[114] R. Fitzmaurice, Manual on stabilized soil construction for housing, (1958).

[115] Indian Road Congress (IRC), Guidelines for the design of flexible pavements, Indian Code Pract. 37 (2012).

[116] Indian Standard, IS : 4332 (Part IV). METHODS OF TEST FOR STABILIZED SOILS, New Delhi, 1986.

[117] M. Banar, Life cycle assessment of waste tire pyrolysis, Fresenius Environ. Bull. 24 (2015) 1215–1226.

[118] A.J. Raymond, M. Asce, J.T. Dejong, F. Asce, A. Kendall, ; J Tanner Blackburn, R. Deschamps, Life Cycle Sustainability Assessment of Geotechnical Ground Improvement Methods, J. Geotech. Geoenvironmental Eng. 147 (2021) 04021161. https://doi.org/10.1061/(ASCE)GT.1943-5606.0002646.

[119] C.G. da Rocha, A. Passuello, N.C. Consoli, R.A. Quiñónez Samaniego, N.M. Kanazawa, Life cycle assessment for soil stabilization dosages: A study for the Paraguayan Chaco, J. Clean. Prod. 139 (2016) 309–318. https://doi.org/10.1016/j.jclepro.2016.07.219.

[120] D.G.A. Holt, Jefferson, P.A. Braithwaite, D.N. Chapman, P.D. Student, Sustainable Geotechnical Design, (2010) 2925–2932. https://doi.org/10.1061/41095(365)298.

[121] K. Johansson, Life cycle assessment of two end-of-life tyre applications: artificial turfs and asphalt rubber, (2018) 71.

[122] I. Samuelsson, S. Larsson, J. Spross, Life cycle assessment and life cycle cost analysis for geotechnical engineering: Review and research gaps, IOP Conf. Ser. Earth Environ. Sci. 710 (2021). https://doi.org/10.1088/1755-1315/710/1/012031.

[123] C. Spaulding, F. Masse, J. LaBrozzi, Ground Improvement Technologies for a Sustainable World, Civ. Eng. Mag. Arch. 78 (2008) 54–59. https://doi.org/10.1061/CIEGAG.0000168.

[124] M.A. Rahgozar, M. Saberian, J. Li, Soil stabilization with non-conventional eco-friendly agricultural waste materials: An experimental study, Transp. Geotech. 14 (2018) 52–60. https://doi.org/10.1016/J.TRGEO.2017.09.004.

[125] A.J. Raymond, M.A. Pinkse, A. Kendall, J.T. DeJong, Life-Cycle Assessment of Ground Improvement Alternatives for the Treasure Island, California, Redevelopment, 2020 (2017) 345–354. https://doi.org/10.1061/9780784480434.037.

[126] S.A. Jefferis, Moving Towards Sustainability in Geotechnical Engineering, (2008). https://doi.org/10.1061/40971.

[127] X. Song, C. Carlsson, R. Kiilsgaard, D. Bendz, H. Kennedy, Life cycle assessment of geotechnical works in building construction: A review and recommendations, Sustain. 12 (2020) 1–17. https://doi.org/10.3390/su12208442.

[128] A. Nordelöf, S. Poulikidou, M. Chordia, F.B. de Oliveira, J. Tivander, R. Arvidsson, Methodological approaches to end-of-life modelling in life cycle assessments of lithium-ion batteries, Batteries. 5 (2019). https://doi.org/10.3390/batteries5030051.

[129] A. Kendall, A.J. Raymond, J. Tipton, J.T. DeJong, Review of life-cycle-

based environmental assessments of geotechnical systems, Proc. Inst. Civ. Eng. Eng. Sustain. 171 (2016) 57–67. https://doi.org/10.1680/JENSU.16.00073/SUPPL_FILE/JENSU.16.00073_SUPPLEMENTARYMATERIAL.PDF.

[130] C.M. Shillaber, S.M. Asce, J.K. Mitchell, P.E.M. Asce, J.E. Dove, M. Asce, Energy and Carbon Assessment of Ground Improvement Works. II: Working Model and Example, J. Geotech. Geoenvironmental Eng. 142 (2016) 04015084. https://doi.org/10.1061/(ASCE)GT.1943-5606.0001411.

[131] C. Chau, K. Soga, D. Nicholson, N. O'Riordan, T. Inui, Embodied Energy as an Environmental Impact Indicator for Basement Wall Construction, (2008) 867–874. https://doi.org/10.1061/40971(310)108.

[132] R. Storesund, M. Asce, J. Massey, A.M. Asce, Y. Kim, Life Cycle Impacts for Concrete Retaining Walls vs. Bioengineered Slopes, (2008) 875–882. https://doi.org/10.1061/40971(310)109.

[133] S.D. Rafalko, J.E. Sankey, N. Freitag, Sustainability Measures for MSE Walls and Baseline Environmental Impact Evaluations, (2010) 486–493. https://doi.org/10.1061/41128(384)48.

[134] L. Li, K. Chen, Quantitative assessment of carbon dioxide emissions in construction projects: A case study in Shenzhen, J. Clean. Prod. 141 (2017) 394–408. https://doi.org/10.1016/J.JCLEPRO.2016.09.134.

[135] S. Bressi, J. Santos, M. Giunta, L. Pistonesi, D. Lo Presti, A comparative life-cycle assessment of asphalt mixtures for railway sub-ballast containing alternative materials, Resour. Conserv. Recycl. 137 (2018) 76–88. https://doi.org/10.1016/j.resconrec.2018.05.028.

[136] A.R. Sánchez, V.C. Ramos, M.S. Polo, M.V.L. Ramón, J. Utrilla, Life cycle assessment of cement production with marble waste sludges, Int. J. Environ. Res. Public Health. 18 (2021). https://doi.org/10.3390/ijerph182010968.

[137] C.G. da Rocha, R.B. Saldanha, M. Tonini de Araújo, N.C. Consoli, Social and environmental assessments of Eco-friendly Pavement alternatives, Constr. Build. Mater. 325 (2022) 126736. https://doi.org/10.1016/j.conbuildmat.2022.126736.

[138] I. Bianco, D. Panepinto, M. Zanetti, End-of-life tyres: Comparative life cycle assessment of treatment scenarios, Appl. Sci. 11 (2021). https://doi.org/10.3390/app11083599.

[139] R. Feraldi, S. Cashman, M. Huff, L. Raahauge, Comparative LCA of treatment options for US scrap tires: Material recycling and tire-derived fuel combustion, Int. J. Life Cycle Assess. 18 (2013) 613–625. https://doi.org/10.1007/s11367-012-0514-8.

[140] Y. Hakyemez, N. Turhan, I. Sönmez, M. Sümengen, The Geology of the Turkish Republic of Northern Cyprus. Department of the Geological Surveys, General Directorate of the Minerals Research and Exploration of Turkey, Unpubl. Rep. 44 (2000).

[141] ASTM D4318-17e1, Standard Test Methods for Liquid Limit, Plastic Limit, and Plasticity Index of Soils, ASTM Int. (2017). https://doi.org/10.1520/D4318-17E01.

[142] ASTM D6913 / D6913M-17, Standard Test Methods for Particle-Size Distribution (Gradation) of Soils Using Sieve Analysis, ASTM Int. (2017). https://doi.org/10.1520/D6913_D6913M-17.

[143] ASTM D854-14, Standard Test Methods for Specific Gravity of Soil Solids by Water Pycnometer, ASTM Int. (2014). https://doi.org/10.1520/D0854-14.

[144] ASTM C150 / C150M-20, Standard Specification for Portland Cement, ASTM Int. (2020). https://doi.org/10.1520/C0150_C0150M-20.

[145] ASTM D698-12e2, Standard Test Methods for Laboratory Compaction Characteristics of Soil Using Standard Effort (12 400 ft-lbf/ft3 (600 kN-

m/m3)), ASTM Int. (2012). https://doi.org/10.1520/D0698-12E02.

[146] R.S. Ladd, Preparing test specimens using undercompaction, Geotech. Test. J. 1 (1978) 16–23.

[147] ASTM C511-19, Standard Specification for Mixing Rooms, Moist Cabinets, Moist Rooms, and Water Storage Tanks Used in the Testing of Hydraulic Cements and Concretes, ASTM Int. (2019). https://doi.org/10.1520/C0511-19.

[148] N.C. Consoli, D. Winter, H.B. Leon, H.C. Scheuermann Filho, Durability, Strength, and Stiffness of Green Stabilized Sand, J. Geotech. Geoenvironmental Eng. 144 (2018) 04018057. https://doi.org/10.1061/(ASCE)GT.1943-5606.0001928.

[149] E.B. Moreira, J.A. Baldovino, J.L. Rose, R. Luis dos Santos Izzo, Effects of porosity, dry unit weight, cement content and void/cement ratio on unconfined compressive strength of roof tile waste-silty soil mixtures, J. Rock Mech. Geotech. Eng. 11 (2019) 369–378. https://doi.org/10.1016/j.jrmge.2018.04.015.

[150] N.C. Consoli, A. da Silva, A.M. Barcelos, L. Festugato, F. Favretto, Porosity/Cement Index Controlling Flexural Tensile Strength of Artificially Cemented Soils in Brazil, Geotech. Geol. Eng. 38 (2020) 713–722. https://doi.org/10.1007/s10706-019-01059-w.

[151] A. Ekinci, M. Hanafi, E. Aydin, Strength, Stiffness, and Microstructure of Wood-Ash Stabilized Marine Clay, Minerals. 10 (2020) 796.

[152] J.J.A. Baldovino, R.L.S. Izzo, J.L. Rose, M.D.I. Domingos, Strength, durability, and microstructure of geopolymers based on recycled-glass powder waste and dolomitic lime for soil stabilization, Constr. Build. Mater. 271 (2021) 121874.

[153] A. Diambra, E. Ibraim, A. Peccin, N.C. Consoli, L. Festugato, Theoretical

derivation of artificially cemented granular soil strength, J. Geotech. Geoenvironmental Eng. 143 (2017) 4017003.

[154] J.A. Baldovino, R.L. dos Santos Izzo, C. Millan-Paramo, An equation to estimate the compressive and tensile strengths of lime-stabilized soils in Curitiba, Brazil, Arab. J. Geosci. 15 (2022) 419. https://doi.org/10.1007/s12517-022-09681-4.

[155] ASTM D1633-17, Standard Test Methods for Compressive Strength of Molded Soil-Cement Cylinders, ASTM Int. (2017). https://doi.org/10.1520/D1633-17.

[156] ASTM C597-02, Standard Test Method for Pulse Velocity Through Concrete, ASTM Int. (2002). https://doi.org/10.1520/C0597-02.

[157] ASTM D559 / D559M-15, Standard Test Methods for Wetting and Drying Compacted Soil-Cement Mixtures, ASTM Int. (2015). https://doi.org/10.1520/D0559_D0559M-15.

[158] OpenLCA v1.10.3, The open source software for sustainability assessment., GreenDelta. (2020). https://www.openlca.org (accessed March 15, 2022).

[159] I.O. for Standardization, Environmental management: life cycle assessment; Principles and Framework, ISO, 2006.

[160] I.O. for Standardization, Environmental management: life cycle assessment; requirements and guidelines, ISO Geneva, Switzerland, 2006.

[161] Ecoinvent, Ecoinvent database version 3.7, Zurich, Switzerland, 2020. https://ecoinvent.org/the-ecoinvent-database/data-releases/ecoinvent-3-7/.

[162] Ecoinvent, Ecoinvent database version 3.7, Zurich, Switzerland, 2020.

[163] A. Ahmed, Simplified regression model to predict the strength of reinforced sand with waste polystyrene plastic type, Geotech. Geol. Eng. 30 (2012) 963–973.

[164] W.S. Adaska, D.R. Luhr, Control of reflective cracking in cement stabilized pavements, in: Proc. 5th Int. RILEM Conf. Crack. Pavements, 2004: pp. 309–316.

[165] T. Scullion, Precracking of soil-cement bases to reduce reflection cracking: Field investigation, Transp. Res. Rec. 1787 (2002) 22–30.

[166] A. Ahmed, M.H. El Naggar, Swelling and geo-environmental properties of bentonite treated with recycled bassanite, Appl. Clay Sci. 121 (2016) 95–102.

[167] G. Habert, S.A. Miller, V.M. John, J.L. Provis, A. Favier, A. Horvath, K.L. Scrivener, Environmental impacts and decarbonization strategies in the cement and concrete industries, Nat. Rev. Earth Environ. 2020 111. 1 (2020) 559–573. https://doi.org/10.1038/s43017-020-0093-3.

APPENDICES

A. ANOVA Responses Tables

Table A.1. ANOVA table of responses regarding unconfined compressive strength, initial shear modulus and elastic modulus of TRP samples.

	Source	Sum of Squares	Df	Mean Square	F-Ratio	P-Value
Unconfined Compressive Strength, q_u	MAIN EFFECTS					
	A: Dry Density (kg/m^3)	140919000	1	140919000	1221.41	0.0000
	B: Cement (%)	122346000	2	61172800	530.21	0.0000
	C: Tyre Rubber Powder (%)	49515300	4	12378800	107.29	0.0000
	D: Curing (Days)	176113000	2	88056700	763.23	0.0000
	INTERACTIONS					
	AB	2567040	2	1283520	11.12	0.0000
	AC	17787400	4	4446850	38.54	0.0000
	AD	12484000	2	6241990	54.1	0.0000
	BC	9168470	8	1146060	9.93	0.0000
	BD	11099600	4	2774910	24.05	0.0000
	CD	41215700	8	5151960	44.65	0.0000
	ABC	3523020	8	440377	3.82	0.0006
	ABD	4923210	4	1230800	10.67	0.0000
	ACD	8385160	8	1048140	9.08	0.0000
	BCD	5393290	16	337081	2.92	0.0005
	RESIDUAL	12229700	106	115374		
	TOTAL (CORRECTED)	617670000	179			
Initial Shear modulus, G_0	MAIN EFFECTS					
	A: Dry Density (kg/m^3)	102484000	1	102484000	1374.09	0.0000
	B: Cement (%)	51435500	2	25717800	344.82	0.0000
	C: Tyre Rubber Powder (%)	21508400	4	5377090	72.1	0.0000
	D: Curing (Days)	63954600	2	31977300	428.75	0.0000
	INTERACTIONS					
	AB	1305980	2	652988	8.76	0.0003
	AC	733934	4	183483	2.46	0.0498
	AD	2633910	2	1316960	17.66	0.0000
	BC	1351280	8	168909	2.26	0.0282
	BD	2082890	4	520723	6.98	0.0000
	CD	5024640	8	628080	8.42	0.0000
	ABC	1707760	8	213470	2.86	0.0064
	ABD	1506420	4	376606	5.05	0.0009
	ACD	483564	8	60445.6	0.81	0.5949
	BCD	671947	16	41996.7	0.56	0.9047
	RESIDUAL	7905790	106	74582.9		
	TOTAL (CORRECTED)	264790000	179			
Elastic modulus, E	MAIN EFFECTS					
	A: Dry Density (kg/m^3)	632879	1	632879	635.31	0.0000
	B: Cement (%)	761284	2	380642	382.11	0.0000
	C: Tyre Rubber Powder (%)	515286	4	128822	129.32	0.0000
	D: Curing (Days)	1524890	2	762444	765.37	0.0000
	INTERACTIONS					
	AB	6046	2	3022.97	3.03	0.0519
	AC	9986	4	2496.58	2.51	0.0459
	AD	80915	2	40457.70	40.61	0.0000
	BC	42236	8	5279.44	5.3	0.0000
	BD	24500	4	6125.06	6.15	0.0002
	CD	160372	8	20046.60	20.12	0.0000
	ABC	30112	8	3763.93	3.78	0.0006
	ABD	10413	4	2603.32	2.61	0.0389
	ACD	19826	8	2478.19	2.49	0.0158
	RESIDUAL	115556	116	996.17		
	TOTAL (CORRECTED)	4489620	173			

Table A.2. ANOVA table of responses regarding unconfined compressive strength, initial shear modulus and elastic modulus of TRF samples.

	Source	Sum of Squares	Df	Mean Square	F-Ratio	P-Value
Unconfined Compressive Strength, q_u	MAIN EFFECTS					
	A: Dry Density (kg/m^3)	122586000	1	122586000	3077.35	0.0000
	B: Cement (%)	124272000	2	62135900	1559.83	0.0000
	C: Tyre Rubber Fiber (%)	60385900	4	15096500	378.97	0.0000
	D: Curing (Days)	163743000	2	81871700	2055.27	0.0000
	INTERACTIONS					
	AB	3530980	2	1765490	44.32	0.0000
	AC	19591800	4	4897960	122.96	0.0000
	AD	15839900	2	7919950	198.82	0.0000
	BC	10849800	8	1356230	34.05	0.0000
	BD	6147820	4	1536960	38.58	0.0000
	CD	26487100	8	3310890	83.12	0.0000
	ABC	2376580	8	297072	7.46	0.0000
	ABD	1339010	4	334751	8.4	0.0000
	ACD	6858890	8	857361	21.52	0.0000
	BCD	4568140	16	285509	7.17	0.0000
	RESIDUAL	4222510	106	39835		
	TOTAL (CORRECTED)	572800000	179			
Initial Shear modulus, G_o	MAIN EFFECTS					
	A: Dry Density (kg/m^3)	101007000	1	101007000	3055.77	0.0000
	B: Cement (%)	47886100	2	23943100	724.35	0.0000
	C: Tyre Rubber Fiber (%)	20344300	4	5086080	153.87	0.0000
	D: Curing (Days)	88042400	2	44021200	1331.78	0.0000
	INTERACTIONS					
	AB	1136910	2	568456	17.2	0.0000
	AC	2402250	4	600562	18.17	0.0000
	AD	1665500	2	832751	25.19	0.0000
	BC	2167240	8	270905	8.2	0.0000
	BD	1380420	4	345104	10.44	0.0000
	CD	1629340	8	203668	6.16	0.0000
	ABC	628476	8	78559.5	2.38	0.0214
	ABD	951092	4	237773	7.19	0.0000
	ACD	1885740	8	235718	7.13	0.0000
	BCD	1242790	16	77674.6	2.35	0.0051
	RESIDUAL	3503770	106	33054.4		
	TOTAL (CORRECTED)	275873000	179			
Elastic modulus, E	MAIN EFFECTS					
	A: Dry Density (kg/m^3)	1145390	1	1145390	1789.57	0.0000
	B: Cement (%)	881730	2	440865	688.81	0.0000
	C: Tyre Rubber Fiber (%)	569087	4	142272	222.29	0.0000
	D: Curing (Days)	1399580	2	699791	1093.36	0.0000
	INTERACTIONS					
	AB	38721	2	19360.40	30.25	0.0000
	AC	28857	4	7214.23	11.27	0.0000
	AD	56597	2	28298.30	44.21	0.0000
	BC	32319	8	4039.93	6.31	0.0000
	BD	24495	4	6123.63	9.57	0.0000
	CD	99485	8	12435.60	19.43	0.0000
	ABC	13213	8	1651.60	2.58	0.0125
	ABD	13718	4	3429.47	5.36	0.0005
	ACD	9739	8	1217.41	1.9	0.0661
	RESIDUAL	74244	116	640.04		
	TOTAL (CORRECTED)	4489620	173			

Table A.3. ANOVA table of responses regarding the validation of the normalized UCS, G_0 and E relation with $n/(X_{iv})^{0.32}$.

TRP					
Normalized UCS		**Normalized G_0**		**Normalized E**	
Model	**R-Squared**	**Model**	**R-Squared**	**Model**	**R-Squared**
Power	89.45%	Power	89.12%	Power	76.77%
Exponential	89.37%	Reciprocal-Y	88.90%	Multiplicative	76.57%
Logarithmic-Y square root-X	89.29%	Reciprocal-Y square root-X	88.69%	Logarithmic-Y square root-X	76.51%
Logarithmic-Y squared-X	89.15%	Reciprocal-Y squared-X	88.68%	Square root-Y reciprocal-X	76.44%
Multiplicative	89.29%	Reciprocal-Y logarithmic-X	88.27%	Exponential	76.28%
Reciprocal-Y squared-X	88.84%	Multiplicative	88.00%	S-curve model	76.23%
Square root-Y logarithmic-X	88.79%	Logarithmic-Y square root-X	87.93%	Square root-Y logarithmic-X	76.16%
Square root-Y reciprocal-X	88.74%	Exponential	87.64%	Reciprocal-Y squared-X	76.00%
Double square root	88.54%	S-curve model	87.51%	Double square root	75.78%
S-curve model	88.12%	Square root-Y reciprocal-X	87.02%	Reciprocal-X	75.78%
Square root-Y	88.10%	Square root-Y logarithmic-X	87.02%	Reciprocal-Y	75.67%
Reciprocal-X	87.44%	Double reciprocal	86.79%	Logarithmic-Y squared-X	75.37%
Reciprocal-Y	87.08%	Double square root	86.69%	Reciprocal-Y square root-X	75.28%
Square root-Y squared-X	86.69%	Logarithmic-Y squared-X	86.46%	Square root-Y	75.25%
Logarithmic-X	86.42%	Square root-Y	86.17%	Logarithmic-X	74.89%
Reciprocal-Y square root-X	85.92%	Reciprocal-X	85.94%	Reciprocal-Y logarithmic-X	74.72%
Square root-X	85.64%	Logarithmic-X	85.45%	Square root-X	74.21%
Linear	84.69%	Square root-X	84.90%	Square root-Y squared-X	73.74%
Reciprocal-Y logarithmic-X	84.59%	Square root-Y squared-X	84.53%	Linear	73.39%
Squared-X	82.32%	Linear	84.14%	Double reciprocal	73.17%
Double reciprocal	81.46%	Squared-X	82.08%	Squared-Y reciprocal-X	72.09%
Squared-Y reciprocal-X	80.17%	Squared-Y reciprocal-X	82.05%	Squared-X	71.34%
Squared-Y logarithmic-X	77.36%	Squared-Y logarithmic-X	80.68%	Squared-Y logarithmic-X	70.14%
Squared-Y square root-X	75.75%	Squared-Y square root-X	79.70%	Squared-Y square root-X	68.95%
Squared-Y	74.02%	Squared-Y	78.55%	Squared-Y	67.65%
Double squared	70.27%	Double squared	75.77%	Double squared	64.73%
Logistic		Logistic		Logistic	
Log probit		Log probit		Log probit	
TRF					
Power	**89.21%**	Power	**89.45%**	Power	**89.41%**
Logarithmic-Y square root-X	89.11%	Logarithmic-Y square root-X	89.37%	Exponential	89.23%
Multiplicative	89.11%	Multiplicative	89.36%	Logarithmic-Y square root-X	89.09%
Exponential	88.93%	Exponential	89.15%	Logarithmic-Y squared-X	88.89%
S-curve model	88.55%	Square root-Y logarithmic-X	89.14%	Square root-Y logarithmic-X	88.82%
Square root-Y reciprocal-X	88.52%	Reciprocal-Y	89.03%	Double square root	88.80%
Reciprocal-Y squared-X	88.43%	Double square root	88.94%	Multiplicative	88.75%
Square root-Y logarithmic-X	88.05%	Square root-Y reciprocal-X	88.85%	Square root-Y	88.57%
Logarithmic-Y squared-X	88.04%	Reciprocal-Y square root-X	88.84%	Square root-Y reciprocal-X	88.22%
Double square root	87.55%	Reciprocal-Y squared-X	88.75%	Reciprocal-X	87.82%
Reciprocal-Y	87.39%	S-curve model	88.66%	Reciprocal-Y squared-X	87.81%
Square root-Y	86.87%	Reciprocal-X	88.60%	Logarithmic-X	87.72%
Reciprocal-Y square root-X	86.60%	Square root-Y	88.52%	Square root-Y squared-X	87.52%
Reciprocal-X	86.55%	Logarithmic-X	88.47%	S-curve model	87.45%
Reciprocal-Y logarithmic-X	85.63%	Reciprocal-Y logarithmic-X	88.42%	Square root-X	87.36%
Logarithmic-X	85.08%	Square root-X	88.07%	Linear	86.79%
Square root-Y squared-X	85.03%	Logarithmic-Y squared-X	88.05%	Reciprocal-Y	86.68%
Square root-X	84.10%	Linear	87.45%	Reciprocal-Y square root-X	85.83%
Double reciprocal	83.19%	Square root-Y squared-X	87.03%	Squared-X	85.07%
Linear	82.96%	Double reciprocal	86.91%	Reciprocal-Y logarithmic-X	84.79%
Squared-X	80.28%	Squared-Y reciprocal-X	86.79%	Squared-Y reciprocal-X	84.13%
Squared-Y reciprocal-X	77.56%	Squared-Y logarithmic-X	85.90%	Squared-Y logarithmic-X	82.83%
Squared-Y logarithmic-X	74.49%	Squared-X	85.59%	Double reciprocal	82.17%
Squared-Y square root-X	72.78%	Squared-Y square root-X	85.12%	Squared-Y square root-X	81.88%
Squared-Y	70.97%	Squared-Y	84.14%	Squared-Y	80.74%
Double squared	67.13%	Double squared	81.62%	Double squared	77.97%
Logistic		Logistic		Logistic	
Log probit		Log probit		Log probit	

B. Validation of Normalized (UCS, G_0, and E) Equations

Table B.1. Error calculation of the UCS, G_0 and E results considering the normalized equation - TRP.

Dry Density (g/cm^3)	Cement (%)	TRP (%)	Curing (Days)	$n/X_{iv}^{0.32}$	q_u(kPa)	$q_{u(n/Xiv^{\wedge}0.32=25)}$	Peridicted q_u (kPa)	Error(%)	G_o(MPa)	$G_{0(n/Xiv^{\wedge}0.32=25)}$	Peridicted G_o(MPa)	Error(%)	E(MPa)	$E_{(n/Xiv^{\wedge}0.32=25)}$	Peridicated E(MPa)	Error(%)
1.6	7	0	7	30.90	1377.08		1380.82	0.27	3580.87		3401.45	5.27	184.30		212.88	13.43
1.6	7	0	7	30.61	1296.95		1415.03	8.34	3584.56		3446.25	4.01	195.50		216.46	9.68
1.6	10	0	7	27.63	1968.38		1847.29	6.55	4170.82		3974.10	4.95	262.50		259.53	1.15
1.6	10	0	7	27.92	2102.52		1797.56	16.97	4152.88		3916.55	6.03	263.70		254.75	3.51
1.6	13	0	7	24.06	2702.74		2646.01	2.14	4307.94		4815.81	10.55	363.90		331.45	9.79
1.6	13	0	7	25.08	2758.42	2380.33	2375.23	16.13	4428.50	4524.16	4545.73	2.58	359.40	299.89	307.97	16.70
1.8	7	0	7	24.08	2563.09		2642.17	2.99	4690.81		4812.07	2.52	327.90		331.12	0.97
1.8	7	0	7	23.35	2289.87		2859.58	19.92	4932.15		5019.86	1.75	260.80		349.44	25.37
1.8	10	0	7	21.92	3107.13		3373.45	7.89	5300.99		5483.55	3.33	342.90		391.05	12.31
1.8	10	0	7	21.91	3228.16		3375.86	4.38	5404.68		5485.64	1.48	341.70		391.24	12.66
1.8	13	0	7	19.67	4209.75		4470.04	5.82	5604.48		6373.99	12.07	498.60		473.64	5.27
1.8	13	0	7	20.11	4371.00		4217.02	3.65	6150.94		6178.50	0.45	508.00		455.22	11.60
1.6	7	0	28	28.29	2364.44		2912.03	18.80	4476.57		4719.86	5.15	382.50		426.13	10.24
1.6	7	0	28	28.72	2364.35		2798.99	15.53	4655.03		4621.01	0.74	388.80		414.80	6.27
1.6	10	0	28	25.84	3533.66		3682.10	4.03	5358.88		5350.65	0.15	540.20		499.94	8.05
1.6	10	0	28	26.11	3818.81		3583.73	6.56	5104.59		5273.75	3.21	526.10		490.81	7.19
1.6	13	0	28	22.90	5863.75		5044.30	16.24	6459.26		6331.28	2.02	648.30		619.41	4.66
1.6	13	0	28	23.34	5791.82	3988.55	4799.98	20.66	6414.37	5551.43	6165.44	4.04	620.30	513.31	598.83	3.59
1.8	7	0	28	22.98	4571.61		4995.80	8.49	6412.72		6298.65	1.81	561.40		615.35	8.77
1.8	7	0	28	23.09	4689.59		4937.04	5.01	6000.90		6258.94	4.12	526.10		610.42	13.81
1.8	10	0	28	21.16	7151.04		6189.42	15.54	7015.40		7063.03	0.67	646.70		711.98	9.17
1.8	10	0	28	21.06	7369.85		6272.19	17.50	7384.30		7113.37	3.81	648.10		718.45	9.79
1.8	13	0	28	18.57	8897.82		8690.79	2.38	7569.82		8468.34	10.61	833.20		897.05	7.12
1.8	13	0	28	18.54	8397.46		8728.57	3.79	7441.64		8488.01	12.33	798.10		899.71	11.29
1.6	7	0	60	27.69	2823.20		3488.58	19.07	5192.36		5241.92	0.95				
1.6	7	0	60	29.35	2524.04		2999.42	15.85	4983.16		4835.19	3.06				
1.6	10	0	60	26.16	4128.65		4045.23	2.06	5954.82		5673.66	4.96				
1.6	10	0	60	25.82	4531.45		4185.08	8.28	6289.52		5777.70	8.86				
1.6	13	0	60	23.35	6036.83		5432.40	11.13	5999.76		6642.33	9.67	636.10		653.03	2.59
1.6	13	0	60	22.93	6522.63	4521.74	5696.73	14.50	6503.44	5986.27	6813.21	4.55	631.10	560.42	674.50	6.43
1.8	7	0	60	22.03	6387.77		6320.35	1.07	6693.91		7202.29	7.06	694.80		723.92	4.02
1.8	7	0	60	22.08	7006.62		6286.46	11.46	6847.11		7181.62	4.66	661.90		721.28	8.23
1.8	10	0	60	19.80	9388.48		8345.14	12.50	7582.18		8355.93	9.26	815.70		874.69	6.74
1.8	10	0	60	20.21	9345.86		7907.39	18.19	7721.42		8118.66	4.89	774.20		843.19	8.18
1.8	13	0	60	18.52	10344.62		9921.50	4.26	8579.13		9165.75	6.40				
1.8	13	0	60	18.52	10344.62		9921.50	4.26	8579.13		9165.75	6.40				
1.6	7	2.5	7	28.24	1754.12		1747.10	0.40	4065.01		4058.00	0.17	223.00		240.45	7.26
1.6	7	2.5	7	29.17	1510.23		1605.27	5.92	3885.56		3878.41	0.18	200.00		226.99	11.89
1.6	10	2.5	7	24.72	2306.18		2469.50	6.61	4644.57		4882.70	4.88	323.90		304.33	6.43
1.6	10	2.5	7	25.91	2290.60		2185.78	4.80	4646.31		4574.29	1.57	330.70		280.07	18.08
1.6	13	2.5	7	22.85	3045.45		3031.09	0.47	5076.19		5447.97	6.82	363.30		349.89	3.83
1.6	13	2.5	7	23.24	2731.94	2382.88	2900.16	5.80	4987.82	4762.19	5320.87	6.26	358.20	288.81	339.52	5.50
1.8	7	2.5	7	23.49	2734.51		2821.45	3.08	5277.90		5243.17	0.66	293.50		333.22	11.92
1.8	7	2.5	7	23.87	2729.43		2704.97	0.90	5404.36		5126.32	5.42	270.30		323.80	16.52
1.8	10	2.5	7	20.41	4261.36		4061.73	4.91	6062.10		6370.76	4.84	400.00		427.03	6.33
1.8	10	2.5	7	21.34	3771.37		3620.01	4.18	5924.57		5990.45	1.10	390.70		394.84	1.05
1.8	13	2.5	7	21.26	3975.59		3655.51	8.76	6204.17		6021.79	3.03	370.00		397.47	6.91
1.8	13	2.5	7	20.18	3944.31		4187.57	5.81	6243.17		6475.53	3.59	437.30		435.99	0.30
1.6	7	2.5	28	28.37	3464.45		3423.50	1.20	5129.27		5069.70	1.18	380.00		365.64	3.93
1.6	7	2.5	28	28.54	3571.07		3367.71	6.04	5244.31		5025.36	4.36	377.50		361.57	4.40
1.6	10	2.5	28	25.48	4571.87		4524.36	1.05	5517.84		5884.60	6.23	434.57		442.07	1.70
1.6	10	2.5	28	25.79	4131.91		4385.46	5.78	5479.48		5787.31	5.32	401.10		432.78	7.32
1.6	13	2.5	28	24.16	5295.80		5196.00	1.92	5716.77		6336.56	9.78	433.45		485.75	10.77
1.6	13	2.5	28	25.00	4623.11	4723.65	4756.12	2.80	5751.82	5986.35	6043.88	4.83	444.50	442.65	457.36	2.81
1.8	7	2.5	28	24.92	4569.43		4793.37	4.67	6313.23		6069.14	4.02	396.50		459.79	13.77
1.8	7	2.5	28	24.76	4332.08		4873.73	11.11	6086.13		6123.32	0.61	382.86		465.03	17.67
1.8	10	2.5	28	22.71	6026.58		6100.84	1.22	7366.10		6904.42	6.69	604.90		541.84	11.64
1.8	10	2.5	28	21.89	7787.85		6714.87	15.98	7962.61		7267.63	9.56	610.60		578.40	5.57
1.8	13	2.5	28	19.51	8808.15		9061.76	2.80	7999.00		8530.73	6.23	693.80		709.33	2.19
1.8	13	2.5	28	19.97	8378.73		8529.03	1.76	7943.51		8258.84	3.82	673.80		680.66	1.01

1.6	7	2.5	60	28.89	2453.81	4207.31	2906.94	15.59	5093.75	6498.52	5364.56	5.05	395.20	438.93	350.96	12.60
1.6	7	2.5	60	30.50	2045.96		2524.30	18.95	4953.45		4974.68	0.43	401.30		318.81	25.87
1.6	10	2.5	60	28.16	2504.42		3106.63	19.38	5238.25		5558.53	5.76	441.30		367.20	20.18
1.6	10	2.5	60	27.56	2769.89		3285.52	15.69	5526.05		5727.42	3.52	474.00		381.47	24.26
1.6	13	2.5	60	25.62	4794.02		3973.21	20.66	6411.97		6339.93	1.14	549.50		434.16	26.57
1.6	13	2.5	60	25.24	4769.13		4130.56	15.46	6595.09		6472.95	1.89	594.60		445.79	33.38
1.8	7	2.5	60	25.68	4020.76		3950.08	1.79	6650.73		6320.17	5.23	563.60		432.44	30.33
1.8	7	2.5	60	25.53	4020.76		4007.65	0.33	6788.80		6369.26	6.59	577.70		436.72	32.28
1.8	10	2.5	60	22.34	6811.87		5671.10	20.12	8080.06		7668.26	5.37	689.80		553.15	24.70
1.8	10	2.5	60	22.43	6223.80		5613.23	10.88	7954.31		7626.32	4.30	635.60		549.30	15.71
1.8	13	2.5	60	21.47	6003.18		6288.71	4.54	7783.00		8103.96	3.96	767.90		593.48	29.39
1.8	13	2.5	60	21.64	6198.93		6162.12	0.60	7873.89		8016.34	1.78	700.40		585.32	19.66
1.6	7	5	7	28.24	1842.33	2316.94	1698.53	8.47	4204.90	4555.66	3881.73	8.33	193.40	258.41	215.12	10.10
1.6	7	5	7	28.33	1775.63		1684.47	5.41	4025.28		3864.51	4.16	233.00		213.91	8.93
1.6	10	5	7	25.53	1987.74		2207.30	9.95	4460.64		4465.38	0.11	289.90		257.12	12.75
1.6	10	5	7	24.91	1833.05		2353.07	22.10	4512.59		4620.68	2.34	285.40		268.57	6.27
1.6	13	5	7	23.79	2927.35		2653.09	10.34	4591.76		4926.84	6.80	306.00		291.43	5.00
1.6	13	5	7	23.25	3007.20		2816.81	6.76	4565.97		5087.12	10.24	305.40		303.55	0.61
1.8	7	5	7	23.99	2309.92		2595.40	11.00	4501.13		4869.28	7.56	280.00		287.10	2.47
1.8	7	5	7	23.73	2336.35		2671.59	12.55	4593.76		4945.19	7.11	270.00		292.81	7.79
1.8	10	5	7	22.03	3285.39		3238.31	1.45	5706.22		5480.85	4.11	358.50		333.78	7.41
1.8	10	5	7	21.72	3279.52		3359.46	2.38	5671.16		5589.54	1.46	349.60		342.23	2.15
1.8	13	5	7	20.45	4585.98		3930.65	16.67	5912.28		6079.03	2.74	366.20		380.84	3.84
1.8	13	5	7	19.71	4617.13		4328.97	6.66	5946.12		6400.96	7.11	392.20		406.71	3.57
1.6	7	5	28	28.48	3311.41	4430.36	3178.32	4.19	4581.77	5399.84	4548.10	0.74	378.50	420.81	345.19	9.65
1.6	7	5	28	28.07	3398.49		3299.83	2.99	5016.76		4640.25	8.11	367.60		354.12	3.81
1.6	10	5	28	25.28	4509.77		4331.33	4.12	5041.49		5366.55	6.06	382.40		426.16	10.27
1.6	10	5	28	25.50	4727.48		4233.95	11.66	4962.82		5301.70	6.39	390.00		419.61	7.06
1.6	13	5	28	23.99	4307.77		4963.61	13.21	5497.93		5772.07	4.75	474.00		467.58	1.37
1.6	13	5	28	23.70	5467.01		5124.81	6.68	5486.57		5871.54	6.56	506.10		477.87	5.91
1.8	7	5	28	23.89	4241.37		5015.11	15.43	5750.99		5804.01	0.91	395.90		470.88	15.92
1.8	7	5	28	23.81	4136.22		5060.07	18.26	5382.25		5831.77	7.71	390.10		473.75	17.66
1.8	10	5	28	21.49	6350.55		6604.26	3.84	7477.77		6724.17	11.21	549.30		567.92	3.28
1.8	10	5	28	21.08	5667.54		6949.56	18.45	7376.17		6909.89	6.75	530.00		587.97	9.86
1.8	13	5	28	19.97	7341.69		7992.57	8.14	7557.94		7446.25	1.50	652.50		646.70	0.90
1.8	13	5	28	20.17	7581.07		7796.52	2.76	7513.63		7348.04	2.25	645.10		635.85	1.45
1.6	7	5	60	29.43	2563.34	4054.44	2669.65	3.98	4571.21	6149.15	4947.19	7.60	400.00	526.01	407.02	1.73
1.6	7	5	60	29.34	2569.47		2692.39	4.57	4640.27		4969.67	6.63	391.00		409.38	4.49
1.6	10	5	60	27.37	2884.11		3224.30	10.55	5364.90		5472.51	1.97	468.10		462.84	1.14
1.6	10	5	60	27.24	2923.46		3265.79	10.48	4972.82		5510.04	9.75	426.00		466.89	8.76
1.6	13	5	60	24.93	4213.88		4111.06	2.50	6345.51		6231.58	1.83	553.20		546.09	1.30
1.6	13	5	60	25.34	4210.54		3941.50	6.83	6469.87		6092.82	6.19	534.00		530.65	0.63
1.8	7	5	60	23.85	4792.26		4613.37	3.88	6185.02		6627.71	6.68	545.00		590.67	7.73
1.8	7	5	60	23.89	4898.75		4594.33	6.63	6517.50		6613.07	1.45	515.10		589.01	12.55
1.8	10	5	60	22.20	6636.43		5559.40	19.37	7895.69		7322.72	7.82	710.00		670.65	5.87
1.8	10	5	60	22.29	6544.49		5502.02	18.95	7862.87		7282.21	7.97	755.63		665.93	13.47
1.8	13	5	60	21.07	5309.46		6361.72	16.54	7190.66		7869.95	8.63	650.40		735.11	11.52
1.8	13	5	60	21.30	5315.81		6188.57	14.10	7566.53		7754.71	2.43	650.30		721.43	9.86
1.6	7	10	7	27.77	1802.81	2202.79	1687.56	6.83	3666.42	4339.70	3785.82	3.15	193.40	258.41	221.67	12.75
1.6	7	10	7	27.88	1778.41		1669.02	6.55	3904.02		3763.53	3.73	181.40		220.01	17.55
1.6	10	10	7	24.41	2226.17		2359.68	5.66	4437.07		4528.93	2.03	314.20		278.49	12.82
1.6	10	10	7	24.82	2343.85		2258.36	3.79	4333.88		4423.91	2.03	320.10		270.30	18.43
1.6	13	10	7	22.72	3039.98		2841.18	7.00	4913.08		5001.62	1.77	354.00		316.02	12.02
1.6	13	10	7	23.07	2965.98		2731.49	8.58	4698.61		4897.44	4.06	331.00		307.66	7.58
1.8	7	10	7	22.35	2313.15		2965.07	21.99	5021.30		5117.05	1.87	289.00		325.34	11.17
1.8	7	10	7	22.14	2753.25		3041.11	9.47	5067.41		5186.80	2.30	304.00		331.00	8.16
1.8	10	10	7	21.05	2977.10		3464.86	14.08	5428.43		5561.44	2.39	350.00		361.74	3.24
1.8	10	10	7	21.72	2697.84		3194.33	15.54	5283.48		5324.91	0.78	313.00		342.26	8.55
1.8	13	10	7	18.85	3626.16		4619.41	21.50	5769.48		6485.76	11.04	450.00		439.97	2.28
1.8	13	10	7	20.11	3293.86		3903.91	15.63	5637.96		5927.72	4.89	430.00		392.34	9.60
1.6	7	10	28	28.36	3023.04	4266.73	3094.85	2.32	4959.52	5398.10	4573.50	8.44	375.40	419.08	346.36	8.38
1.6	7	10	28	28.61	3241.84		3023.02	7.24	4642.81		4516.44	2.80	331.60		340.87	2.72
1.6	10	10	28	26.18	3885.24		3809.52	1.99	4776.61		5110.78	6.54	384.90		398.99	3.53
1.6	10	10	28	25.46	4036.20		4094.09	1.41	4684.82		5311.45	11.80	396.00		419.04	5.50
1.6	13	10	28	23.61	5378.07		4980.14	7.99	5797.82		5897.95	1.70	474.10		478.83	0.99
1.6	13	10	28	23.80	5524.48		4879.86	13.21	5909.46		5834.16	1.29	490.00		472.24	3.76
1.8	7	10	28	24.29	4099.43		4630.54	11.47	5470.94		5672.86	3.56	420.00		455.68	7.83
1.8	7	10	28	23.96	4091.32		4794.52	14.67	5450.12		5779.39	5.70	415.00		466.60	11.06
1.8	10	10	28	21.14	6202.26		6644.34	6.65	7159.28		6880.82	4.05	540.00		582.66	7.32
1.8	10	10	28	21.37	6157.20		6459.68	4.68	7096.79		6777.92	4.70	520.00		571.59	9.03
1.8	13	10	28	19.94	6639.07		7729.67	14.11	7088.53		7460.52	4.99	560.00		645.88	13.30
1.8	13	10	28	19.87	6882.83		7799.96	11.76	7732.99		7496.72	3.15	600.00		649.87	7.67

1.6	7	10	60	28.88	2314.39	3468.95	2400.13	3.57	4629.53	5778.93	4774.09	3.03	380.00	401.60	321.42	18.23
1.6	7	10	60	28.35	2312.55		2518.60	8.18	4660.44		4898.66	4.86	365.40		332.14	10.01
1.6	10	10	60	26.74	3336.52		2930.12	13.87	5498.46		5311.48	3.52	450.20		368.18	22.28
1.6	10	10	60	26.87	3218.71		2894.96	11.18	5541.74		5277.32	5.01	416.60		365.17	14.08
1.6	13	10	60	24.00	4222.84		3883.69	8.73	6194.09		6174.92	0.31	475.50		446.03	6.61
1.6	13	10	60	24.45	4164.39		3698.16	12.61	6299.02		6015.41	4.71	520.70		431.41	20.70
1.8	7	10	60	23.57	4270.54		4067.46	4.99	6746.57		6329.44	6.59	548.90		460.29	19.25
1.8	7	10	60	23.54	4309.86		4080.34	5.63	6062.09		6340.14	4.39	523.40		461.28	13.47
1.8	10	10	60	21.52	4404.02		5157.01	14.60	6342.75		7185.72	11.73	586.70		541.00	8.45
1.8	10	10	60	22.44	4334.53		4624.36	6.27	6364.26		6778.89	6.12	586.80		502.31	16.82
1.8	13	10	60	20.57	4980.33		5794.81	14.06	7519.44		7647.93	1.68	640.90		585.70	9.42
1.8	13	10	60	20.41	5024.09		5918.89	15.12	7306.71		7735.05	5.54	622.80		594.21	4.81
1.6	7	20	7	26.23	1445.79	1742.26	1547.79	6.59	3292.46	3749.03	3539.98	6.99	139.20	184.36	174.92	20.42
1.6	7	20	7	26.43	1704.71		1517.90	12.31	3508.69		3503.27	0.15	156.10		172.62	9.57
1.6	10	20	7	23.96	1876.33		1958.07	4.17	4370.87		4014.15	8.89	264.00		205.29	28.60
1.6	10	20	7	24.03	1725.65		1943.76	11.22	4071.05		3998.44	1.82	232.80		204.27	13.97
1.6	13	20	7	21.99	2515.86		2448.43	2.75	4148.47		4523.59	8.29	236.70		239.02	0.97
1.6	13	20	7	22.30	2736.64		2359.14	16.00	4364.46		4434.64	1.58	257.50		233.05	10.49
1.8	7	20	7	21.42	2231.14		2620.08	14.84	4680.85		4690.46	0.20	235.30		250.31	6.00
1.8	7	20	7	22.25	2426.71		2373.61	2.24	4592.44		4449.15	3.22	221.20		234.03	5.48
1.8	10	20	7	19.98	2916.14		3142.49	7.20	5109.36		5169.25	1.16	326.60		283.29	15.29
1.8	10	20	7	20.08	2733.87		3101.43	11.85	4993.55		5133.04	2.72	321.00		280.76	14.33
1.8	13	20	7	19.28	3387.62		3446.20	1.70	5462.12		5430.61	0.58	338.40		301.65	12.18
1.8	13	20	7	18.92	3830.36		3619.08	5.84	6063.07		5574.59	8.76	366.00		311.87	17.36
1.6	7	20	28	28.01	1914.98	2951.10	2209.78	13.34	3320.61	4154.40	3580.18	7.25	200.00	294.23	248.50	19.52
1.6	7	20	28	27.57	2316.22		2302.25	0.61	3138.61		3659.51	14.23	214.30		255.53	16.14
1.6	10	20	28	24.15	3127.51		3250.54	3.78	4473.16		4400.58	1.65	350.00		323.17	8.30
1.6	10	20	28	24.10	3802.79		3266.70	16.41	4537.16		4412.26	2.83	370.00		324.26	14.11
1.6	13	20	28	23.35	4515.75		3545.11	27.38	4905.59		4609.47	6.42	418.30		342.83	22.01
1.6	13	20	28	23.63	4378.09		3438.26	27.33	5344.36		4534.66	17.86	394.30		335.76	17.44
1.8	7	20	28	22.11	3847.85		4085.62	5.82	5304.24		4972.77	6.67	340.70		377.60	9.77
1.8	7	20	28	22.81	3448.93		3767.82	8.46	4555.94		4762.09	4.33	330.00		357.35	7.65
1.8	10	20	28	21.10	4074.50		4617.02	11.75	6226.66		5308.70	17.29	404.60		410.38	1.41
1.8	10	20	28	20.20	4890.59		5171.20	5.43	6460.63		5640.37	14.54	466.00		443.30	5.12
1.8	13	20	28	18.62	6824.97		6385.41	6.88	6864.85		6313.59	8.73	526.10		511.75	2.81
1.8	13	20	28	19.91	6046.74		5364.91	12.71	6129.97		5752.36	6.56	520.00		454.54	14.40
1.6	7	20	60	26.89	2003.11	2764.03	2300.99	12.95	3748.17	4531.68	4132.87	9.31	261.70	316.73	287.51	8.98
1.6	7	20	60	26.85	2088.37		2311.32	9.65	3859.11		4142.78	6.85	279.20		288.39	3.19
1.6	10	20	60	25.39	2820.86		2672.45	5.55	4704.56		4477.12	5.08	338.00		318.35	6.17
1.6	10	20	60	24.97	3046.66		2791.70	9.13	4867.78		4582.84	6.22	314.00		327.95	4.25
1.6	13	20	60	23.30	3536.05		3339.02	5.90	5243.60		5043.15	3.97	315.40		370.46	14.86
1.6	13	20	60	23.00	3153.94		3455.52	8.73	5083.99		5136.46	1.02	334.60		379.21	11.76
1.8	7	20	60	23.83	3447.04		3152.15	9.36	5050.07		4890.23	3.27	390.50		356.22	9.62
1.8	7	20	60	23.27	3480.25		3351.75	3.83	4961.23		5053.42	1.82	388.60		371.42	4.63
1.8	10	20	60	21.31	3719.33		4213.78	11.73	6577.29		5711.18	15.17	451.10		434.04	3.93
1.8	10	20	60	21.36	3568.10		4186.41	14.77	6171.92		5691.32	8.44	460.00		432.12	6.45
1.8	13	20	60	20.14	4453.78		4878.73	8.71	7360.92		6176.55	19.18	590.00		479.57	23.03
1.8	13	20	60	19.65	4515.87		5201.06	13.17	7693.27		6391.46	20.37	590.00		500.92	17.78
						Average Error		9.16		**Average Error**		5.13		**Average Error**		10.04

Table B.2. Error calculation of the UCS, G0 and E results considering the normalized equation - TRF.

Dry Density (g/cm^3)	Cement (%)	TRP (%)	Curing (Days)	$n/X_{iv}^{0.32}$	q_u(kPa)	$q_{u(n/Xiv^{0.32}=25)}$	Peridicted q_u (kPa)	Error(%)	G_o(MPa)	$G_{0(n/Xiv^{0.32}=25)}$	Peridicted G_o(MPa)	Error(%)	E(MPa)	$E_{(n/Xiv^{0.32}=25)}$	Peridicated E(MPa)	Error(%)
1.6	7	0	7	30.90	1377.08		1486.46	7.36	3580.87		3445.15	3.94	184.30		198.80	7.30
1.6	7	0	7	30.61	1296.95		1518.27	14.58	3584.56		3485.93	2.83	195.50		202.73	3.57
1.6	10	0	7	27.63	1968.38		1912.21	2.94	4170.82		3962.57	5.26	262.50		250.92	4.61
1.6	10	0	7	27.92	2102.52		1867.58	12.58	4152.88		3910.92	6.19	263.70		245.50	7.41
1.6	13	0	7	24.06	2702.74		2609.66	3.57	4307.94		4709.82	8.53	363.90		334.49	8.79
1.6	13	0	7	25.08	2758.42	2380.33	2376.90	16.05	4428.50	4524.16	4471.60	0.96	359.40	312.90	306.82	17.14
1.8	7	0	7	24.08	2563.09		2606.38	1.66	4690.81		4706.53	0.33	327.90		334.10	1.86
1.8	7	0	7	23.35	2289.87		2790.98	17.95	4932.15		4888.90	0.88	330.00		355.92	7.28
1.8	10	0	7	21.92	3107.13		3220.08	3.51	5300.99		5293.18	0.15	382.90		406.23	5.74
1.8	10	0	7	21.91	3228.16		3222.07	0.19	5404.68		5295.00	2.07	381.70		406.46	6.09
1.8	13	0	7	19.67	4209.75		4108.18	2.47	5604.48		6060.17	7.52	498.60		508.82	2.01
1.8	13	0	7	20.11	4371.00		3906.16	11.90	6150.94		5892.76	4.38	508.00		485.64	4.60
1.6	7	0	28	28.29	2364.44		3039.24	22.20	4476.57		4721.66	5.19	382.50		389.49	1.79
1.6	7	0	28	28.72	2364.35		2936.88	19.49	4655.03		4632.64	0.48	388.80		377.35	3.03
1.6	10	0	28	25.84	3533.66		3723.47	5.10	5358.88		5285.49	1.39	540.20		469.91	14.96
1.6	10	0	28	26.11	3818.81		3637.23	4.99	5104.59		5217.13	2.16	526.10		459.84	14.41
1.6	13	0	28	22.90	5863.75		4889.35	19.93	6459.26		6149.07	5.04	648.30		604.48	7.25
1.6	13	0	28	23.34	5791.82	3988.55	4683.73	23.66	6414.37	5551.43	6004.03	6.83	620.30	510.01	580.94	6.77
1.8	7	0	28	22.98	4571.61		4848.63	5.71	6412.72		6120.57	4.77	561.40		599.83	6.41
1.8	7	0	28	23.09	4689.59		4799.24	2.28	6000.90		6085.85	1.40	526.10		594.17	11.46
1.8	10	0	28	21.16	7151.04		5836.32	22.53	7015.40		6784.61	3.40	646.70		711.97	9.17
1.8	10	0	28	21.06	7369.85		5903.81	24.83	7384.30		6828.08	8.15	648.10		719.58	9.93
1.8	13	0	28	18.57	8897.82		7828.97	13.65	7569.82		7987.20	5.23	833.20		934.09	10.80
1.8	13	0	28	18.54	8397.46		7858.42	6.86	7441.64		8003.88	7.02	798.10		937.34	14.85
1.6	7	0	60	27.69	2823.20		3630.49	22.24	5192.36		5267.01	1.42				
1.6	7	0	60	29.35	2524.04		3185.56	20.77	4983.16		4898.01	1.74				
1.6	10	0	60	26.16	4128.65		4126.71	0.05	5954.82		5655.55	5.29				
1.6	10	0	60	25.82	4531.45		4249.89	6.62	6289.52		5748.72	9.41				
1.6	13	0	60	24.21	6036.83		4913.08	22.87	6126.23		6231.00	1.68	636.10		624.06	1.93
1.6	13	0	60	22.93	6522.63	4542.32	5549.73	17.53	6503.44	6030.50	6667.40	2.46	631.10	591.12	698.47	9.64
1.8	7	0	60	22.03	6387.77		6071.75	5.20	6693.91		7008.85	4.49	694.80		758.99	8.46
1.8	7	0	60	22.08	7006.62		6043.57	15.94	6847.11		6990.76	2.05	661.90		755.73	12.42
1.8	10	0	60	19.80	9388.48		7722.53	21.57	7582.18		8010.73	5.35	815.70		947.96	13.95
1.8	10	0	60	20.21	9345.86		7370.70	26.80	7721.42		7805.88	1.08	774.20		907.97	14.73
1.8	13	0	60	18.52	10344.62		8969.90	15.33	8579.13		8705.60	1.45				
1.8	13	0	60	18.52	10344.62		8969.90	15.33	8579.13		8705.60	1.45				
1.6	7	2.5	7	28.42	1754.12		2249.54	22.02	3435.22		3986.93	13.84	172.32		228.83	24.69
1.6	7	2.5	7	28.60	1510.23		2218.30	31.92	3368.75		3956.08	14.85	175.12		225.89	22.48
1.6	10	2.5	7	26.04	2306.18		2739.36	15.81	4422.77		4448.04	0.57	276.00		274.54	0.53
1.6	10	2.5	7	26.04	2290.60		2738.99	16.37	4297.12		4447.71	3.39	266.02		274.50	3.09
1.6	13	2.5	7	24.14	3045.45		3249.95	6.29	4840.59		4891.10	1.03	309.80		321.53	3.65
1.6	13	2.5	7	23.38	2731.94	2984.58	3489.88	21.72	4871.97	4716.09	5088.53	4.26	390.40	302.67	343.41	13.68
1.8	7	2.5	7	24.68	2734.51		3091.97	11.56	5313.92		4757.56	11.69	336.84		307.05	9.70
1.8	7	2.5	7	26.85	2729.43		2556.24	6.78	4725.19		4280.32	10.39	297.16		257.53	15.39
1.8	10	2.5	7	22.32	4261.36		3876.94	9.92	6636.55		5394.72	23.02	464.49		378.48	22.72
1.8	10	2.5	7	21.91	3771.37		4041.68	6.69	6439.86		5520.90	16.65	496.69		393.33	26.28
1.8	13	2.5	7	20.74	3975.59		4568.94	12.99	7149.19		5910.10	20.97	540.80		440.54	22.76
1.8	13	2.5	7	20.47	3944.31		4706.93	16.20	7024.08		6008.61	16.90	508.32		452.82	12.26

1.6	7	2.5	28	28.68	3464.45	4702.49	3472.41	0.23	4529.52	5830.56	4873.24	7.05	369.70	465.04	344.98	7.17
1.6	7	2.5	28	29.14	3571.07		3350.19	6.59	4426.48		4777.19	7.34	324.80		333.74	2.68
1.6	10	2.5	28	26.05	4571.87		4310.51	6.06	5408.20		5495.19	1.58	467.90		421.30	11.06
1.6	10	2.5	28	26.61	4131.91		4112.53	0.47	5498.06		5353.52	2.70	382.40		403.38	5.20
1.6	13	2.5	28	24.65	5295.80		4883.43	8.44	5841.09		5889.69	0.83	453.19		472.82	4.15
1.6	13	2.5	28	25.07	4623.11		4700.01	1.64	5922.66		5765.75	2.72	499.31		456.38	9.41
1.8	7	2.5	28	23.96	4569.43		5206.72	12.24	6335.37		6103.21	3.80	476.24		501.69	5.07
1.8	7	2.5	28	24.01	4332.08		5178.48	16.34	6483.27		6084.80	6.55	484.10		499.17	3.02
1.8	10	2.5	28	22.52	6026.58		5983.19	0.73	6948.70		6593.21	5.39	593.90		570.48	4.11
1.8	10	2.5	28	21.49	7787.85		6652.00	17.08	7433.12		6992.99	6.29	655.70		629.19	4.21
1.8	13	2.5	28	20.67	8808.15		7259.10	21.34	7850.26		7340.67	6.94	676.94		682.10	0.76
1.8	13	2.5	28	20.30	8378.73		7558.09	10.86	7842.43		7507.13	4.47	717.90		708.03	1.39
1.6	7	2.5	60	29.54	2453.81	5242.88	3623.94	32.29	5445.85	6509.94	5244.99	3.83	367.50	529.92	369.82	0.63
1.6	7	2.5	60	30.41	2045.96		3394.98	39.74	5307.35		5058.22	4.93	331.20		348.16	4.87
1.6	10	2.5	60	27.23	2504.42		4351.85	42.45	5694.20		5806.40	1.93	475.72		438.00	8.61
1.6	10	2.5	60	27.32	2769.89		4319.33	35.87	5509.71		5782.26	4.71	430.00		434.97	1.14
1.6	13	2.5	60	25.62	4794.02		4992.68	3.98	6447.71		6266.88	2.89	444.70		497.31	10.58
1.6	13	2.5	60	25.22	4769.13		5170.44	7.76	6336.49		6389.88	0.84	520.00		513.65	1.24
1.8	7	2.5	60	25.21	4020.76		5177.10	22.34	6044.21		6394.45	5.48	522.05		514.27	1.51
1.8	7	2.5	60	25.05	4020.76		5252.30	23.45	6476.54		6445.89	0.48	553.04		521.17	6.12
1.8	10	2.5	60	22.31	6811.87		6813.39	0.02	7937.86		7448.49	6.57	756.40		662.91	14.10
1.8	10	2.5	60	21.93	6223.80		7084.29	12.15	7821.42		7611.59	2.76	757.00		687.24	10.15
1.8	13	2.5	60	20.59	6003.18		8158.45	26.42	8581.56		8232.61	4.24	826.50		783.04	5.55
1.8	13	2.5	60	20.12	6198.93		8599.45	27.91	8396.73		8476.94	0.95	811.26		822.09	1.32
1.6	7	5	7	29.01	1842.33	2726.23	1962.63	6.13	3526.57	4601.76	3792.32	7.01	168.88	269.39	195.20	13.48
1.6	7	5	7	28.91	1775.63		1978.37	10.25	3438.77		3809.19	9.72	151.90		196.65	22.76
1.6	10	5	7	26.34	1987.74		2437.53	18.45	4407.97		4277.50	3.05	262.50		238.50	10.06
1.6	10	5	7	25.20	1833.05		2693.32	31.94	4341.91		4521.33	3.97	231.40		261.55	11.53
1.6	13	5	7	23.85	2927.35		3048.02	3.96	4684.49		4843.02	3.27	329.00		293.24	12.20
1.6	13	5	7	24.14	3007.20		2968.26	1.31	4737.58		4772.20	0.73	295.40		286.14	3.24
1.8	7	5	7	24.36	2309.92		2907.82	20.56	5075.83		4717.97	7.59	317.40		280.75	13.06
1.8	7	5	7	24.14	2336.35		2967.25	21.26	5103.77		4771.30	6.97	283.10		286.05	1.03
1.8	10	5	7	22.98	3285.39		3315.82	0.92	5762.98		5074.99	13.56	366.60		316.98	15.65
1.8	10	5	7	22.73	3279.52		3397.47	3.47	5742.28		5144.04	11.63	377.70		324.19	16.51
1.8	13	5	7	21.82	4585.98		3723.76	23.15	6013.21		5412.90	11.09	424.80		352.87	20.38
1.8	13	5	7	20.80	4617.13		4148.08	11.31	6435.13		5747.33	11.97	483.80		389.89	24.09
1.6	7	5	28	29.43	3311.41	4222.97	2943.81	12.49	4997.49	5839.10	4726.71	5.73	328.70	433.33	304.79	7.85
1.6	7	5	28	29.14	3398.49		3008.99	12.94	4825.48		4784.56	0.86	344.50		311.02	10.76
1.6	10	5	28	26.23	4509.77		3813.18	18.27	5420.94		5457.46	0.67	394.90		387.15	2.00
1.6	10	5	28	26.74	4727.48		3651.99	29.45	5450.90		5328.06	2.31	364.90		372.00	1.91
1.6	13	5	28	24.39	4307.77		4492.52	4.11	5831.45		5977.89	2.45	450.40		450.51	0.02
1.6	13	5	28	24.05	5467.01		4634.90	17.95	5897.26		6082.41	3.04	488.50		463.69	5.35
1.8	7	5	28	24.77	4241.37		4336.13	2.19	5960.41		5861.37	1.69	401.00		435.99	8.03
1.8	7	5	28	24.44	4136.22		4471.86	7.51	5990.50		5962.60	0.47	420.90		448.60	6.17
1.8	10	5	28	21.80	6350.55		5784.10	9.79	6783.42		6878.88	1.39	595.70		569.06	4.68
1.8	10	5	28	21.68	5667.54		5851.52	3.14	7048.36		6923.31	1.81	598.30		575.19	4.02
1.8	13	5	28	20.05	7341.69		6978.47	5.20	7475.66		7634.99	2.09	624.60		676.90	7.73
1.8	13	5	28	20.45	7581.07		6674.40	13.58	6885.53		7448.34	7.56	640.20		649.59	1.45
1.6	7	5	60	30.27	2563.34	4821.76	3154.36	18.74	4824.69	6415.76	5013.43	3.76	294.90	491.89	326.25	9.61
1.6	7	5	60	30.62	2569.47		3073.03	16.39	4827.78		4941.20	2.30	335.70		318.46	5.41
1.6	10	5	60	27.90	2884.11		3790.55	23.91	5874.77		5552.18	5.81	445.80		386.64	15.30
1.6	10	5	60	27.27	2923.46		3988.22	26.70	5827.48		5711.22	2.04	425.80		405.25	5.07
1.6	13	5	60	25.62	4213.88		4590.11	8.20	6390.61		6175.07	3.49	450.60		461.48	2.36
1.6	13	5	60	25.18	4210.54		4771.00	11.75	6503.26		6309.10	3.08	505.40		478.26	5.67
1.8	7	5	60	25.44	4792.26		4662.07	2.79	6495.98		6228.67	4.29	489.30		468.16	4.52
1.8	7	5	60	24.84	4898.75		4922.98	0.49	6225.75		6419.98	3.03	467.00		492.33	5.15
1.8	10	5	60	22.02	6636.43		6456.36	2.79	7470.35		7463.72	0.09	715.40		632.59	13.09
1.8	10	5	60	21.61	6544.49		6735.26	2.83	7737.06		7641.16	1.26	622.50		657.81	5.37
1.8	13	5	60	20.19	5309.46		7849.44	32.36	8255.62		8319.46	0.77	753.00		757.81	0.63
1.8	13	5	60	20.47	5315.81		7608.09	30.13	8285.33		8176.36	1.33	720.00		736.24	2.21
1.6	7	10	7	29.36	1802.81	2787.40	1952.57	7.67	3858.69	4473.83	3631.35	6.26	217.10	281.22	198.70	9.26
1.6	7	10	7	29.77	1778.41		1893.49	6.08	3774.80		3569.89	5.74	194.50		193.13	0.71
1.6	10	10	7	26.46	2226.17		2467.07	9.76	3955.93		4135.22	4.34	211.40		246.65	14.29
1.6	10	10	7	26.20	2343.85		2522.50	7.08	4085.02		4186.59	2.43	232.31		251.77	7.73
1.6	13	10	7	23.95	3039.98		3088.06	1.56	4544.01		4684.55	3.00	293.60		303.55	3.28
1.6	13	10	7	23.95	2965.98		3087.30	3.93	4615.24		4683.91	1.47	321.36		303.48	5.89
1.8	7	10	7	24.39	2313.15		2963.03	21.93	4817.32		4578.21	5.22	292.22		292.17	0.02
1.8	7	10	7	24.24	2753.25		3005.94	8.41	4654.05		4614.93	0.85	276.10		296.08	6.75
1.8	10	10	7	22.58	2977.10		3524.31	15.53	5081.77		5041.39	0.80	362.80		342.99	5.78
1.8	10	10	7	22.90	2697.84		3417.66	21.06	5004.57		4956.06	0.98	378.80		333.38	13.62
1.8	13	10	7	20.86	3626.16		4212.18	13.91	5510.52		5566.33	1.00	446.40		404.45	10.37
1.8	13	10	7	21.72	3293.86		3849.33	14.43	5242.48		5294.62	0.98	430.00		372.13	15.55

1.6	7	10	28	29.15	3023.04		2642.65	14.39	4487.59		4510.43	0.51	334.50		291.11	14.91
1.6	7	10	28	28.48	3241.84		2784.61	16.42	4594.79		4643.46	1.05	310.30		305.53	1.56
1.6	10	10	28	27.25	3885.24		3074.29	26.38	4970.96		4905.92	1.33	356.90		334.81	6.60
1.6	10	10	28	26.42	4036.20		3296.79	22.43	5175.82		5100.11	1.48	353.70		357.15	0.97
1.6	13	10	28	25.10	5378.07		3699.15	45.39	5692.88		5437.05	4.71	373.30		397.26	6.03
1.6	13	10	28	24.84	5524.48		3786.80	45.89	5618.56		5508.24	2.00	414.00		405.96	1.98
1.8	7	10	28	23.82	4099.43	3711.04	4161.06	1.48	5933.94	5506.36	5804.34	2.23	421.20	405.81	442.91	4.90
1.8	7	10	28	24.65	4091.32		3852.68	6.19	5873.24		5561.28	5.61	389.40		412.48	5.60
1.8	10	10	28	21.43	6202.26		5282.00	17.42	6142.34		6626.83	7.31	487.40		552.19	11.73
1.8	10	10	28	21.46	6157.20		5260.88	17.04	6681.61		6612.09	1.05	511.70		550.15	6.99
1.8	13	10	28	20.54	6639.07		5807.56	14.32	7198.91		6985.41	3.06	626.60		602.80	3.95
1.8	13	10	28	20.06	6882.83		6128.15	12.31	6861.93		7197.08	4.66	605.90		633.49	4.36
1.6	7	10	60	29.50	2314.39		2854.42	18.92	4841.79		4919.96	1.59	355.72		326.63	8.91
1.6	7	10	60	28.44	2312.55		3098.58	25.37	4928.58		5149.49	4.29	370.10		352.37	5.03
1.6	10	10	60	27.81	3336.52		3258.47	2.40	5163.67		5295.46	2.49	391.23		369.15	5.98
1.6	10	10	60	27.68	3218.71		3293.88	2.28	5307.98		5327.35	0.36	394.00		372.86	5.67
1.6	13	10	60	26.27	4222.84		3705.90	13.95	6403.52		5687.85	12.58	500.40		415.78	20.35
1.6	13	10	60	25.78	4164.39		3863.96	7.78	6043.31		5821.37	3.81	472.00		432.14	9.22
1.8	7	10	60	24.38	4270.54	4116.92	4382.31	2.55	6184.27	6096.10	6243.06	0.94	440.30	466.70	485.48	9.31
1.8	7	10	60	24.35	4309.86		4392.58	1.88	6288.01		6251.18	0.59	467.30		486.53	3.95
1.8	10	10	60	22.51	4404.02		5246.13	16.05	7282.55		6899.32	5.55	614.90		573.32	7.25
1.8	10	10	60	21.69	4334.53		5700.61	23.96	7490.30		7225.24	3.67	584.05		619.09	5.66
1.8	13	10	60	19.33	4980.33		7387.85	32.59	8126.92		8344.61	2.61	692.60		786.77	11.97
1.8	13	10	60	19.46	5024.09		7280.48	30.99	8021.03		8277.02	3.09	751.30		776.19	3.21
1.6	7	20	7	30.02	1445.79		1551.93	6.84	3749.91		3292.02	13.91	135.40		162.53	16.69
1.6	7	20	7	29.73	1704.71		1586.39	7.46	3683.71		3332.44	10.54	151.10		165.87	8.90
1.6	10	20	7	26.27	1876.33		2095.28	10.45	3859.98		3889.47	0.76	210.70		214.52	1.78
1.6	10	20	7	27.00	1725.65		1969.28	12.37	3897.61		3757.74	3.72	209.30		202.57	3.32
1.6	13	20	7	24.90	2515.86		2363.54	6.44	4118.17		4158.70	0.97	258.60		239.79	7.84
1.6	13	20	7	24.46	2736.64		2459.69	11.26	4268.79		4251.86	0.40	276.90		248.80	11.30
1.8	7	20	7	24.72	2231.14	2328.02	2401.30	7.09	4135.68	4169.00	4195.48	1.43	275.80	240.83	243.33	13.34
1.8	7	20	7	25.20	2426.71		2300.95	5.47	4232.93		4097.16	3.31	262.30		233.92	12.13
1.8	10	20	7	22.25	2916.14		3043.75	4.19	4613.66		4786.12	3.60	300.20		302.96	0.91
1.8	10	20	7	22.95	2733.87		2837.75	3.66	4532.96		4603.36	1.53	303.40		283.95	6.85
1.8	13	20	7	21.37	3387.62		3331.73	1.68	4893.79		5032.63	2.76	323.80		329.36	1.69
1.8	13	20	7	21.40	3830.36		3323.47	15.25	4817.91		5025.69	4.13	345.00		328.61	4.99
1.6	7	20	28	30.07	1914.98		2273.61	15.77	4287.43		3999.22	7.21	227.10		222.53	2.05
1.6	7	20	28	30.42	2316.22		2215.51	4.55	4430.54		3942.13	12.39	240.80		217.27	10.83
1.6	10	20	28	27.75	3127.51		2724.51	14.79	4521.86		4422.08	2.26	266.90		263.04	1.47
1.6	10	20	28	27.46	3802.79		2789.89	36.31	4495.73		4480.73	0.33	250.00		268.87	7.02
1.6	13	20	28	24.67	4515.75		3548.33	27.26	5051.28		5121.17	1.36	356.90		335.81	6.28
1.6	13	20	28	25.06	4378.09		3425.55	27.81	4860.05		5021.96	3.22	327.50		325.05	0.75
1.8	7	20	28	25.00	3847.85	3424.05	3443.09	11.76	5323.32	5075.68	5036.23	5.70	317.00	330.93	326.59	2.94
1.8	7	20	28	24.71	3448.93		3537.56	2.51	5468.32		5112.53	6.96	320.00		334.87	4.44
1.8	10	20	28	21.05	4074.50		5070.02	19.64	6044.84		6244.14	3.19	439.10		467.05	5.99
1.8	10	20	28	21.38	4890.59		4898.53	0.16	6108.25		6125.90	0.29	442.80		452.43	2.13
1.8	13	20	28	20.28	6824.97		5515.77	23.74	6617.85		6543.40	1.14	550.30		504.89	8.99
1.8	13	20	28	20.82	6046.74		5200.24	16.28	6234.30		6332.73	1.55	536.40		478.13	12.19
1.6	7	20	60	29.87	2003.11		2534.25	20.96	4620.60		4440.66	4.05	277.40		278.01	0.22
1.6	7	20	60	31.05	2088.37		2322.81	10.09	4653.47		4230.85	9.99	263.10		256.50	2.57
1.6	10	20	60	27.58	2820.86		3033.29	7.00	4887.83		4907.01	0.39	361.30		328.27	10.06
1.6	10	20	60	27.54	3046.66		3043.20	0.11	4948.27		4915.91	0.66	323.40		329.26	1.78
1.6	13	20	60	25.88	3536.05		3500.36	1.02	5100.06		5313.39	4.01	381.50		374.74	1.80
1.6	13	20	60	25.38	3153.94		3658.05	13.78	5226.55		5445.06	4.01	403.50		390.32	3.38
1.8	7	20	60	25.42	3447.04	3761.03	3645.71	5.45	5472.92	5590.22	5434.85	0.70	346.30	407.87	389.11	11.00
1.8	7	20	60	24.90	3480.25		3817.69	8.84	5348.71		5575.83	4.07	382.50		406.04	5.80
1.8	10	20	60	22.08	3719.33		5000.88	25.63	6972.04		6478.07	7.63	603.30		521.15	15.76
1.8	10	20	60	21.74	3568.10		5181.70	31.14	6584.15		6607.17	0.35	524.00		538.54	2.70
1.8	13	20	60	19.92	4453.78		6309.90	29.42	7309.77		7371.29	0.83	615.00		646.11	4.82
1.8	13	20	60	19.96	4515.87		6281.10	28.10	7386.77		7352.58	0.46	593.10		643.39	7.82
						Average Error		**13.90**		**Average Error**		**4.20**		**Average Error**		**7.64**

C. ALM versus Cycle Number Graphs

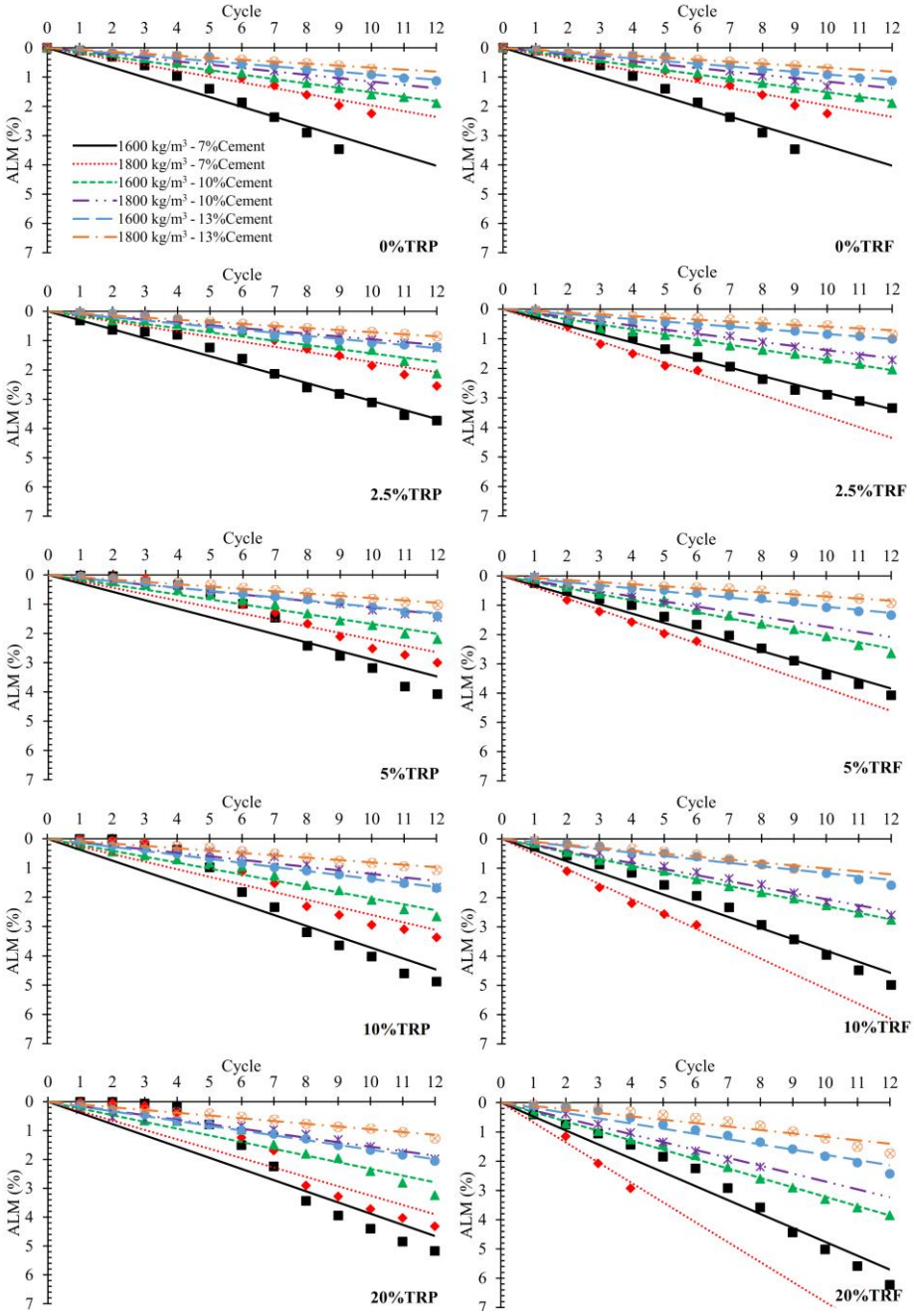

Figure C.1. The Accumulated Loss of Mass (ALM) over the wet/dry cycles for blends containing (7, 10, and 13%) cement content, (0, 2.5, 5, 10, and 20%) TRP and TRF, (1600 kg/m^3 and 1800 kg/m^3) dry densities and cured for 28 days.

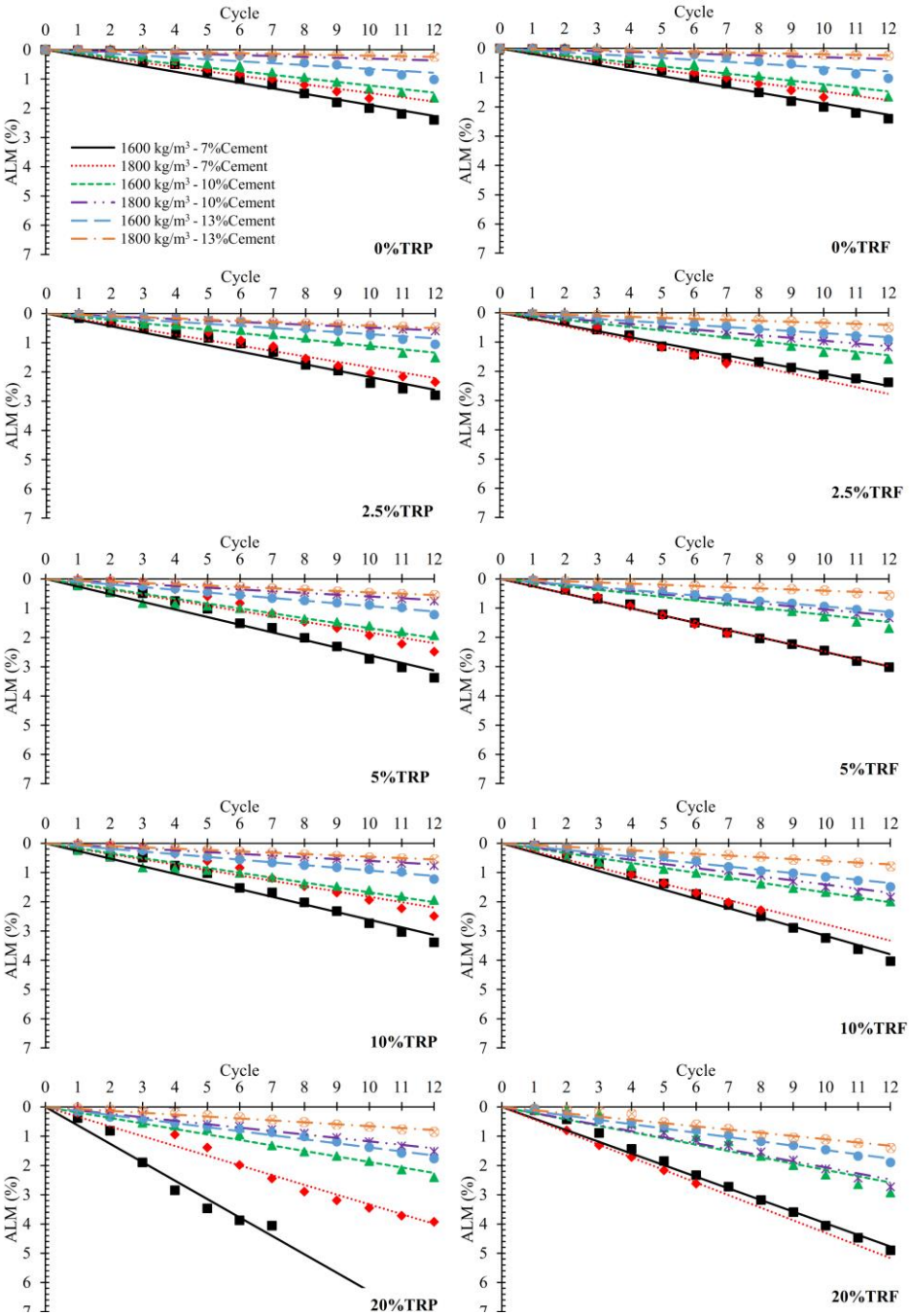

Figure C.2. The Accumulated Loss of Mass (ALM) over the wet/dry cycles for blends containing (7, 10, and 13%) cement content, (0, 2.5, 5, 10, and 20%) TRP and TRF, (1600 kg/m^3 and 1800 kg/m^3) dry densities and cured for 60 days.

D. Environmental Assessment

Table D.1. Mix design of 1 m^3 of tire rubber (TR) (either as fiber (TRF) or Powder for (TRP)) with cemented clay.

Dry Density (kg/m^3)	Cement (%)	TR Content (%)	blend Name	Clay (kg)	Cement (kg)	Additive (kg)	Water (kg)
1600	7	0	1.6C7	1495.33	104.67	0.00	403.91
		2.5	1.6C7TR2.5	1495.33	102.06	0.94	403.19
		5	1.6C7TR5	1495.33	99.44	1.88	402.47
		10	1.6C7TR10	1495.33	94.21	3.75	401.04
		20	1.6C7TR20	1495.33	83.74	7.51	398.20
	10	0	1.6C10	1454.55	145.45	0.00	406.04
		2.5	1.6C10TR2.5	1454.55	141.82	1.30	405.04
		5	1.6C10TR5	1454.55	138.18	2.61	404.04
		10	1.6C10TR10	1454.55	130.91	5.22	402.04
		20	1.6C10TR20	1454.55	116.36	10.44	398.09
	13	0	1.6C13	1415.93	184.07	0.00	408.07
		2.5	1.6C13TR2.5	1415.93	179.47	1.65	406.79
		5	1.6C13TR5	1415.93	174.87	3.30	405.52
		10	1.6C13TR10	1415.93	165.66	6.60	402.99
		20	1.6C13TR20	1415.93	147.26	13.21	397.98
1800	7	0	1.8C7	1682.24	117.76	0.00	329.62
		2.5	1.8C7TR2.5	1682.24	114.81	1.06	328.77
		5	1.8C7TR5	1682.24	111.87	2.11	327.93
		10	1.8C7TR10	1682.24	105.98	4.22	326.25
		20	1.8C7TR20	1682.24	94.21	8.45	322.90
	10	0	1.8C10	1636.36	163.64	0.00	332.09
		2.5	1.8C10TR2.5	1636.36	159.55	1.47	330.92
		5	1.8C10TR5	1636.36	155.45	2.94	329.74
		10	1.8C10TR10	1636.36	147.27	5.87	327.40
		20	1.8C10TR20	1636.36	130.91	11.74	322.75
	13	0	1.8C13	1592.92	207.08	0.00	334.44
		2.5	1.8C13TR2.5	1592.92	201.90	1.86	332.95
		5	1.8C13TR5	1592.92	196.73	3.71	331.46
		10	1.8C13TR10	1592.92	186.37	7.43	328.49
		20	1.8C13TR20	1592.92	165.66	14.86	322.60

Table D.2. LCA results of tire rubber cement-clay mix considering 18 environmental impacts.

Indicator	agricultural land occupation - ALOP	climate change - GWP100	fossil depletion - FDP	freshwater ecotoxicity - FETPinf	freshwater eutrophication - FEP	human toxicity - HTPinf	ionising radiation - IRP_HE	marine ecotoxicity - METPinf	marine eutrophication - MEP
Unit / Mix	m^2a	kg CO_2-Eq	kg oil-Eq	kg 1,4-DCB-Eq	kg P-Eq	kg 1,4-DCB-Eq	kg U_{235}-Eq	kg 1,4-DCB-Eq	kg N-Eq
1.6C7	0.9771	93.1383	10.7233	0.4744	0.0098	10.4891	2.0387	0.4307	0.0770
1.6C7TR2.5	0.5668	88.5209	10.3268	0.1254	0.0095	9.5993	1.9327	0.1275	0.0743
1.6C7TR5	0.1565	83.9035	9.9303	-0.2236	0.0092	8.7096	1.8267	-0.1757	0.0716
1.6C7TR10	-0.6641	74.6688	9.1372	-0.9215	0.0085	6.9301	1.6146	-0.7822	0.0663
1.6C7TR20	-2.3052	56.1992	7.5511	-2.3174	0.0072	3.3710	1.1905	-1.9951	0.0555
1.6C10	1.3495	128.2660	14.5110	0.6525	0.0136	14.4295	2.7438	0.5925	0.1056
1.6C10TR2.5	0.7793	121.8490	13.9600	0.1675	0.0131	13.1931	2.5965	0.1711	0.1019
1.6C10TR5	0.2092	115.4330	13.4090	-0.3174	0.0126	11.9566	2.4491	-0.2502	0.0982
1.6C10TR10	-0.9311	102.6000	12.3070	-1.2873	0.0117	9.4838	2.1545	-1.0929	0.0907
1.6C10TR20	-3.2116	76.9347	10.1030	-3.2270	0.0099	4.5381	1.5652	-2.7784	0.0758
1.6C13	1.7021	161.5280	18.0976	0.8212	0.0171	18.1606	3.4114	0.7457	0.1327
1.6C13TR2.5	0.9806	153.4080	17.4004	0.2075	0.0165	16.5959	3.2250	0.2125	0.1280
1.6C13TR5	0.2591	145.2880	16.7031	-0.4062	0.0159	15.0313	3.0386	-0.3208	0.1233
1.6C13TR10	-1.1839	129.0480	15.3085	-1.6336	0.0148	11.9019	2.6657	-1.3872	0.1138
1.6C13TR20	-4.0699	96.5691	12.5193	-4.0883	0.0124	5.6432	1.9199	-3.5201	0.0950
1.8C7	1.0938	104.3280	11.9154	0.5295	0.0110	11.7096	2.2519	0.4809	0.0861
1.8C7TR2.5	0.6322	99.1333	11.4693	0.1370	0.0106	10.7086	2.1327	0.1398	0.0831
1.8C7TR5	0.1706	93.9387	11.0232	-0.2556	0.0103	9.7076	2.0134	-0.2014	0.0801
1.8C7TR10	-0.7525	83.5496	10.1311	-1.0408	0.0095	7.7057	1.7748	-0.8836	0.0740
1.8C7TR20	-2.5988	62.7714	8.3467	-2.6112	0.0080	3.7017	1.2978	-2.2481	0.0620
1.8C10	1.5127	143.8460	16.1766	0.7299	0.0152	16.1425	3.0452	0.6629	0.1183
1.8C10TR2.5	0.8713	136.6280	15.5567	0.1844	0.0147	14.7515	2.8794	0.1889	0.1141
1.8C10TR5	0.2299	129.4090	14.9368	-0.3612	0.0141	13.3606	2.7137	-0.2852	0.1099
1.8C10TR10	-1.0529	114.9720	13.6971	-1.4523	0.0131	10.5786	2.3822	-1.2332	0.1015
1.8C10TR20	-3.6185	86.0988	11.2175	-3.6345	0.0110	5.0147	1.7192	-3.1294	0.0847
1.8C13	1.9095	181.2660	20.2116	0.9197	0.0191	20.3401	3.7963	0.8352	0.1487
1.8C13TR2.5	1.0978	172.1310	19.4271	0.2293	0.0185	18.5798	3.5865	0.2354	0.1434
1.8C13TR5	0.2861	162.9960	18.6426	-0.4611	0.0178	16.8195	3.3768	-0.3645	0.1381
1.8C13TR10	-1.3373	144.7270	17.0737	-1.8419	0.0165	13.2990	2.9573	-1.5643	0.1275
1.8C13TR20	-4.5841	108.1870	13.9359	-4.6034	0.0139	6.2580	2.1183	-3.9638	0.1063

Table D.2. *Cont*. LCA results of tire rubber cement-clay mix considering 18 environmental impacts

Indicator	metal depletion - MDP	natural land transformation - NLTP	ozone depletion - ODPinf	particulate matter formation - PMFP	photochemical oxidant formation - POFP	terrestrial acidification - TAP100	terrestrial ecotoxicity - TETPinf	urban land occupation - ULOP	water depletion - WDP
Unit / Mix	kg Fe-Eq	m^2	kg CFC-11-Eq	kg PM10-Eq	kg NMVOC	kg SO2-Eq	kg 1,4-DCB-Eq	m^2a	m^3
1.6C7	12.8452	0.0082	0.0000	0.0894	0.2167	0.1921	0.0036	1.9202	1.0219
1.6C7TR2.5	11.9677	0.0079	0.0000	0.0869	0.2083	0.1841	0.0033	1.5044	0.9950
1.6C7TR5	11.0903	0.0076	0.0000	0.0844	0.1999	0.1760	0.0030	1.0885	0.9681
1.6C7TR10	9.3355	0.0070	0.0000	0.0794	0.1832	0.1599	0.0025	0.2568	0.9143
1.6C7TR20	5.8258	0.0057	0.0000	0.0693	0.1497	0.1277	0.0014	-1.4067	0.8068
1.6C10	17.7875	0.0110	0.0000	0.1225	0.2965	0.2636	0.0049	2.6571	1.0723
1.6C10TR2.5	16.5682	0.0106	0.0000	0.1190	0.2849	0.2524	0.0045	2.0792	1.0349
1.6C10TR5	15.3489	0.0102	0.0000	0.1155	0.2733	0.2412	0.0042	1.5013	0.9976
1.6C10TR10	12.9104	0.0093	0.0000	0.1086	0.2500	0.2188	0.0034	0.3455	0.9229
1.6C10TR20	8.0333	0.0076	0.0000	0.0947	0.2034	0.1740	0.0019	-1.9661	0.7734
1.6C13	22.4674	0.0137	0.0000	0.1538	0.3721	0.3313	0.0062	3.3548	1.1201
1.6C13TR2.5	20.9244	0.0131	0.0000	0.1494	0.3574	0.3171	0.0057	2.6235	1.0728
1.6C13TR5	19.3815	0.0126	0.0000	0.1450	0.3427	0.3030	0.0052	1.8921	1.0255
1.6C13TR10	16.2955	0.0115	0.0000	0.1362	0.3132	0.2746	0.0042	0.4295	0.9310
1.6C13TR20	10.1236	0.0094	0.0000	0.1186	0.2543	0.2179	0.0023	-2.4958	0.7419
1.8C7	14.4169	0.0091	0.0000	0.0998	0.2421	0.2148	0.0040	2.1536	0.8697
1.8C7TR2.5	13.4298	0.0087	0.0000	0.0970	0.2326	0.2057	0.0037	1.6858	0.8395
1.8C7TR5	12.4427	0.0084	0.0000	0.0941	0.2232	0.1966	0.0034	1.2179	0.8092
1.8C7TR10	10.4685	0.0077	0.0000	0.0885	0.2044	0.1785	0.0028	0.2822	0.7487
1.8C7TR20	6.5201	0.0063	0.0000	0.0772	0.1667	0.1422	0.0015	-1.5892	0.6278
1.8C10	19.9770	0.0123	0.0000	0.1370	0.3319	0.2952	0.0055	2.9826	0.9264
1.8C10TR2.5	18.6053	0.0118	0.0000	0.1331	0.3188	0.2826	0.0051	2.3324	0.8844
1.8C10TR5	17.2337	0.0113	0.0000	0.1292	0.3057	0.2700	0.0046	1.6823	0.8424
1.8C10TR10	14.4903	0.0103	0.0000	0.1214	0.2795	0.2448	0.0038	0.3821	0.7583
1.8C10TR20	9.0036	0.0084	0.0000	0.1057	0.2272	0.1944	0.0021	-2.2185	0.5902
1.8C13	25.2419	0.0153	0.0000	0.1723	0.4170	0.3713	0.0069	3.7675	0.9802
1.8C13TR2.5	23.5061	0.0147	0.0000	0.1673	0.4004	0.3554	0.0064	2.9448	0.9270
1.8C13TR5	21.7702	0.0140	0.0000	0.1624	0.3838	0.3394	0.0058	2.1220	0.8738
1.8C13TR10	18.2985	0.0128	0.0000	0.1525	0.3507	0.3076	0.0047	0.4766	0.7674
1.8C13TR20	11.3552	0.0104	0.0000	0.1327	0.2844	0.2438	0.0026	-2.8143	0.5547

TEZ İZİN FORMU / THESIS PERMISSION FORM

PROGRAM / PROGRAM

Sürdürülebilir Çevre ve Enerji Sistemleri / Sustainable Environment and Energy Systems ☑

Siyaset Bilimi ve Uluslararası İlişkiler / Political Science and International Relations ☐

İngilizce Öğretmenliği / English Language Teaching ☐

Elektrik Elektronik Mühendisliği / Electrical and Electronics Engineering ☐

Bilgisayar Mühendisliği / Computer Engineering ☐

Makina Mühendisliği / Mechanical Engineering ☐

YAZARIN / AUTHOR
Soyadı / Surname : Al-Subari

Adı / Name : Lutf Nagi Ahmed

Programı / Program : Sustainable Environment and Energy Systems

TEZİN ADI / TITLE OF THE THESIS (**İngilizce** / English) : Utilization of Waste Rubber Tires in Artificially Cemented Alluvial Clay

TEZİN TÜRÜ / DEGREE**:** **Yüksek Lisans** / Master ☑ **Doktora** / PhD ☐

1. **Tezin tamamı dünya çapında erişime açılacaktır. /** Release the entire work immediately for access worldwide. ☐

2. **Tez iki yıl süreyle erişime kapalı olacaktır.** / Secure the entire work for patent and/or proprietary purposes for a period of **two years. *** ☑

3. **Tez altı ay süreyle erişime kapalı olacaktır.** / Secure the entire work for period of **six months**. * ☐

Yazarın imzası / Author Signature ..... **Tarih** / Date .....

Tez Danışmanı / Thesis Advisor Full Name: .....

Tez Danışmanı İmzası / Thesis Advisor Signature: .....

Eş Danışmanı / Co-Advisor Full Name: .....

Eş Danışmanı İmzası / Co-Advisor Signature: .....

Program Koordinatörü / Program Coordinator Full Name: .....

Program Koordinatörü İmzası / Program Coordinator Signature: .....